THE UNIVERSITY OF OKLAHOMA

GRADUATE COLLEGE

CHARACTERIZATION OF DYNAMIC ADSORPTION OF PENTANE ON SILICA GEL

A DISSERTATION

SUBMITTED TO THE GRADUATE FACULTY

in partial fulfillment of the requirements for the

degree of

DOCTOR OF PHILOSOPHY

By

RILEY BYRAN NEEDHAM

Norman, Oklahoma

1965

CHARACTERIZATION OF DYNAMIC ADSORPTION

OF PENTANE ON SILICA GEL

APPROVED BY

J. R. Campbell

Preston L. Moore

John C. Briscoe

Frank Canfield

Sherrill D. Christian

DISSERTATION COMMITTEE

ACKNOWLEDGMENT

The author wishes to express his appreciation to the following people for their invaluable contributions to this dissertation.

Special thanks is extended to Dr. John M. Campbell, research director throughout this investigation, for his enthusiastic interest and constructive criticism.

The financial assistance and continued interest in fundamental research of the Davison Chemical Co., a division of W. R. Grace and Co., is gratefully acknowledged.

Finally, appreciation is extended to my wife, Shirley, for her patience and skillful preparation of this manuscript.

TABLE OF CONTENTS

LIST OF TABLES

LIST OF ILLUSTRATIONS

CHARACTERIZATION OF DYNAMIC ADSORPTION OF PENTANE ON SILICA GEL

CHAPTER I

INTRODUCTION

The application of fixed bed dynamic adsorption for the recovery of liquids from natural gas has enjoyed an extremely rapid growth in recent years.(1) This process has generally been successfully applied, although little is known about the actual adsorption mechanism(s) involved.

The status of the art of dynamic adsorption is two fold. First, there have been several purely mathematical developments based upon simplifying assumptions. The most seriously limiting of these assumptions are that the adsorption is isothermal, only one adsorbing component is present, and some particular mass transfer rate equation predicts the adsorption rate. There has been no general attempt to apply these mathematical developments to dynamic hydrocarbon adsorption.

Second, there have been some dynamic hydrocarbon adsorption data on silica gel reported in the literature, but the resulting correlations of the data have been purely empirical. Thus their application is limited to the conditions under which the data were obtained.

Although the problem of dynamic adsorption is in the general class of simultaneous mass and heat transfer, there have been no reported experimental efforts to analyze the heat transfer portion of the problem.

By relying on experience and over design, the application of dynamic adsorption to hydrocarbon recovery has generally been successful. However, in the improvement of current operations and expansion to broader applications of dynamic hydrocarbon adsorption, a fundamental understanding of the adsorption process is indispensable.

CHAPTER II

DISCUSSION AND REVIEW OF PREVIOUS INVESTIGATIONS

Introduction to Single Component Adsorption

Single component adsorption is characterized by the formation of an adsorption zone or wave. This zone is in reality a concentration profile which forms near the inlet to the bed and then travels to the outlet. Figure 1 is a graphical representation of this zone. The desiccant behind the zone, (A), is virtually saturated and the desiccant in front of the zone, (B), is essentially virgin.

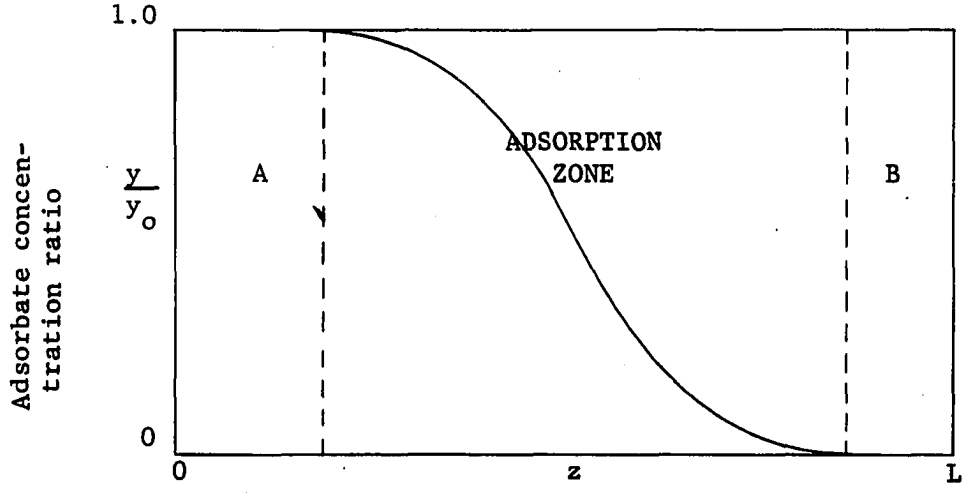

FIGURE 1.--REPRESENTATION OF THE ADSORPTION ZONE

The adsorption zone is formed when the desiccant at the inlet to the bed is saturated. After the adsorption zone is formed, it can follow any one of the four types of behavior listed below:

A. The adsorption zone can continue to increase in length throughout the desiccant bed even if the bed is infinitely long. This type of adsorption zone is termed a non-stabilizing zone.

B. The zone can quickly stabilize; that is, become of constant length so that the formation time and stabilization time are small in comparison to the total traverse time through the bed.

C. The zone can eventually stabilize, but in this case the formation time and stabilization time may be nearly as large as the total traverse time. Indeed, if the desiccant bed is short compared to the adsorption zone, the zone may reach the exit end before it has stabilized.

D. The zone shape becomes dependent upon only dimensionless time and independent of the length of the desiccant bed.

Only types A, B and C are of importance in the adsorption of hydrocarbons on silica gel.

The above described behavior is largely dependent upon the type of adsorption isotherm that the adsorbate exhibits upon the particular adsorbent.

Adsorption Isotherms

Figure 2 shows the three general types of isotherms which control the development of the adsorption zone.

The favorable type of isotherm gives rise to the zone behavior described in B and C. The actual position of the isotherm, the bed length,

and the type and magnitude of mass transfer mechanism determine whether the zone behaves as described in B or C. The linear isotherm results in the type A behavior; whereas, the unfavorable isotherm produces the type D.

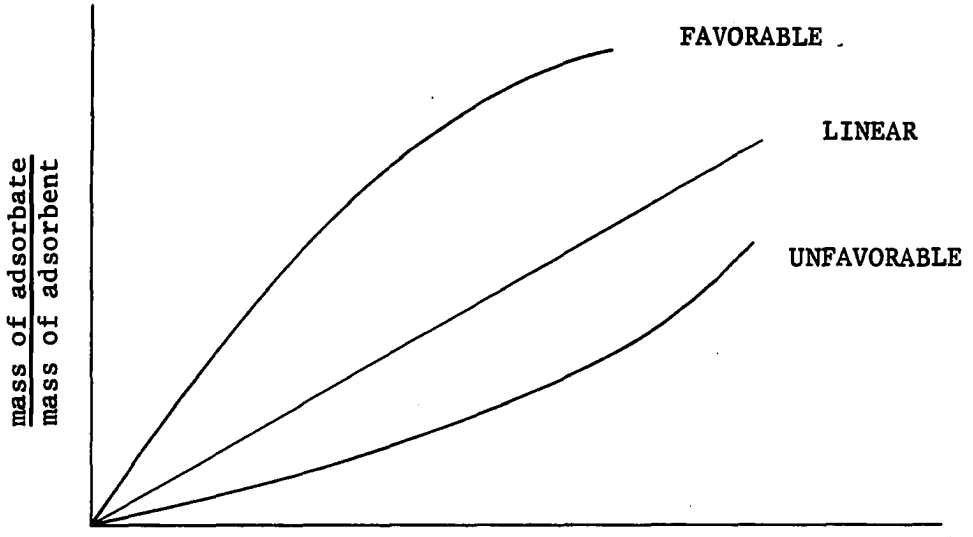

FIGURE 2.--ADSORPTION ISOTHERMS

Most hydrocarbon adsorption on silica gel follows the favorable type of isotherm.(2) At low concentrations the linear isotherm is a workable approximation.(3)

The above discussion of the behavior of the adsorption zone is somewhat qualitative. In order to be more specific, the type(s) of mass transfer mechanism(s) which are controlling the adsorption in a particular case must be known.

Mechanisms of Adsorption Mass Transfer

For isothermal adsorption of hydrocarbons on silica gel the overall mechanisms which probably dominate the rate of mass transfer are:(4)

1. The diffusion through the gas film which surrounds each desiccant particle. This mechanism will be called the "G" mechanism.

2. The diffusion inside the desiccant particle. This mechanism will be called the "P" mechanism. It is recognized that diffusion inside the particle can include a variety of transport processes.

3. A combination of gas film diffusion and particle diffusion. This mechanism will be called the "PG" mechanism. This mechanism is important only when the P and G resistances are about equal.

A more complete discussion of the adsorption zone can be found in recent publications of Vermeulen(4) and Carter.(5,6,7,8)

There have been several mathematical attempts to quantitatively describe single component adsorption which utilize the types of behavior previously described and utilize various assumptions about the controlling mechanism.

Previous Mathematical Developments

Each mathematical development is based upon a particular set of assumptions which in turn determines the ability of the resulting equations to realistically describe dynamic hydrocarbon adsorption.

All of the developments have several common assumptions which are listed below:(9)

1. The adsorption process is isothermal.

2. The pressure gradient along the length of the tower can be neglected.

3. There is no diffusion or dispersion in the longitudinal direction.

4. The mass gas velocity is constant.

5. The flowing gas contains a single adsorbing component.

6. The average particle concentration and gas composition do not vary across any given tower cross section.

7. The mass transfer rate constants are not functions of concentration.

8. The concentration of the adsorbate in the inlet gas is constant.

Assumptions 1 - 6 are necessary in order to develop the differential form of the mass balance, which is one of the necessary equations in each model. One form of this differential mass balance is:

$$-G\left(\frac{\partial y}{\partial z}\right) = \rho_B\left(\frac{\partial w}{\partial t}\right) + \phi_m \rho_g\left(\frac{\partial y}{\partial t}\right) \qquad \text{----------1)}$$

where:

G = mass velocity of carrier gas, $\frac{\text{lb. gas}}{\text{hr - ft.}^2}$.

y = adsorbate concentration in the carrier gas, $\frac{\text{lb. adsorbate}}{\text{lb. gas}}$.

z = distance from the inlet of the adsorption column, feet.

ρ_B = bulk density of the packed column, $\frac{\text{lb. gel}}{\text{ft.}^3}$.

ρ_g = density of the gas under adsorption conditions, $\frac{\text{lb. gas}}{\text{ft.}^3 \text{ void space}}$.

ϕ_m = macroscopic porosity of packed column, $\frac{\text{ft.}^3 \text{ void}}{\text{ft.}^3}$.

t = time, hrs.

w = adsorbate concentration on the adsorbent, $\frac{\text{lb. adsorbate}}{\text{lb. gel}}$.

In addition to the eight assumptions listed above each development contains assumptions as to the mechanism and the type of adsorption isotherm.

In general the resulting mathematical models can be classified into three types corresponding to the first three types of adsorption zone behavior previously described.

Non-stabilizing Models

The non-stabilizing models are characterized by a linear adsorption isotherm which results in the behavior of the adsorption zone described in type A. The mathematical developments are of two main types. The first type assumes that the mass transfer resistances can be described by a linear driving force equation.

Linear Driving Force Concepts

One of the first linear driving force developments was adapted to mass transfer by Hougen and Marshall.(10) In this work the following additional assumptions were utilized:

1. The controlling mass transfer mechanism is the G mechanism.
2. This diffusional mechanism can be represented by a linear driving force of the following form:

$$\left(\frac{\partial w}{\partial t}\right) = \frac{k_G}{B}\left(y - y^*\right) \qquad \text{----------2)}$$

where:

k_G = rate constant which depends on the conditions of adsorption such as gas velocity, adsorbent particle size, type of adsorbate, temperature, and pressure.

y^* = the adsorbate concentration in the gas phase which would be in equilibrium with a solid phase concentration w.

B = the slope of the linear isotherm $y^* = Bw$.

3. The relationship between y^* and w is linear.
4. The adsorbent particles and their packing arrangement can be represented by a single parameter taken as the radius of an equivalent sphere.

5. The static gas phase film around the particle is uniform in thickness.

6. The concentration in the flowing phase around each particle is uniform. That is, the particle is small enough that the concentration change in the flowing phase across the particle can be neglected.

With these assumptions the adsorption behavior is described by the following equation:

$$\frac{y}{y_o} = 1 - e^{-T} \int_0^X e^{-S} I_o\left(2\sqrt{TS}\right) dS \qquad \text{----------3)}$$

where:

y_o = constant adsorbate concentration inlet the column - $\frac{\text{lb.adsorbate}}{\text{lb. gas}}$.

T = dimensionless time = $k_G \left(t - \frac{\varphi_m \rho_g}{G} z\right)$.

X = dimensionless distance = $k_G D z$.

$D = \frac{\rho_B}{G B}$.

I_o = the imaginary Bessel function of zero order.

where all of the symbols used before are as previously defined.

Although the above development has historically been applied to mass transfer operations where the gas film was presumed to be the controlling mechanism, it is also applicable in the case of particle diffusion.(4) For the particle diffusion case the following assumptions are necessary:

1. The mass transfer is controlled by the P mechanism.

2. This mechanism can be represented by a linear driving force of the following form:

$$\left(\frac{\partial w}{\partial t}\right) = k_p \left(w^* - w\right) \qquad \text{----------4)}$$

where:

k_p = mass transfer rate constant for mechanism P.

w^* = concentration of the adsorbate in the adsorbent which would be in equilibrium with the gas phase concentration y.

3. The relationship between w^* and y is $Bw^* = y$.

4. The adsorbent particles and their packing arrangement can be represented by a single parameter taken as the radius of an equivalent sphere.

5. The concentration in the flowing phase around each particle is uniform. That is, the particle is small enough that the concentration gradient in the flowing phase across the particle can be neglected.

With these assumptions the adsorption behavior is again described by Equation 3; but now the dimensionless time and distance are defined as below:

$$T = k_p \left(t - \frac{\phi_m \rho_g z}{G}\right) .$$

$$X = k_p D z .$$

The third case where Equation 3 is valid is for a PG mechanism where both of the mechanisms can be approximated by the linear driving force Equations 2 and 4 for mechanism G and P respectively.

All of the assumptions in the two above cases are again necessary. With these assumptions the rate equation then becomes:(4)

$$\left(\frac{\partial w}{\partial t}\right) = \frac{k_{pG}}{B}\left(y - Bw\right) \qquad \text{----------5)}$$

where:

k_{pG} = combination mechanism rate constant and related to both k_G and k_p by the following equation.

$$\frac{1}{k_{pG}} = \frac{1}{k_G} + \frac{1}{k_p} \qquad \text{----------6)}$$

With rate Equation 5 the solution to this combined mechanism problem is again Equation 3 where now the dimensionless time and distance are defined as follows:

$$T = k_{pG}\left(t - \frac{\phi_m \rho_g z}{G}\right) .$$

$$X = k_{pG} D z .$$

Since equation 3 frequently occurs in problems dealing with heat transfer, there have been several analytical approximations proposed. (11,12,13) One of the approximations, proposed by Jury and Licht,(11) has been applied to adsorption of water on silica gel. This approximation is valid for $TX \geqslant 3600$ and is given below.(4)

$$\frac{y}{y_o} = \frac{1}{2}\left\{1 + \text{ERF}\left(\sqrt{T} - \sqrt{X}\right)\right\} \qquad \text{----------7)}$$

where:

ERF x denotes the error function of x which is

$$\text{ERF } x = \frac{2}{\sqrt{\pi}}\int_0^x e^{-s^2} ds$$

A second approximation proposed by Klinkenberg,(12, 13) which as yet has only been used in heat transfer, is:

$$\frac{y}{y_o} = \frac{1}{2}\left\{1 + \text{ERF}\left[\sqrt{T} - \sqrt{X} + \frac{1}{8\sqrt{T}} + \frac{1}{8\sqrt{X}}\right]\right\} \qquad \text{----------8)}$$

Klinkenberg (13) states that the above equation is accurate to within 0.006 for X = 2, 0.002 for X = 4 and 0.001 for X = 8. This equation should not be used for $X \leq 2$ and for $T \leq 1$.

It can be seen from the previous discussion that the mathematical development is rather complete for single component, isothermal adsorption of an adsorbate which exhibits a linear adsorption isotherm and a linear type driving force.

Combined Solid Phase Diffusion and Gas Film Diffusion

A second type of mathematical development is the case where the diffusion inside the particle (the P mechanism) is not represented by a linear driving force.

In this case the following assumptions were utilized:

1. The mass transfer is controlled by diffusion of the adsorbate into the adsorbent particles possibly coupled with some gas phase diffusion resistance.

2. The particle diffusion occurs by Fick's law diffusion with a constant diffusion coefficient.

3. The gas phase diffusion can be evaluated using a linear driving force equation such as:

$$\left(\frac{\partial w}{\partial t}\right) = \frac{k_G}{B}\left(y - y_r^*\right) \qquad \text{----------9)}$$

where:

y_r^* = the gas phase adsorbate concentration which would be in equilibrium with a solid phase concentration (w_r) at the surface of the adsorbent particle.

4. The relationship between y_r^* and w_r is linear.

5. The adsorbent particles are spheres of uniform size.

6. The static gas film around the particle is uniform in thickness.

7. The concentration in the flowing phase around each particle is uniform. That is, the particle is small enough that the concentration change in the flowing phase across the particle can be neglected.

With these assumptions Rosen (14, 15) numerically solved the resulting equations for the adsorbate breakout curve. These results have been presented in both tabular and graphical form.(15)

Comparison of Exact Solutions to the Film Concepts

One of the cases considered by Rosen (14, 15) was the case of zero gas film resistance. A comparison of the numerical solutions of Rosen to the Klinkenberg equation shows the range of dimensionless time and length where the solid diffusion can be considered as a solid film without appreciable error. Figures 3 and 4 show a comparison between the Klinkenberg equation and the numerical calculations of Rosen for the case of solid diffusion. The dashed curve in these figures is the lower limit of the validity of the Klinkenberg equation to represent Equation 3.

It is apparent from these figures that the solid phase diffusion can be represented as a film type resistance when the dimensionless distance is 10 or greater. Figures 3 and 4 exaggerate the deviation between the two solutions. Therefore, Figures 5 and 6 were prepared to give a more realistic representation. From Figure 5 it can be seen that for $X = 10$ the two solutions are very close; whereas, in Figure 6 for $X = 5$ the deviation is significant.

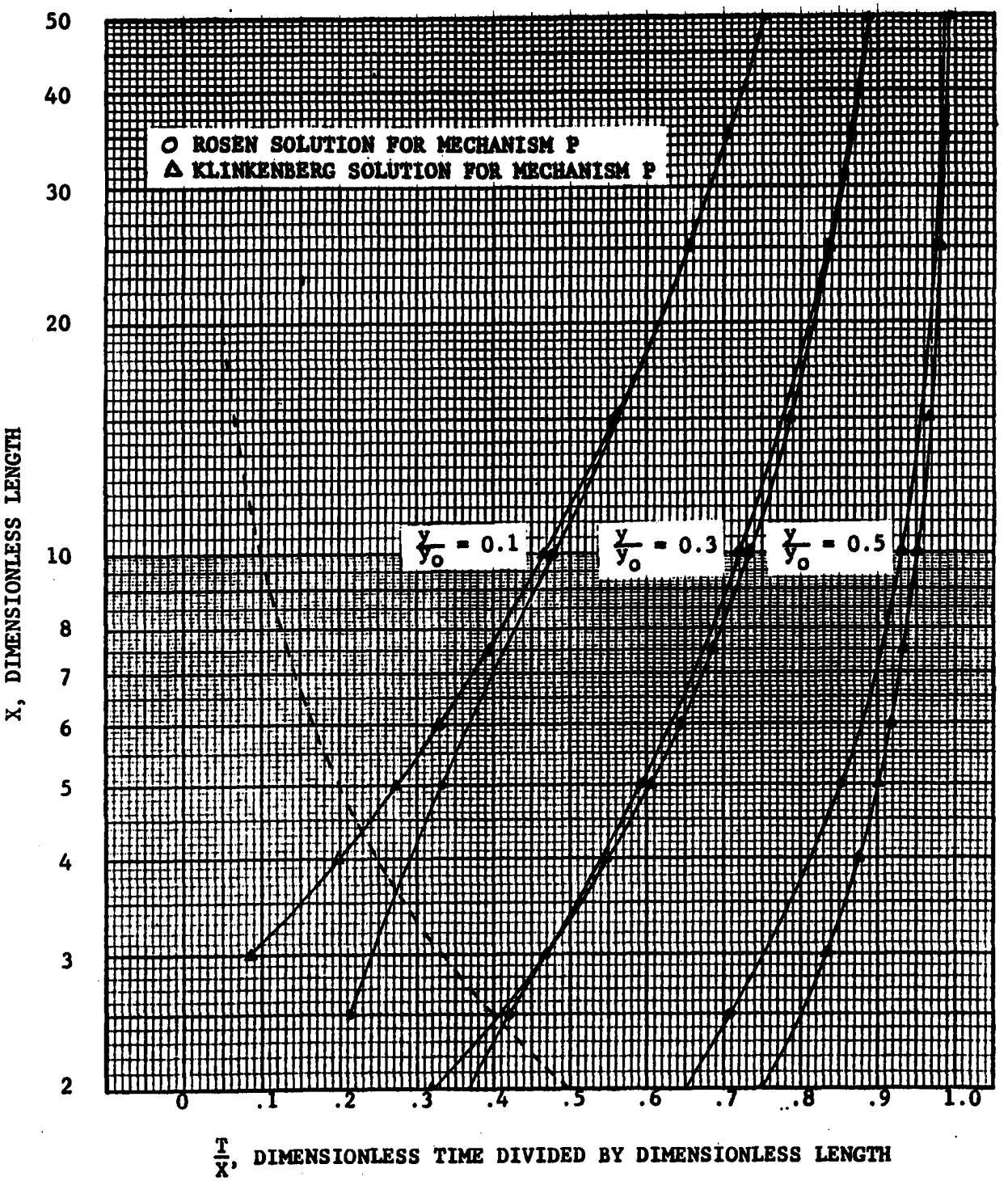

FIGURE 3.--REGIONS OF DEVIATION IN ROSEN AND KLINKENBERG SOLUTIONS

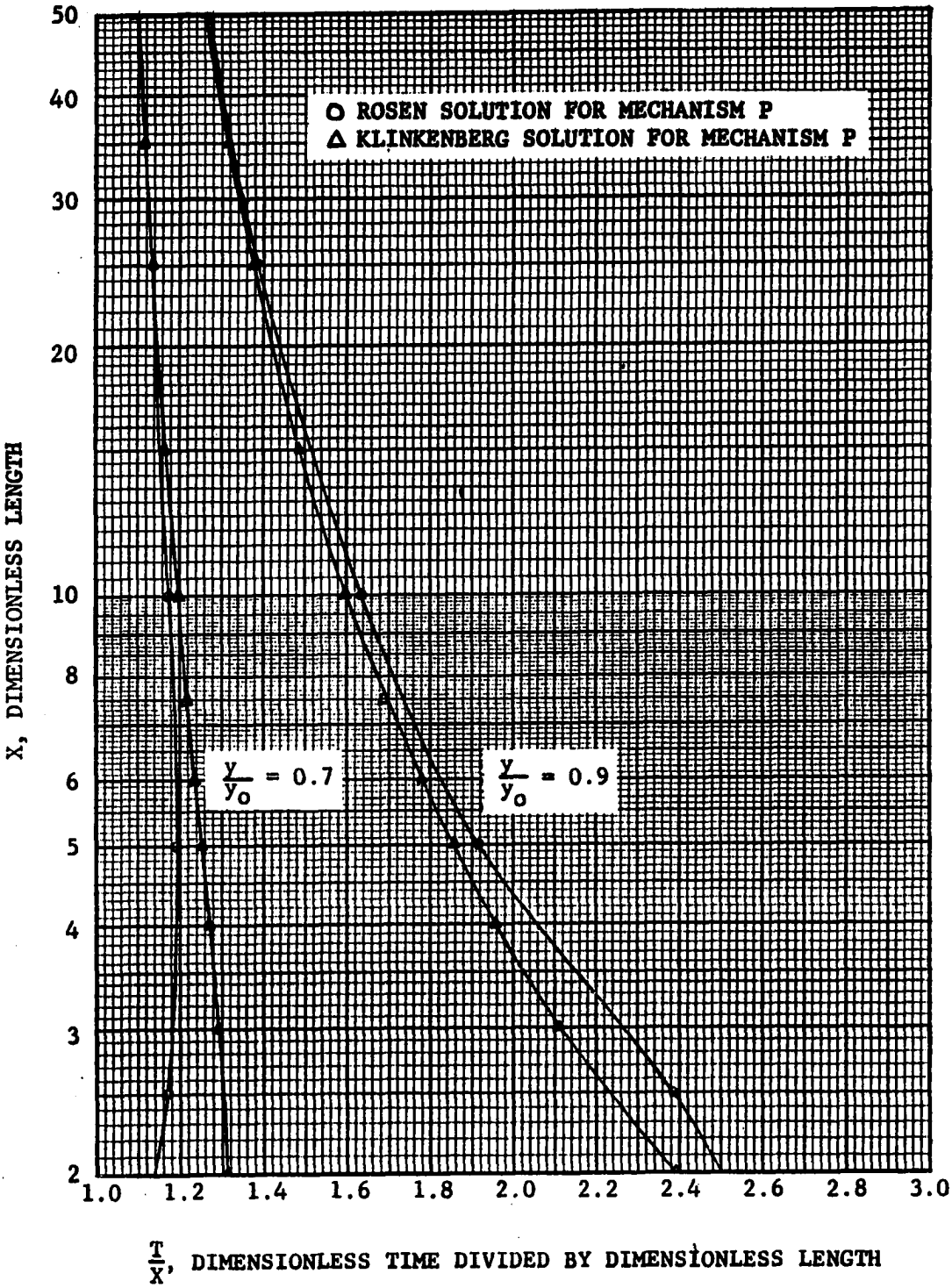

FIGURE 4.--REGIONS OF DEVIATIONS IN ROSEN AND KLINKENBERG SOLUTIONS

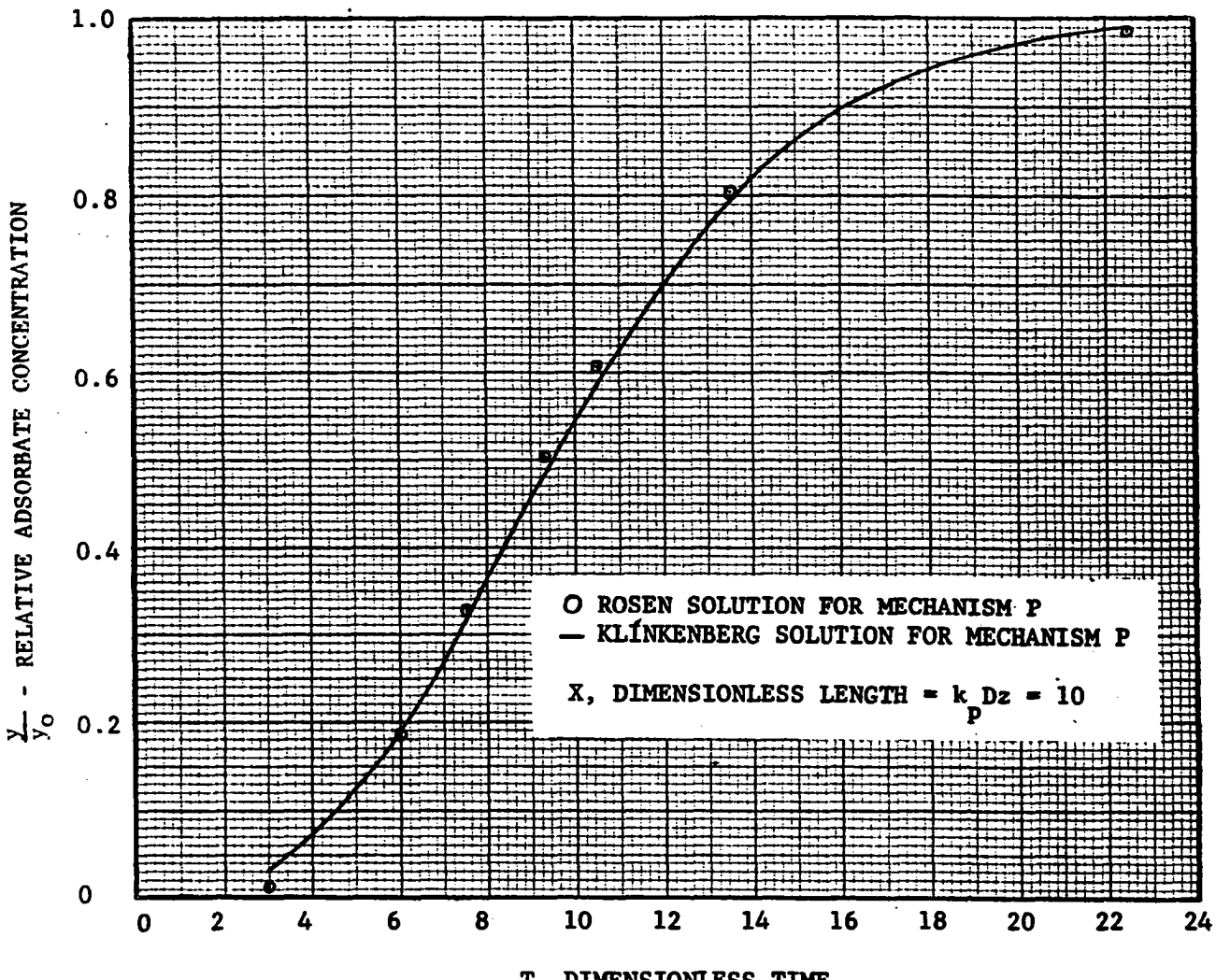

FIGURE 5.--COMPARISON OF BREAKOUT CURVE FOR ROSEN AND KLINKENBERG SOLUTIONS FOR X = 10

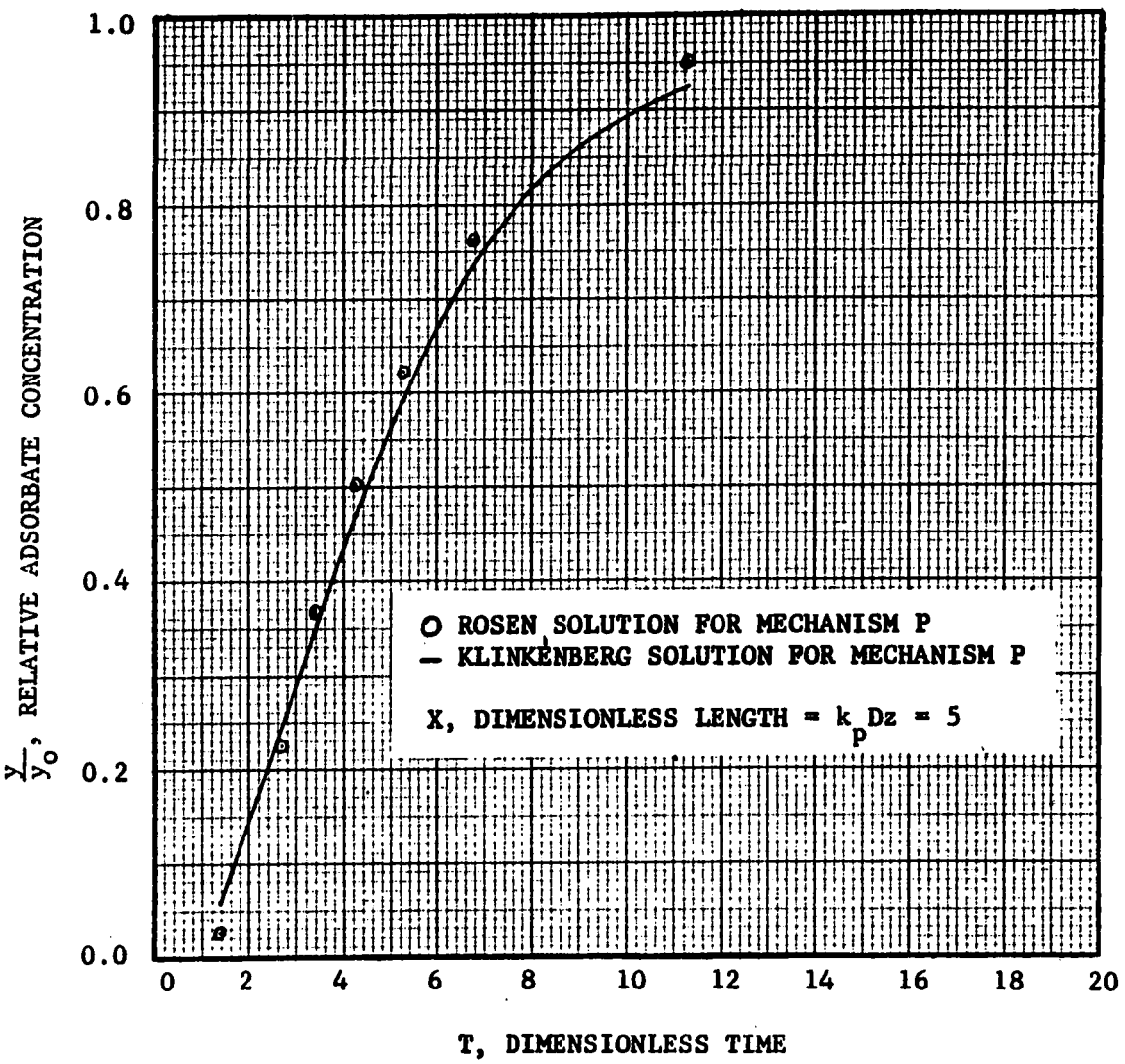

FIGURE 6.--COMPARISON OF BREAKOUT CURVE FOR ROSEN AND KLINKENBERG SOLUTIONS FOR X = 5

Using the numerical calculations of Rosen (15) for a combination mechanism, a second comparison of the film concept to the actual numerical solution can be made. If it is assumed that the P and G mechanisms can be represented as films (linear driving force) then the Klinkenberg equation can be used to calculate the breakout adsorption curve by utilizing Equation 6. By comparing the Klinkenberg results with those of Rosen, the influence of the dual film concept can be checked. Table I shows the results of such calculations for four cases. These results show that the difference between the solutions decreases with increasing $k_p Dz$ and the Klinkenberg approximation is acceptable when $k_p Dz \geqslant 10$. Also at a particular value of $k_p Dz$, the deviation decreases when the values of $k_p Dz$ and $k_G Dz$ are close to the same value.

Therefore, it can be concluded that Equation 8 is a workable solution for all three types of mechanisms (P, G, PG) when the value of $k_p Dz \geqslant 10$ and for the G mechanism when the conditions represented by the dashed line on Figures 3 and 4 are fulfilled.

In all of the above developments the adsorption zone continues to grow in length throughout the adsorption column.

Stabilized Zone with Stabilization Time Less than the Traverse Time

In the stabilized adsorption zone models it is assumed that the zone is stabilized before the end of the column is reached. Also it can be shown that once stabilization is reached, the zone travels through the remaining portion of the column at a substantially constant velocity. The first of these models was developed by Michaels (16) for the G mechanism.

TABLE 1

COMPARISON OF THE ROSEN AND KLINKENBERG SOLUTIONS FOR THE PG MECHANISM

$k_p Dz = 5$, $k_G Dz = 5$				$k_p Dz = 5$, $k_G Dz = 40$			
$\frac{T}{X}$	$\left(\frac{y}{y_o}\right)_R$	$\left(\frac{y}{y_o}\right)_K$	$\left(\frac{y}{y_o}\right)_R - \left(\frac{y}{y_o}\right)_K$	$\frac{T}{X}$	$\left(\frac{y}{y_o}\right)_R$	$\left(\frac{y}{y_o}\right)_K$	$\left(\frac{y}{y_o}\right)_R - \left(\frac{y}{y_o}\right)_K$
0.15	0.133	0.166	-0.033	0.225	0.051	0.096	-0.045
0.30	0.241	0.244	-0.003	0.525	0.270	0.267	0.003
0.525	0.374	0.361	0.013	0.675	0.384	0.366	0.018
0.828	0.532	0.514	0.018	0.855	0.507	0.427	0.080
1.20	0.677	0.665	0.012	1.05	0.620	0.595	0.025
1.65	0.800	0.799	0.001	1.35	0.754	0.680	0.074
3.0	0.963	0.960	0.003	2.25	0.945	0.951	-0.006
$k_p Dz = 10$, $k_G Dz = 5$				$k_p Dz = 10$, $k_G Dz = 40$			
0.15	0.097	0.109	-0.012	0.3	0.034	0.051	-0.017
0.30	0.181	0.186	-0.005	0.6	0.225	0.224	-0.001
0.525	0.317	0.316	0.001	0.75	0.354	0.344	0.010
0.828	0.491	0.487	0.004	0.93	0.500	0.494	0.006
1.20	0.670	0.668	0.002	1.05	0.602	0.588	0.004
1.65	0.820	0.818	0.002	1.35	0.784	0.777	0.007
3.0	0.979	0.980	-0.001	2.25	0.979	0.982	-0.003

K denotes the Klinkenberg solution for the PG mechanism
R denotes the numerical solutions of Rosen for the PG mechanism

The Gas Film Mechanism

In addition to the above assumption of stabilization, the following were utilized:

1. The relationship between y^* and w is represented by the Langmuir adsorption isotherm.

2. The other assumptions are identical to assumptions 1, 2, 4, 5, and 6 of page 8.

The second of these models was developed by Glueckauf and Coates(17) for the P mechanism.

The Solid Diffusion Mechanism

Once stabilization is assumed the other necessary assumptions are:

1. The mass transfer is controlled by diffusion of the adsorbate into the adsorbent particles.

2. This diffusion can be represented by a linear driving force equation such as Equation 4.

3. The adsorbent particles are spheres of uniform size.

4. The equilibrium adsorption condition is represented either by the Freundlich isotherm or the Langmuir with a constant separation factor r.

For the Freundlich isotherm the resulting equation is:

$$t - t_1 = \frac{1}{k_p(1-n)} \ln\left(\frac{1 - \left(\frac{y_1}{y_o}\right)^{1-n}}{1 - \left(\frac{y}{y_o}\right)^{1-n}}\right) \qquad \text{----------10)}$$

where:

t = time in hours.

t_1 = time when $y = y_1$.

n = exponent in the Freundlich isotherm, $w = Ay^n$.

y_o = adsorbate concentration at the inlet to the column,

$$\frac{\text{lbs. adsorbate}}{\text{lb. gas}} .$$

ln = the natural logarithm.

If the length necessary for stabilization and the adsorption bed length are of the same order of magnitude, the task of applying these models to adsorption is formidable. Also the length for stabilization can only be determined experimentally. It changes with adsorbate, adsorbent, adsorbate concentration, gas velocity, temperature, etc.

The third type of mathematical development is for a zone where the stabilization time can be greater than the traverse time.

Stabilizing Zone where Stabilizing Time May Be Greater than the Traverse Time

The mathematical developments in this section are much more complex than those in the preceding sections. The first of these developments was accomplished by Thomas (18) and adapted to adsorption by Vermeulen.(4, 19,20)

Second Order Reaction Rate Mechanism

The assumptions used by Thomas are:

1. The phase change in the adsorption process is the controlling mechanism.
2. This phase change can be represented by a kinetic reaction rate equation of the following form:

$$\left(\frac{\partial w}{\partial t}\right) = k_1\, y(w_o - w) - k_2\, w\,(y_o - y)$$

where:

k_1 and k_2 are constants.

y_o is the adsorbate concentration in the gas phase at the tower inlet.

w_o is the adsorbate concentration on the adsorbent, which would be in equilibrium with y_o.

3. The solid phase concentration is related to the equilibrium gas phase concentration by the Langmuir adsorption isotherm.

$$\frac{w}{w_o} = \frac{\frac{y}{y_o}}{r + (1-r)\frac{y}{y_o}} \qquad \text{----------11)}$$

4. The separation factor (r) is assumed to be constant.

5. The degree of saturation of each particle in a given cross section of the adsorbent bed can be represented by the same average concentration parameter. Thus the particles are uniform and are contacted by the flowing gas stream in the same manner.

It can be shown that the Thomas solution reduces to other known solutions of the adsorption process in several limiting cases. Two of the cases are generally applicable to hydrocarbon adsorption.

Case A - If the G, P, and PG mechanisms can be represented by the linear driving force (Equations 2, 4, and 5), the Thomas solution can be reduced to Equation 3 by setting r = 1 and re-defining dimensionless length and time.

Case B - For $r < 1$ and large dimensionless distances and times, the Thomas solution reduces to a stabilized zone.

Although there is no evidence that the adsorption of normal hydrocarbons on silica gel involves any appreciable resistance from phase change, the Thomas solution is given some theoretical validity by the fact that it reduces to the above two limiting cases.

Combined Solid Diffusion with a Gas Film

This development is accredited to Tien.(21) The assumptions necessary for the resulting numerical solution are:

1. Assumptions 1, 2, 3, 5, 6, and 7 on page 12.
2. The relationship between y_r^* and w_r is the Freundlich isotherm $w_r = A\,(y_r^*)^n$.

The solutions of Tien are of little value for practical hydrocarbon adsorption since the value of n = 1/2 was the only value used and the resulting numerical solutions apply only for values of dimensionless length and time that are outside the practical range. However, the same procedure developed by Tien could be used to compute the desired results.

All of the mathematical developments discussed contain two or more constants which must be evaluated with experimental data. Since the constants change with adsorption conditions, there must be some provision made to determine the values of the constants for the particular adsorption condition at hand.

There is very little hydrocarbon dynamic adsorption data in the literature. The next section reviews this and related data.

Previous Experimental Investigations

There have been several techniques used to correlate single component adsorption data. One of these is to correlate the mass transfer constant, which is determined from the application of one of the previously discussed mathematical developments to the adsorption data, with the process variables such as adsorbent particle size, linear gas velocity, and bed length. These correlations will now be reviewed.

Dependence of the Mass Transfer Constant upon Particle Size, Velocity, and Length

One of the original correlations of the mass transfer constant was obtained by Gamson, Thodos and Hougen (22) for the evaporation of water into air at atmospheric pressure. The water was evaporated from granular porous solids. For a particle Reynolds number $\left(\frac{d_p G}{\mu}\right)$ greater than 350, the mass transfer constant (k_G), as defined in Equation 2, is as follows:

$$k_G = \frac{C_1 B a_v}{\rho_B} \quad \frac{G^{.59} \quad \mu^{.41}}{d_p^{.41}} \quad \left(\frac{\rho D_v}{\mu}\right)_g^{2/3} \qquad \text{----------12)}$$

where:

a_v = is the superficial area of the bed per unit volume of bed, $\frac{ft.^2}{ft.^3}$.

μ = gas viscosity, $\frac{lb_f.}{hr - ft.}$.

D_v = gas diffusivity, $\frac{ft.^2}{hr.}$.

C_1 - proportionality constant.

Leland and Holmes (23) have suggested that this correlation could be utilized for the prediction of single component hydrocarbon adsorption.

Wilke and Hougen (24) have found that a correlation for the mass transfer constant below a modified Reynolds number of 350 could be obtained with the following relationship:

$$k_G = \frac{C_2 B a_v}{\rho_B} \quad \frac{\mu^{.51} G^{.49}}{d_p^{.51}} \left(\frac{\rho D_v}{\mu}\right)_g^{2/3} \qquad \text{----------13)}$$

Hougen and Marshall (10) found that this equation could be applied to water adsorption data on silica gel in the following modified form:

$$k_G = \frac{C_3 B a_v}{\rho_B} \quad \frac{\mu^{.51} G^{.49}}{d_p^{.51}} \qquad \text{----------14)}$$

for $Re < 350$

The silica gel used in the water adsorption had a specific surface area represented by:

$$a_v = \frac{2.58}{d_p} \qquad \text{----------15)}$$

Making use of this Equation in 14 the results are:

$$k_G = \frac{2.58\ C_3 B}{\rho_B} \quad \frac{\mu^{.51} G^{.49}}{d_p^{1.51}} \qquad \text{----------16)}$$

Eagleton and Bliss (25) have found, for the adsorption of water upon silica gel, that the mass transfer constant varies directly with the factor $G^{.55}$ at low adsorbate concentrations and for a given particle size.

Marks et al.(3) have applied Equation 3 to hydrocarbon adsorption on silica gel in order to determine the mass transfer constant. Attempts to correlate this constant using the technique employed by Gamson et al. were unsatisfactory; therefore, a modified approach was used which yielded the following result. According to their analysis the mass transfer constant varies as follows:

$$k_G = C_4 \frac{L^{1/2} a_v K^{1/2}}{d_p^{1.745} G^{.245}} \left(\frac{\rho D_v}{\mu}\right)_g^{2/3} \qquad (17)$$

where:

L = the tower adsorption length, ft.

C_4 = a proportionality factor.

K = slope of the adsorption isotherm .

Since Marks et al.(3) used the a_v described by Equation 15, then:

$$k_G = \frac{2.58\, C_4\, L^{1/2} K^{1/2}}{d_p^{2.745} G^{.245}} \left(\frac{\rho D_v}{\mu}\right)_g^{2/3} \qquad (18)$$

It can be seen that Equation 18 differs from the generalized correlation of Gamson et al.(22) and the water adsorption correlations of Hougen and Marshall (10) and Eagleton and Bliss (25) in three respects.

1. Equation 18 contains a length dependence.
2. The dependence of k_G on mass velocity is inverted with a lower exponent.
3. The k_G dependence on d_p is very great (exponent of 2.745).

The implications of Equation 18 are discussed in Chapter IV.

Sieg (26) has applied the method outlined by Hougen and Marshall (10) to dynamic adsorption of pentane on 3-8 mesh silica gel. However, only trends were obtained from the correlations for the resulting constants.

Empirical Correlation of Breakout Curve

The correlations in the above section utilize assumptions as to the type of mass transfer mechanism which is controlling the adsorption. Without hypothesizing a mechanism an empirical "s" shaped curve (The Gompertz equation) has been "fit" to hydrocarbon adsorption data and the three equation constants determined and correlated with the important adsorption parameters. This equation duplicated quite accurately the breakout curve and is especially applicable for preliminary design calculations.(27,28) Although any "s" shaped curve can be empirically fit to the adsorption breakout curve, the results are only applicable for the conditions under which the data were run. Thus utilizing a purely empirical approach necessitates obtaining data for the full range of each significant parameter.

An approach which takes advantage of the mass transfer phenomena relates many of the fundamental parameters. This reduces the copious data otherwise necessary for prediction of adsorption over a wide range of conditions.

Furthermore, a theoretical or semi-empirical approach yields greater strides in the improvement of the existing processing art by providing an insight into the interrelationship of the fundamental variables.

The Dependence of Dynamic Equilibrium Capacity upon Particle Size

Although it is a well established fact that both the static and dynamic equilibrium capacities are functions of adsorbate concentration, pressure, and temperature; it has only been established recently that

the dynamic capacity also depends upon the adsorbent particle size. Dale et al.(29) have shown that the dynamic equilibrium capacity increases as the particle size decreases. For the adsorption of isobutane and isopentane upon silica gel this increase over 6-8 mesh was 50 per cent for 60-100 mesh and 20 per cent for 20-60 mesh silica gel.

The Behavior of the Adsorption Zone

There is experimental evidence that the adsorption zones for adsorption of pentane and hexane eventually stabilize if the tower length is sufficient. Figure 7 is an example of hexane zone stabilization.(9) Marks et al.(3) show that under some experimental conditions the pentane adsorption zone stabilizes at a column length of 9.9 feet. However, since the stabilization phenomenon is the result of the counteraction of the sharpening tendencies of the dynamic adsorption isotherm and the diffusing tendencies of the mass transfer resistance, the length at which the zone stabilizes is dependent upon many factors and thus varies accordingly.

The length of the adsorption zone has been found to vary mainly as functions of adsorbent particle size and gas velocity.(29) The results of Dale et al.(29) show the variation with velocity is as follows:

$$h_z = \lambda_1 G^{.49} \quad \text{(isopentane on 6-8 mesh silica gel)} \quad \text{----------19)}$$

$$h_z = \lambda_2 G^{.40} \quad \text{(isobutane on 6-8 mesh silica gel)} \quad \text{----------20)}$$

where:

h_z = adsorption zone length, feet.

λ_1, λ_2 are functions of the adsorbate, adsorbent, desiccant bed length and other adsorption conditions.

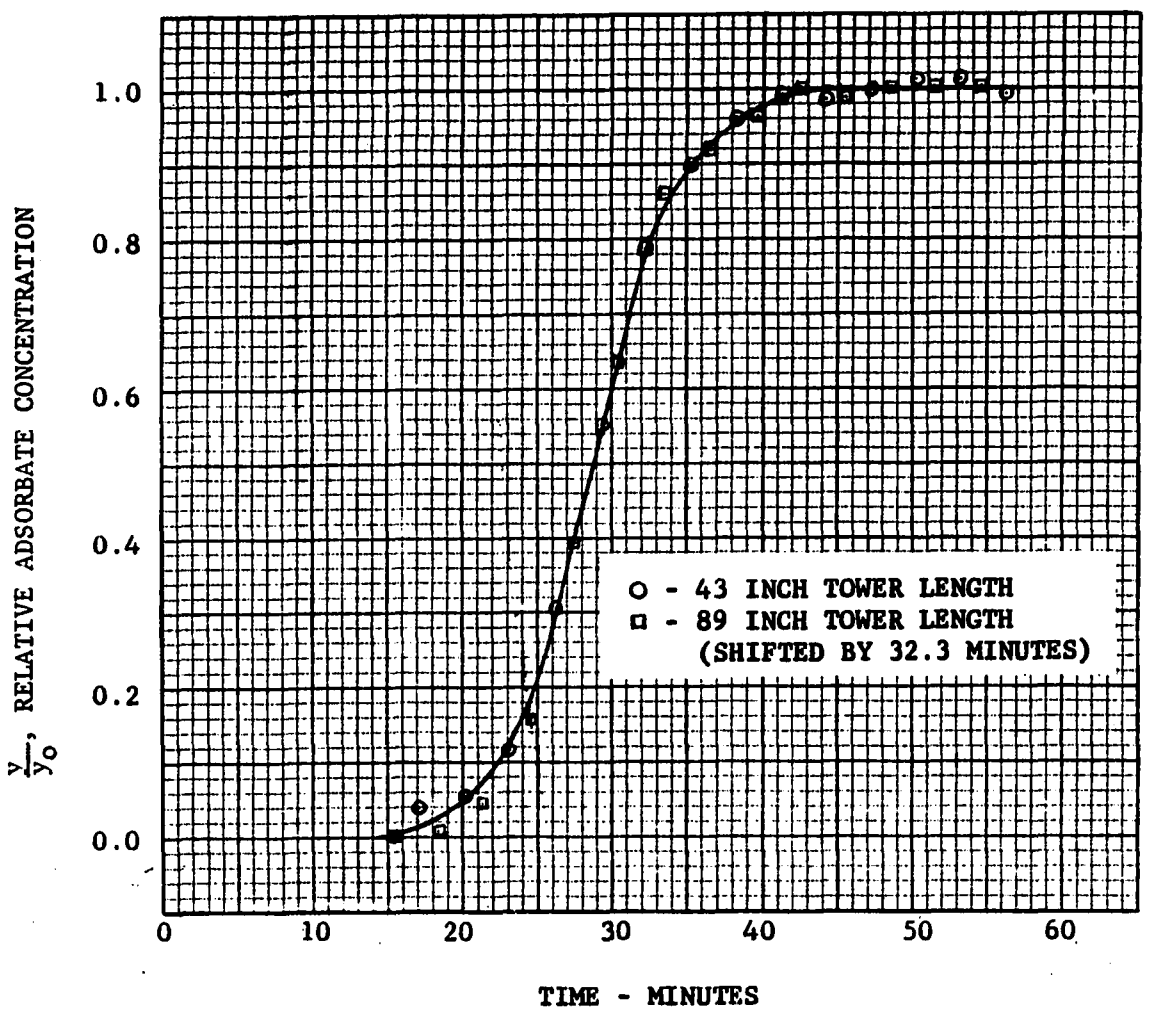

FIGURE 7.--EXAMPLE OF HEXANE ZONE STABILIZATION

Michaels (16) has shown that stabilized zones also form in the related mass transfer operation of ion exchange.

Observations on Heat Effects During Adsorption

It has long been recognized that considerable heat is liberated as a result of gas adsorption. In static systems this results in an associated rise in temperature. Wicke (30,31,32) has measured this temperature rise for the adsorption of carbon dioxide upon carbon and silica gel.

Sanlaville (33) measured temperature rises in excess of 100°C for the dynamic adsorption of water vapor on activated alumina. By assuming that the mass transfer was instantaneous and considering the rate of heat transfer, the outlet composition and temperature were calculated and compared to experimental results. The comparison showed fair agreement.

Recently, Getty (34) has presented the effect of heat generation from adsorption upon the mass transfer zone in water adsorption on molecular sieves. Of particular interest is the development of a secondary mass transfer zone as a result of the cooling of the adsorbent after the first adsorption zone has passed. The temperature rise was on the order of 120°F, which is many times greater than for hydrocarbon adsorption on silica gel. A similar type of phenomenon has been reported by Leavitt (35) for adsorption of carbon dioxide on molecular sieves.

The available information on the heat effects during the dynamic adsorption of hydrocarbons on silica gel shows that the resulting temperature rise can be considerable when the gas composition is high.(9)

Figures 8 and 9 show the results of measurements of gas temperatures at various positions in a desiccant bed.

This chapter has presented a review of mathematical developments and experimental investigations necessary for an understanding of hydrocarbon adsorption on silica gel. It can be seen from this review that no attempt has been made to analyze hydrocarbon adsorption on silica gel with respect to the mass transfer mechanism or to determine which of the numerous mathematical developments is most applicable.

The primary objective of this current investigation is to establish the mass transfer mechanism and provide concrete guide lines for future mathematical developments. A second part of this objective is to present, mainly for design purposes, a method of calculating the dynamic adsorption behavior of pentane on silica gel.

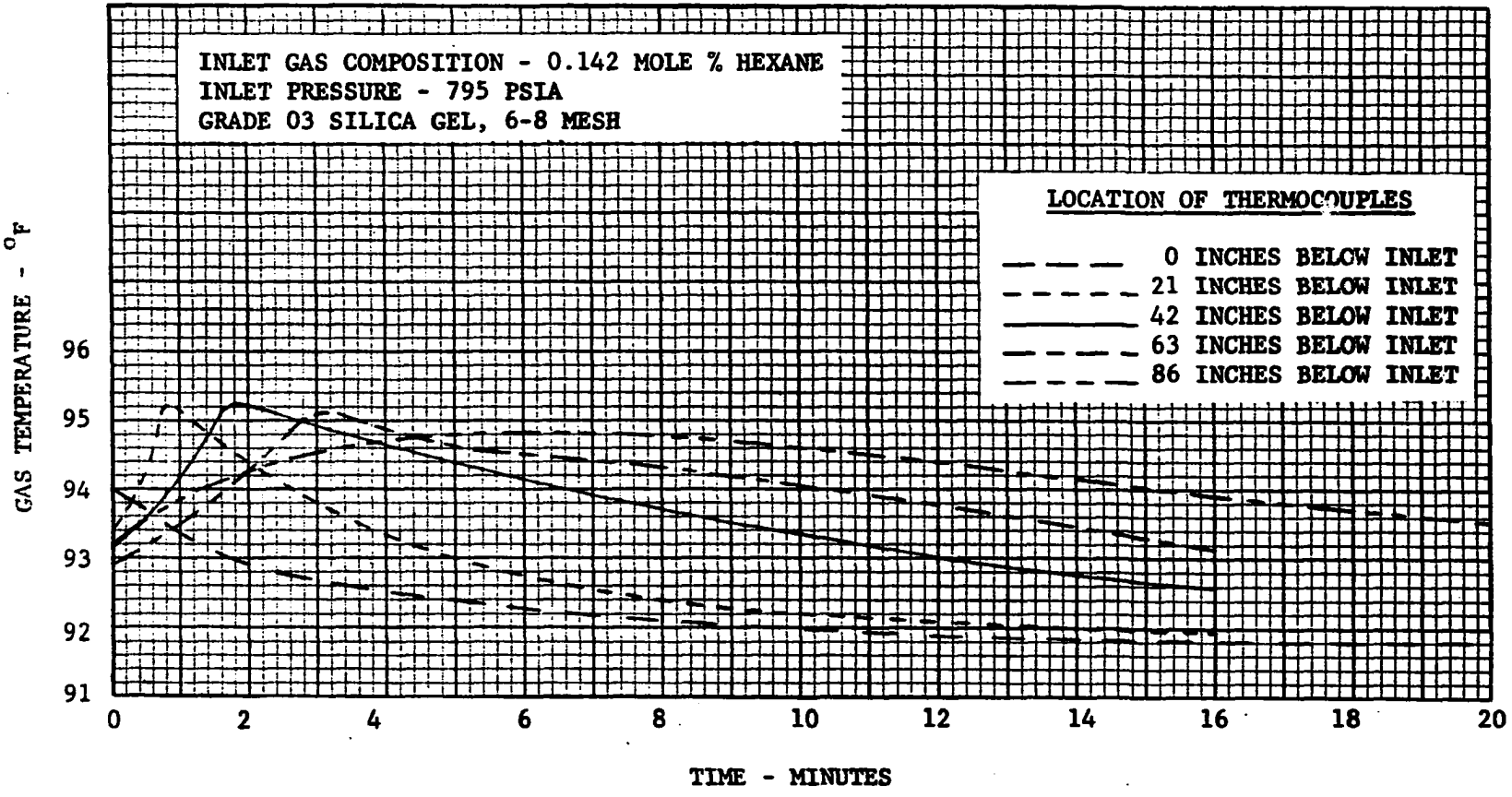

FIGURE 8.--GAS TEMPERATURE AT VARIOUS POINTS IN THE TOWER vs. TIME

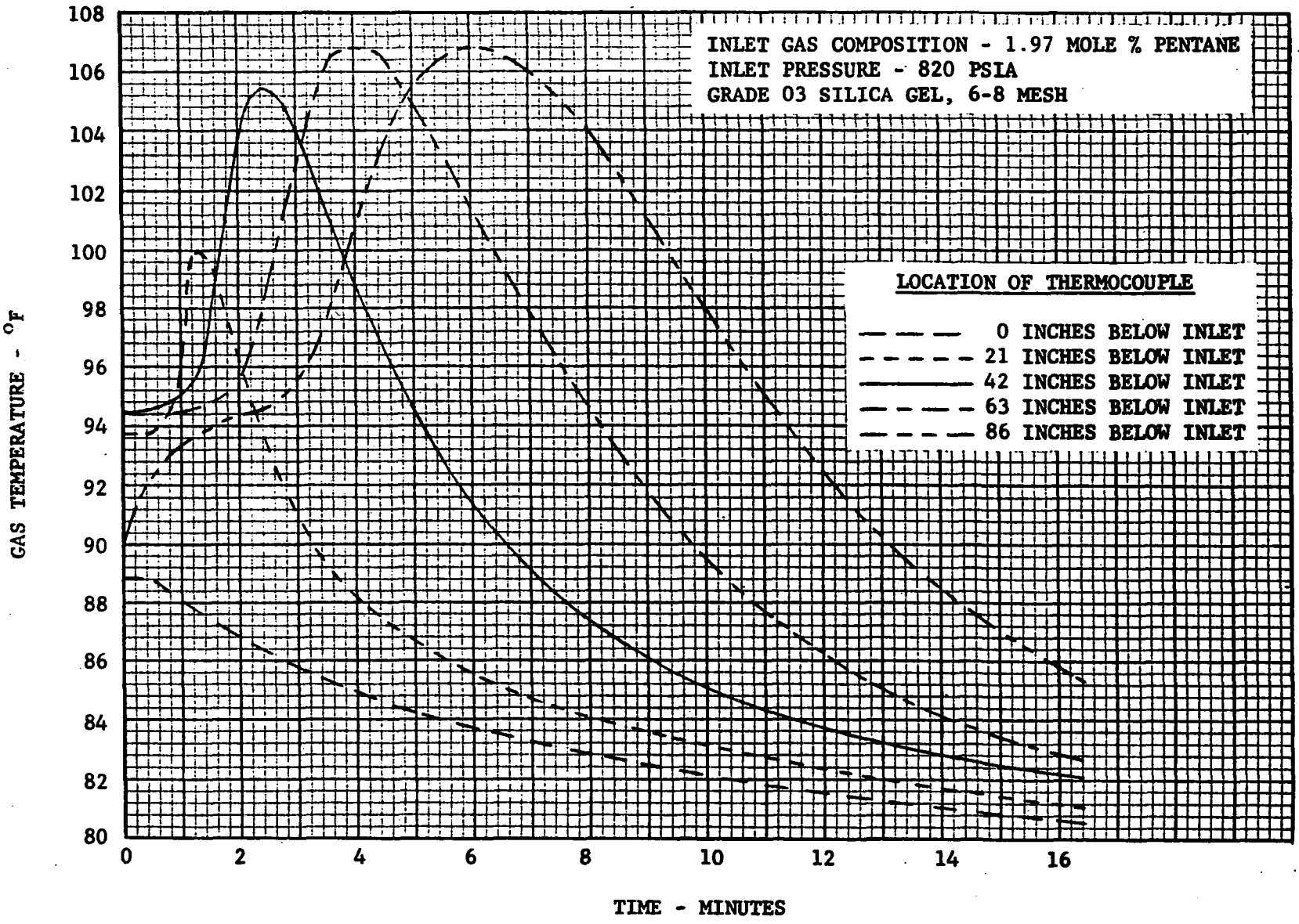

FIGURE 9.--GAS TEMPERATURE AT VARIOUS POINTS IN THE TOWER vs. TIME

CHAPTER III

EXPERIMENTAL APPARATUS AND PROCEDURES

The laboratory equipment was designed to reproduce, as nearly as possible on a small scale, current field operating practices. Figure 10 is a simplified flow sheet of this laboratory installation.(36)

Description of Equipment

The description and function of the equipment can best be accomplished by following the gas flow in Figure 10 through an adsorption cycle and a regeneration cycle.

The Adsorption Cycle

The natural gas is supplied to the laboratory at 100 psig from the Oklahoma Natural Gas Company line serving the city of Norman, Oklahoma. The gas from this supply enters a spherical separator where any entrained liquid is removed. Pressure regulator no. 1 reduces the inlet gas pressure in order to control the capacity of the compressor. The compressor was built by Chicago Pneumatic Tool Company and is capable of a natural gas delivery of 1200 psi and 15,000 S.C.F. per hour. This C.P. compressor is driven by a 60 h.p., 440 v, 3 phase, electric motor. To facilitate gas flow rate control the compressor is equipped with both clearance bottles and valves.

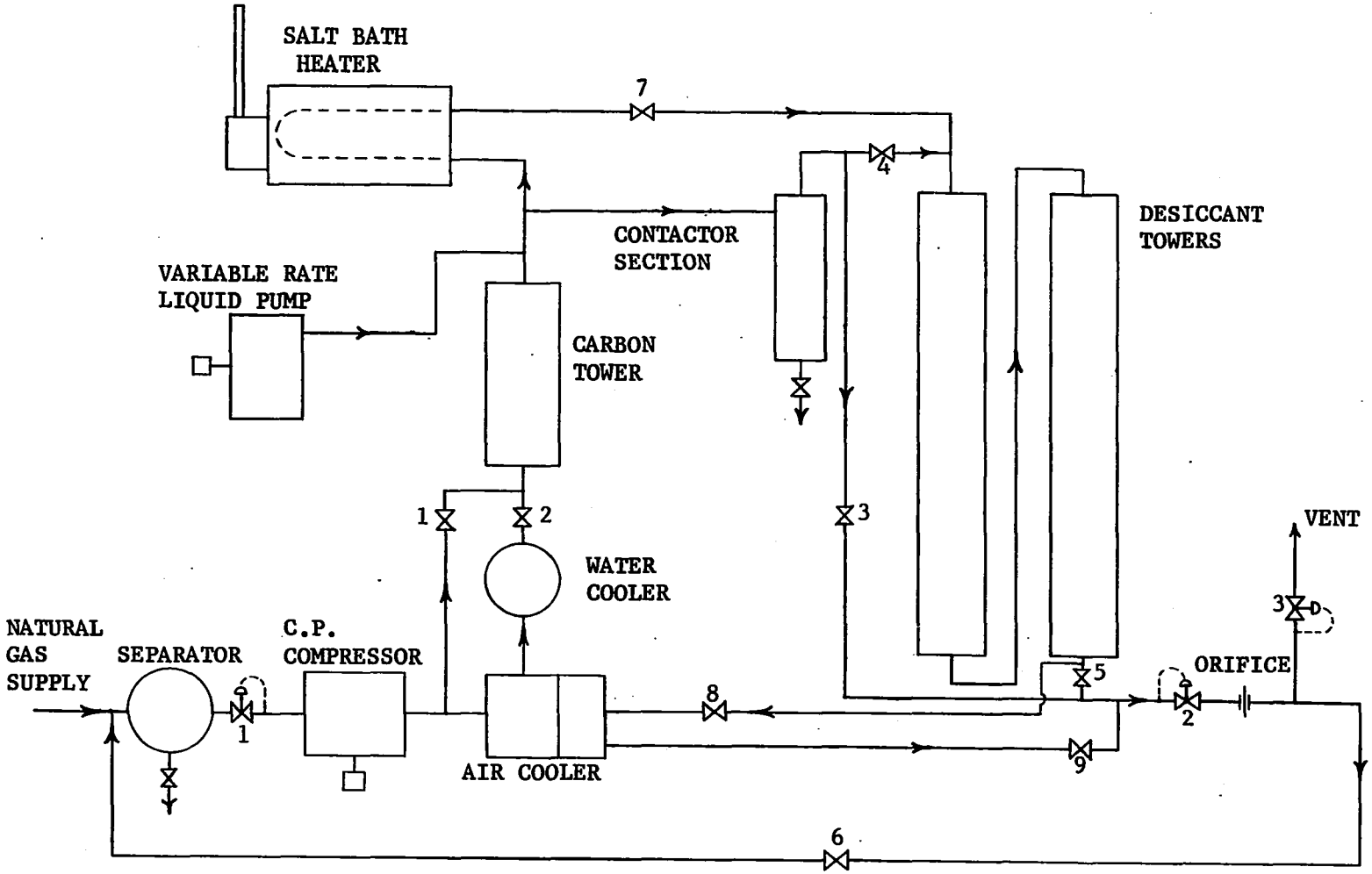

FIGURE 10.--SIMPLIFIED FLOW SHEET OF LABORATORY INSTALLATION

After being compressed to the desired pressure, the gas stream is then split. One part passes through two coolers in series. The first cooler is a twin coil Happy air cooler. The second cooler is a Brown Fintube double pipe heat exchanger with water supplied to the tube side from a cooling tower. The first part and second part of the split stream are recombined after passing through valves 2 and 1 respectively. The gas temperature is regulated by adjusting these two valves.

The gas is next passed through a bed of activated carbon to remove any heavy hydrocarbons, particularly lubricating oil from the compressor. After contacting the activated carbon the natural gas consists primarily of methane and ethane.

In order to obtain the desired natural gas composition for the adsorption tests, known amounts of liquid hydrocarbons are injected into the gas stream. This injection is controlled by a variable stroke Wallace and Tiernan triplex pump coupled to an electric motor through a variable speed drive. The amounts of hydrocarbons injected are weighed to keep a constant check on the operation of the liquid pump. The injection line from the liquid pump is steam traced to increase the vaporization rate. To further promote vaporization and mixing, the gas is then passed through a contactor section. This section is filled with steel wool and contains a liquid trap so that the operator is quickly aware of incomplete liquid vaporization.

Until the proper gas composition is obtained the gas is bypassed around the desiccant towers through valve 3. During the adsorption cycle valve 3 is closed and valves 4 and 5 are opened to direct the gas through the desiccant towers.

In this investigation two towers were used. The tower used for runs 1 through 61 was a four inch diameter tower. Whereas, the tower designed especially for run 62 was two inches in diameter. The details of the design of these towers are included in a later section.

The system pressure is maintained at the desired level (800 psia for this investigation) by pressure regulator 2. The gas flow rate is continuously measured by an orifice and manometer combination. The pressure in this section of the system is regulated (about 125 psia for this investigation) by pressure regulator 3. The used gas is then vented.

The Regeneration Cycle

In the regeneration cycle valves 1, 2, 7, 8 and 9 are open. Valves 3, 4, 5, and 6 are closed. In this operation the only new piece of equipment used is the salt bath heater which elevates the gas temperature to about 525^{o}F.

Provisions have also been made to regenerate the carbon towers as needed. After prolonged operation the carbon towers are dumped and recharged with new activated carbon. This keeps the desiccant tower from being contaminated by compressor oil.

The Desiccant Towers

Two types of towers were used in this investigation. The first tower (tower no. 4) was used in runs 1 through 61. The second tower (tower no. 5) was used for run 62.

Tower no. 4 was constructed in two identical parts. The body of each part was a 7 foot length of 4" schedule 80 seamless pipe. On the

lower end was welded a 4" x 1/2" swage nipple. The top end was welded to a 4" hammer union which in turn was welded to another 4" x 1/2" swage nipple. The lower swage nipple contained a small mesh screen to support the desiccant. Five thermocouple wells were inserted at various positions along the length of each part of the tower. Figure 11 shows the location of these wells. The tower was then externally insulated to reduce heat losses during regeneration.

Tower no. 5 was constructed from a 7 foot, thin wall (0.022 inch), 2 inch diameter, stainless steel tube. A 4" schedule 80 seamless pipe was fitted concentrically around the 2" tube to act as a pressure vessel. The lower ends of both the pressure vessel and the tube were connected to a flange. The upper end of the pressure vessel was welded to a 4" hammer union which was welded to a 4" x 1/2" swage nipple. The upper end of the stainless tube was free so that the system pressure can equalize on the outside and inside of the tube. The outside of the stainless tube was insulated to reduce heat losses during adsorption and regeneration. Eleven thermocouples and two gas sampling tubes were positioned in the tube. Figure 12 shows their location.

Five of the thermocouples were placed inside five desiccant particles by drilling a 3/128 inch hole into the center of each particle. Five more of the thermocouples were left bare, but shielded from the desiccant particles. The shields were made of a white insulating silicone rubber and were perforated to permit easy gas flow around the thermocouples. One thermocouple was inserted in a 1/8 inch O.D. stainless tube and placed into the top of the tower to measure the inlet gas temperature.

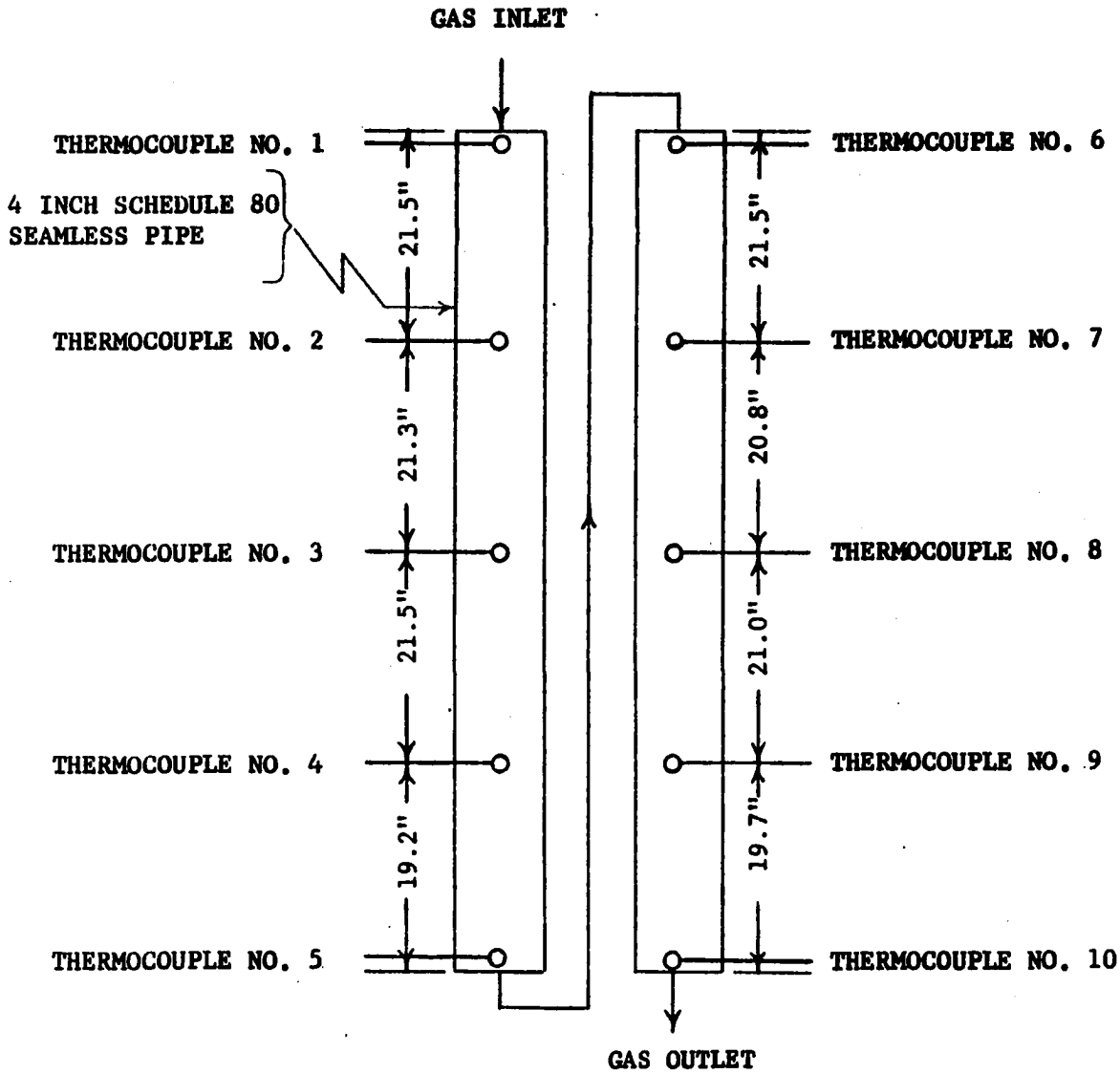

FIGURE 11.--THERMOCOUPLE LOCATION IN TOWER NO. 4

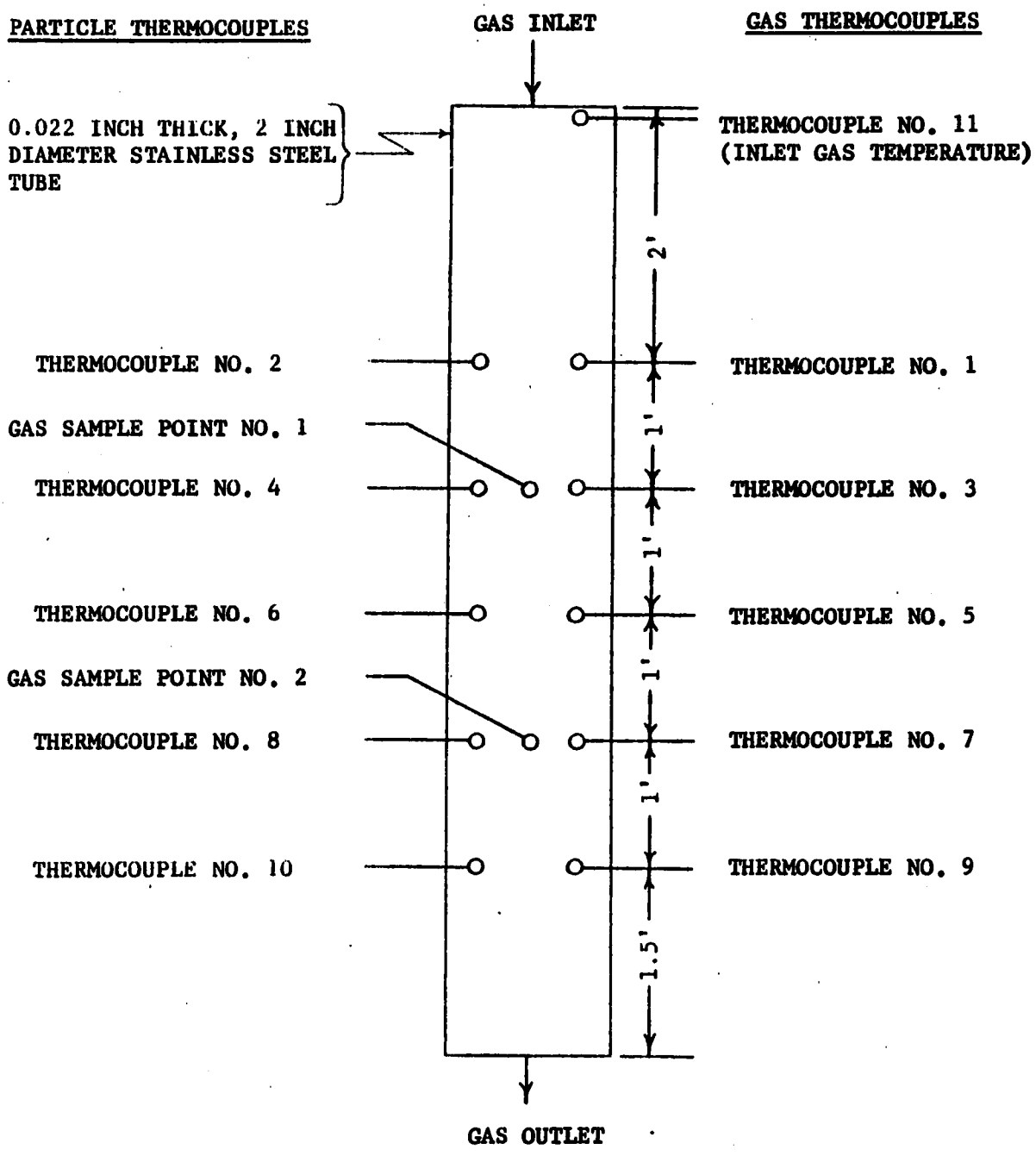

FIGURE 12.--THERMOCOUPLE AND GAS SAMPLE LOCATIONS IN TOWER NO. 5

The ten thermocouples and two gas sampling tubes were led down the annulus between the pressure vessel and the stainless tube and through the bottom flange to a temperature recorder and a process gas chromatograph, respectively.

The Gas Sampling and Temperature Recording Systems

In the runs taken on tower no. 4, gas samples could be taken from both the tower bypass line and the tower exit. These samples decrease in pressure then flow through a 1/8" O.D. steam traced copper tube to a chromatograph analyzer and a gravitometer. A continuous gas vent was maintained to provide a fresh sample at the analyzer at all times. The chromatograph used in this investigation was a Consolidated Electrodynamics Corporation Model 26-212 Process Chromatograph. This chromatograph automatically sampled and analyzed the desired gas stream every two or three minutes as programed. The results of the analysis were recorded on a Honeywell Recorder.

In the run taken on tower no. 5, gas samples could be taken from the tower bypass line and the two sample points inside the tower.

In all runs, gas samples were also taken from the tower exit and the specific gravity continuously determined by a Kimray Gravitometer. This specific gravity determination was used in the flow rate calculations.

Both the thermocouples used in tower no. 4 and those used in tower no. 5 were connected to a 12 point Honeywell Temperature Recorder. Two temperature ranges were provided, a 0-600^{o}F for regeneration and a 0-150^{o}F for the adsorption cycle.

Experimental Procedure

The experimental procedures employed on tower no. 4 and tower no. 5 were the same. Before each run, the desiccant in the tower was regenerated to an exit temperature between 450 and 475°F. During regeneration, valves 1, 2, 7, 8, and 9, as shown in Figure 10, are open. All other valves are closed. Pressure regulator 1 and the compressor clearances were regulated to the desired flow rate. The system pressure was set at about 800 psi by adjusting pressure regulator 2.

After the tower exit temperature had been maintained above 450°F for several minutes, valves 4 and 6 were opened and valve 7 closed. This allowed dry lean cool gas to flow through the desiccant bed and the same gas to be continually cycled through the system until the desiccant bed temperature was reduced to the desired level (usually 90°F). The cycling of the gas during the cooling period minimizes the pentane which will be adsorbed from the lean gas.

Near the end of the cooling period gas samples were analyzed at both the tower inlet and exit. When the two samples were the same the gas flow was bypassed around the towers by opening valve 3 and closing valves 4 and 5. In nearly all cases the amount of pentane in the cooling gas stream was negligibly small; however, the value determined from the analysis was recorded and used to calculate the amount of adsorption during cooling.

With the cooling completed, the gas flow rate and pressure was adjusted, as required, by pressure regulators 1 and 2. Then valve 6 was closed so that the gas was continuously vented. At this time the feed tank for the liquid pump was filled with pentane and weighed. Next the

liquid pump stroke and variable speed drive were adjusted to obtain the desired pentane enrichment in the natural gas stream. At this point the chromatograph was set to analyze the tower bypass stream, the liquid pump was started, and the temperature recorder set on the 0-150^{o}F temperature range. When the chromatograph indicated that the gas composition of the bypass stream had been stabilized, valves 4 and 5 were opened, valve 3 was closed, and the chromatograph samples were taken from the tower exit. This started the adsorption cycle.

Throughout the adsorption cycle the system pressure, flow rate, gas composition exit the tower, gas specific gravity exit the tower, and temperatures from thermocouples located in the tower were recorded. The temperatures were recorded every 24 seconds. The gas composition exit the tower was analyzed by the chromatograph every 2 or 3 minutes depending upon the run.

The adsorption cycle was terminated when the pentane composition in the gas stream exit the tower remained constant at about the tower inlet pentane composition for a considerable time. After the adsorption cycle is finished, the feed tank for the liquid pump is weighed to determine the amount and rate of pentane injection into the lean gas stream. This ended the run.

Before the next run was started the composition of the gas exit the carbon tower was analyzed and the carbon tower regenerated and cooled if necessary.

After the desired amount of data was collected on the desiccant in the tower, the gel was regenerated, removed from the tower, and weighed.

CHAPTER IV

PRESENTATION AND DISCUSSION OF RESULTS

Two types of data were obtained with the equipment and experimental procedures described in Chapter III. The first of these was the concentration breakout curve for the dynamic adsorption of pentane on silica gel.

The Dynamic Adsorption Concentration Data

The breakout concentration curves for the dynamic adsorption of normal pentane on silica gel were obtained by varying superficial velocity, inlet adsorbate concentration, adsorbent particle size, tower length, and temperature. Tables 2 and 3 show the range of each of the above variables investigated. Detailed information on each of the 61 runs is included in the Appendix. An example of the information obtained from the chromatographic analysis of the effluent gas stream from the desiccant bed is given in Figure 13. From such a curve the mass transfer constant and dynamic equilibrium capacity were obtained for each run.

The Mass Transfer Constant

Determination of the Mass Transfer Constant

The mass transfer constant (k) was determined by fitting the experimental breakout curve to the Klinkenberg solution and to the numerical solutions of Rosen. The following procedure was used:

TABLE 2

RANGE OF VELOCITY AND ADSORBATE CONCENTRATION INVESTIGATED

Superficial Gas Velocity ft/min.	Inlet Adsorbate Concentration in the Gas Phase in Mole Per Cent Pentane							
	.05	.10	.20	.40	.80	1.20	2.00	3.00
10	x	o x	o & + *	o x x	o x o	o x	o x +	o
20	o	o x +	o x	o x o	x	x	o x #	
30	o	o x +	o x	x	x	x	o x #	
40	o x +	o x *	o x	o x	o x	o x	o x	

TABLE 3

RANGE OF OTHER VARIABLES INVESTIGATED

Symbol	Bed Length Feet	Inlet gas and Initial Bed Temperature - ^{o}F	Tyler Mesh Size	Bed Diameter Inches
o	13.96	90	3-4	3.826
+	7.00	90	3-4	3.826
x	13.82	90	6-8	3.826
&	13.82	115	6-8	3.826
#	6.83	90	6-8	3.826
*	6.90	90	6-8	3.826

Note:

All data are for an adsorption pressure of 800 psia, silica gel (750-800 m^2/gm surface area, .43 cc/gm pore volume, 21 angstrom average pore diameter).

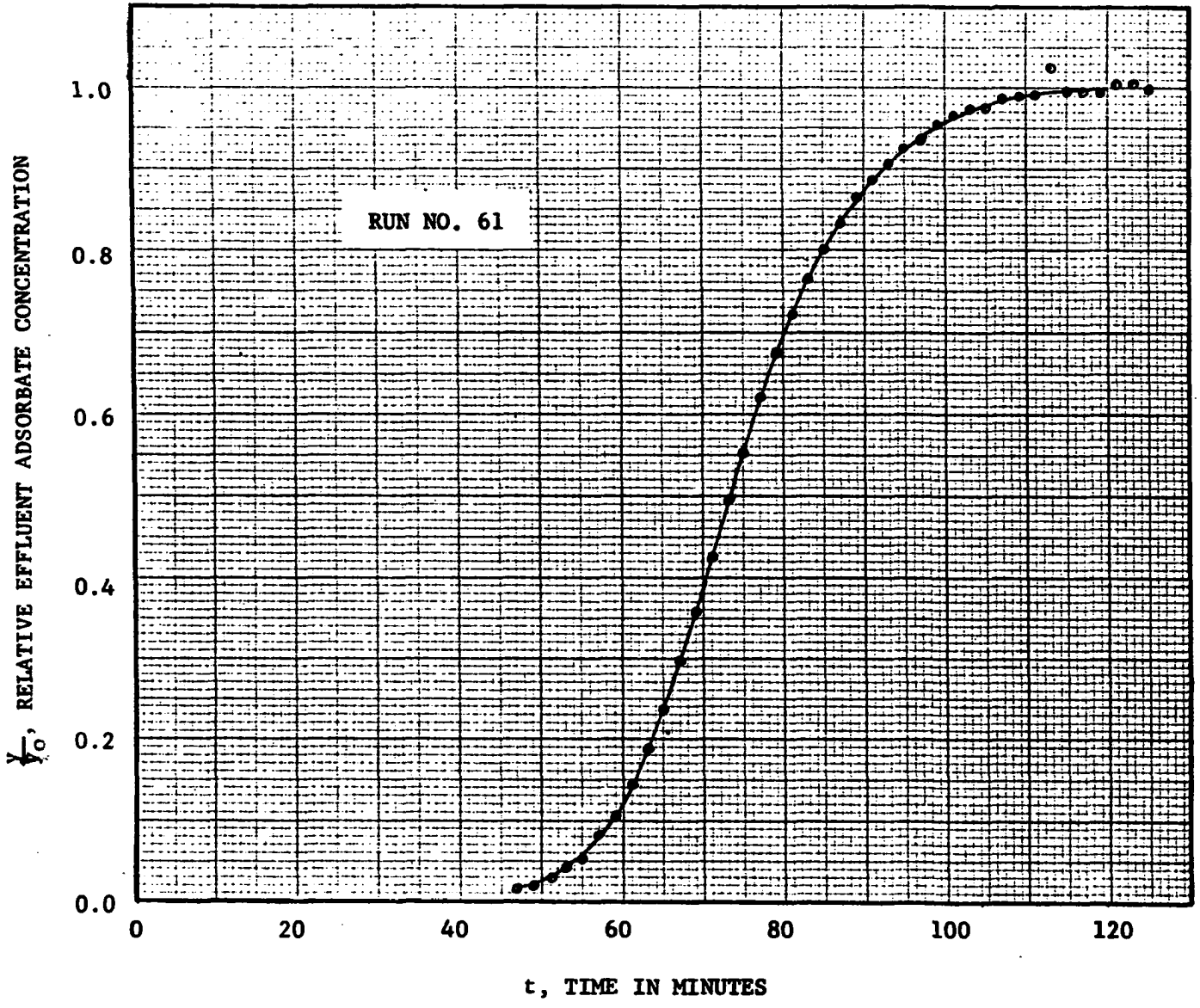

FIGURE 13.--EXAMPLE OF RESULTS OF CHROMATOGRAPHIC ANALYSIS

1. From the chromatographic analysis of the effluent gas from the desiccant bed, a curve similar to Figure 13 was constructed for each run.

2. A smooth curve was drawn through the data points and the values of time were picked off for $\frac{y}{y_o} = 0.8$ and $\frac{y}{y_o} = 0.2$. These values were termed $t_{.8}$ and $t_{.2}$ respectively.

3. Next the breakout curve was integrated by the Trapezoidal rule to obtain Dz. This integral is:

$$\int_{t_{.05}}^{t_{.95}} \left[1 - \frac{y}{y_o}\right] \, dt = Dz$$

4. Utilizing the terms and definitions previously presented, it can be seen that:

$$\frac{t_{.8} - t_{.2}}{Dz} = \frac{T_{.8} - T_{.2}}{X}$$

In this way it is possible to obtain the ratio $\frac{T}{X}$, although neither T nor X is known at this point.

5. Figure 14 was used to determine X from the known value $\frac{t_{.8} - t_{.2}}{Dz}$. Figure 14 was constructed from the numerical solutions of Rosen and from Equation 8, which is the Klinkenberg solution.

6. When X is known then the value of k can be determined from:

$$X = kDz$$

7. The mass transfer constant was calculated for both the Klinkenberg "fit" and the Rosen "fit". Although it is evident from the small deviations between the two curves in Figure 14 that the difference is small when the value of X is above 5.

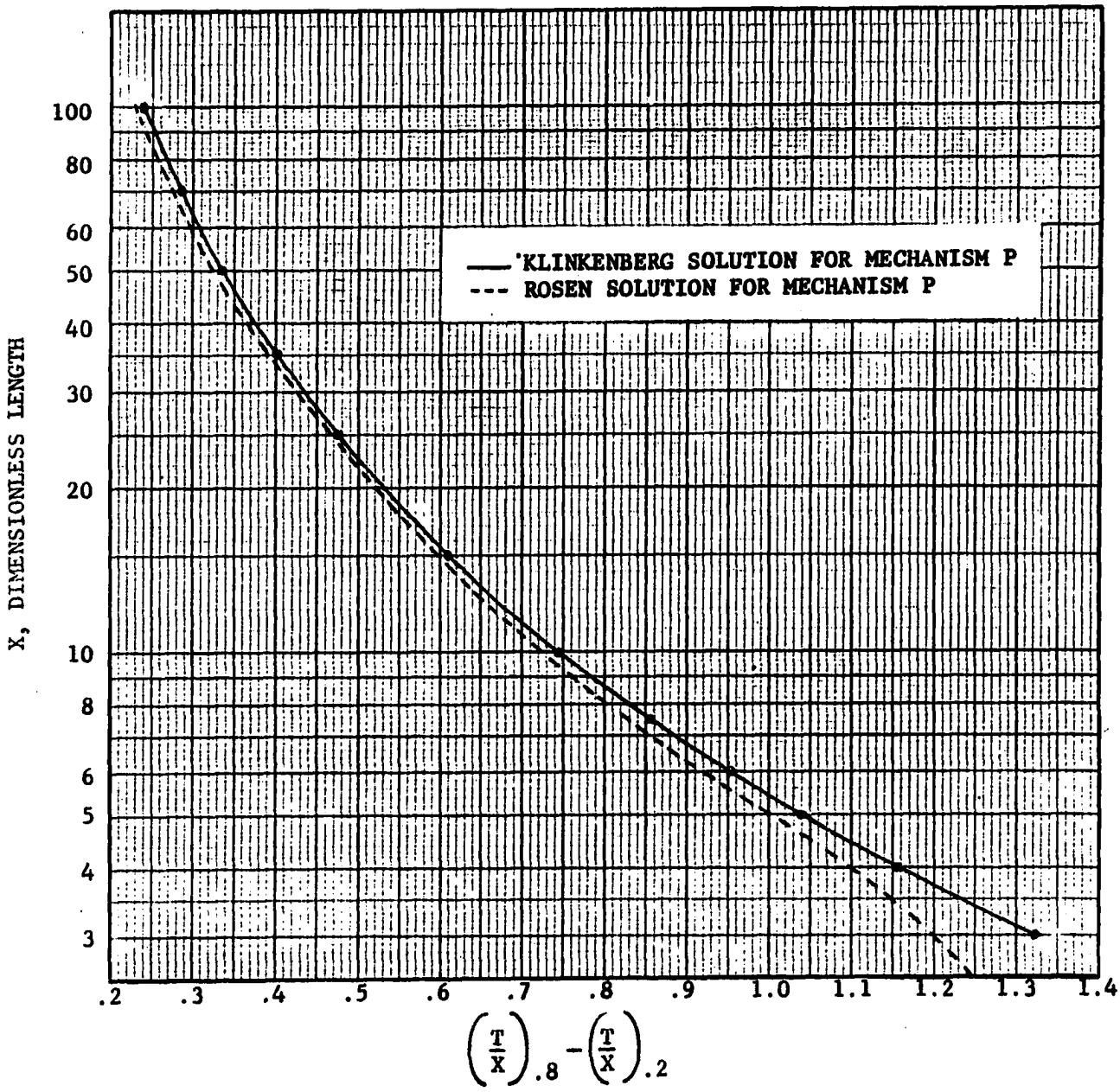

FIGURE 14.--DETERMINATION OF DIMENSIONLESS LENGTH

This procedure was found to be rapid, yet produces a satisfactory fit to the entire breakout curve as can be seen from Figure 15. Some of the curves were not reproduced as well as those in Figure 15; however, these were picked at random and others can be easily checked by using the information in the Appendix.

Dependence of the Mass Transfer Constant upon Velocity

Figures 16 and 17 show the variation of the mass transfer constant with velocity for both the 6-8 mesh gel and the 3-4 mesh gel. Figure 16 was determined from the Klinkenberg solution and Figure 17 from the Rosen solution. It can be seen that the scatter is appreciable for the 3-4 mesh gel; whereas, the data for the 6-8 mesh gel correlate well. The scatter in the 3-4 mesh data may have been caused by irregular bed packing resulting from the large angular particles used. A comparison of Figures 16 and 17 shows that the k determined from the Klinkenberg equation is consistently slightly larger than the corresponding k from the Rosen solutions.

The only significant trend with velocity was obtained with 6-8 mesh gel below a concentration of 0.5 mole per cent pentane. The mass transfer constant deviates only for the data where the superficial velocity is 10 feet per minute. This deviation cannot be accounted for by a simple combination mechanism. The influence of the velocity dependent part of the combination mechanism would increase with concentration instead of diminish. The apparent deviation in the data for a superficial velocity of 10 feet per minute probably results from the comparatively higher temperature exhibited by these runs, coupled with a possible PG mechanism.

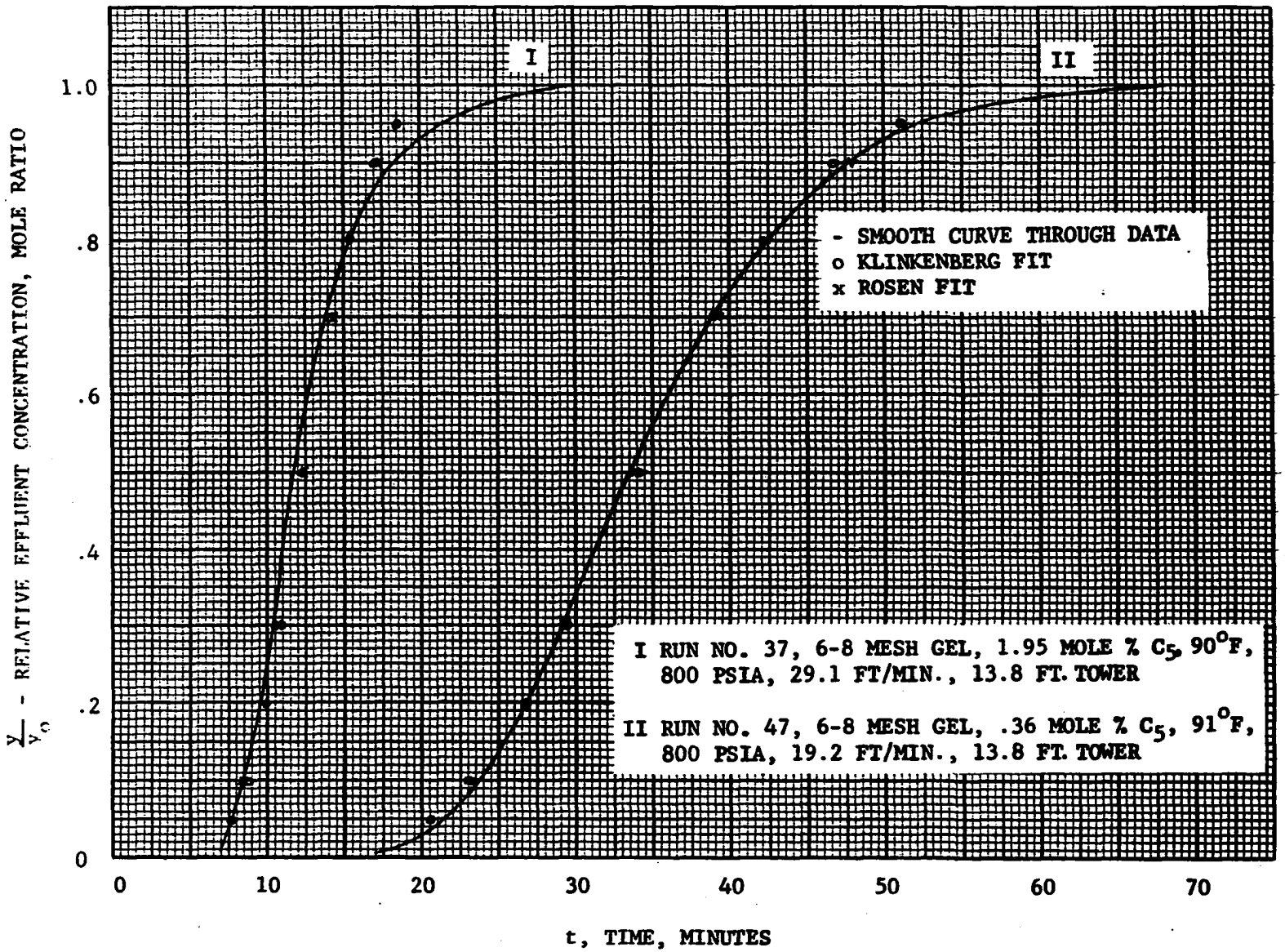

FIGURE 15.--CURVE FITS OF ROSEN AND KLINKENBERG SOLUTIONS

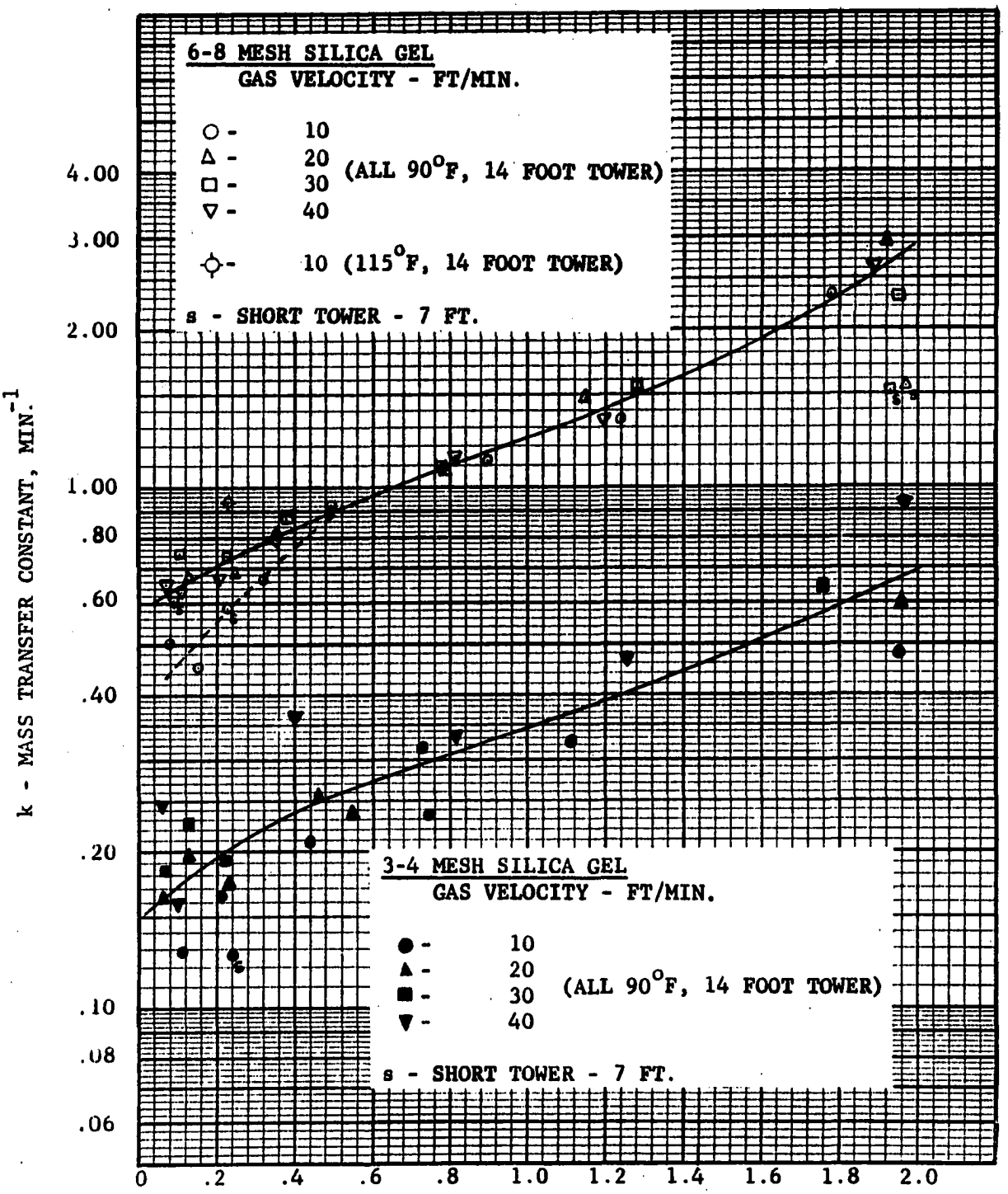

FIGURE 16.--KLINKENBERG DETERMINED MASS TRANSFER CONSTANT

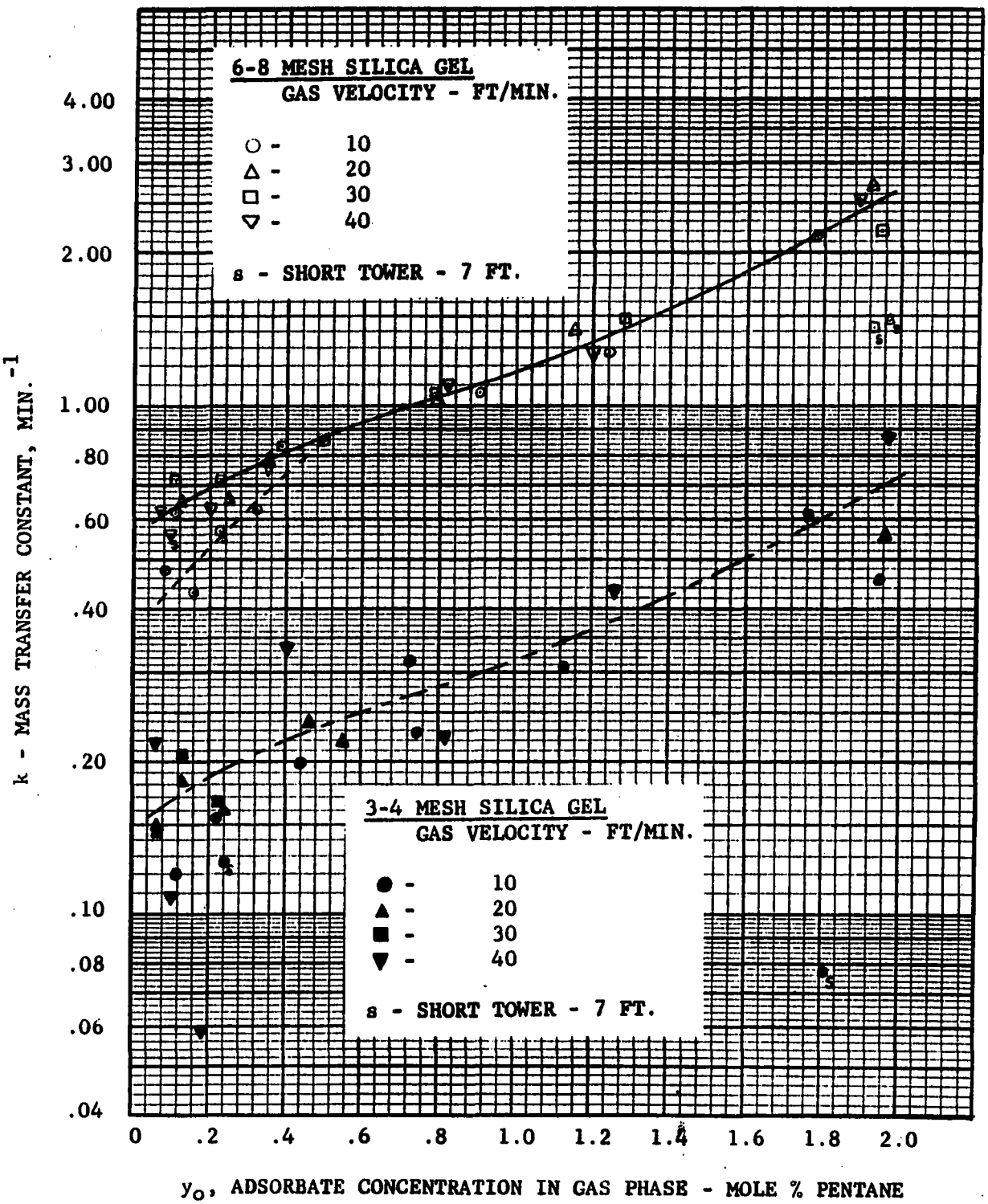

FIGURE 17.--ROSEN DETERMINED MASS TRANSFER CONSTANT

It is more significant that the mass transfer constant in general is not a function of velocity. This is one of many facts which indicate that the particle diffusion mechanism (P) is rate controlling for the adsorption of pentane on silica gel.

Dependence of the Mass Transfer Constant upon Adsorbent Particle Size

The dependence of the mass transfer constant upon the adsorbent particle size is greater than for any other variable investigated. This dependence is shown in Figure 16 and can be represented as:

$$k = \frac{\lambda_3}{d_p^{1.88}}$$

where:

λ_3 is a function dependent upon the other adsorption parameters such as length, velocity, etc.

For spherical particles where mechanism P is controlling, the exponent on d_p should theoretically be 2. For systems where the mass transfer is controlled by the G mechanism, the exponent on d_p has been found to be 1.51.(10) The value of 1.88 determined for the data presented in Figure 16 is another indication that the controlling mechanism is particle diffusion. The deviation of the exponent from 2 might be due to particle shape.

Dependence of the Mass Transfer Constant upon Desiccant Bed Length

At concentrations below 0.3 mole per cent pentane, the effect of bed length is negligible. At high concentrations, about 2 mole per cent pentane, the effect is large and the resulting mass transfer is lower for the shorter bed. This is probably due to the second type of temperature effect discussed in the next section.

Dependence of the Mass Transfer Constant upon Temperature

There are two types of temperature phenomena which are of major importance. The first is the variation of the mass transfer constant with temperature when the adsorption process is essentially isothermal. Most of the data were obtained where the inlet gas and initial bed temperature were 90°F. Although one run was performed where this temperature was 115°F. A comparison of this run to the corresponding runs at 90°F shows that the mass transfer constant increased from 0.58 min^{-1} at 90°F to 0.94 min^{-1} at 115°F. The magnitude of this variation has some important implications. All of the general correlations to date have attempted to account for the temperature variation of the mass transfer constant through the gaseous diffusivity only. In the range of temperature and pressure used in these experiments (90-115°F and 800 psia), the variation in the gaseous diffusivity is less than 5 per cent for a 25°F change in temperature.(37) Thus it is apparent that the gaseous diffusivity does not adequately explain the temperature variation in this data. Furthermore, it is a known fact that the diffusion coefficient for activated pore diffusion of normal butane through silica varies exponentially with temperature.(38) This is another indication that the particle diffusion process is controlling mass transfer.

The second temperature effect upon the mass transfer constant is more subtle. This effect is caused by the increase of the temperature of the gas and desiccant due to the release of the heat of adsorption. This effect is essentially negligible at low adsorbate concentrations and increases as the concentration increases. This temperature increase is shown in Figure 18 and causes the calculated mass transfer constant

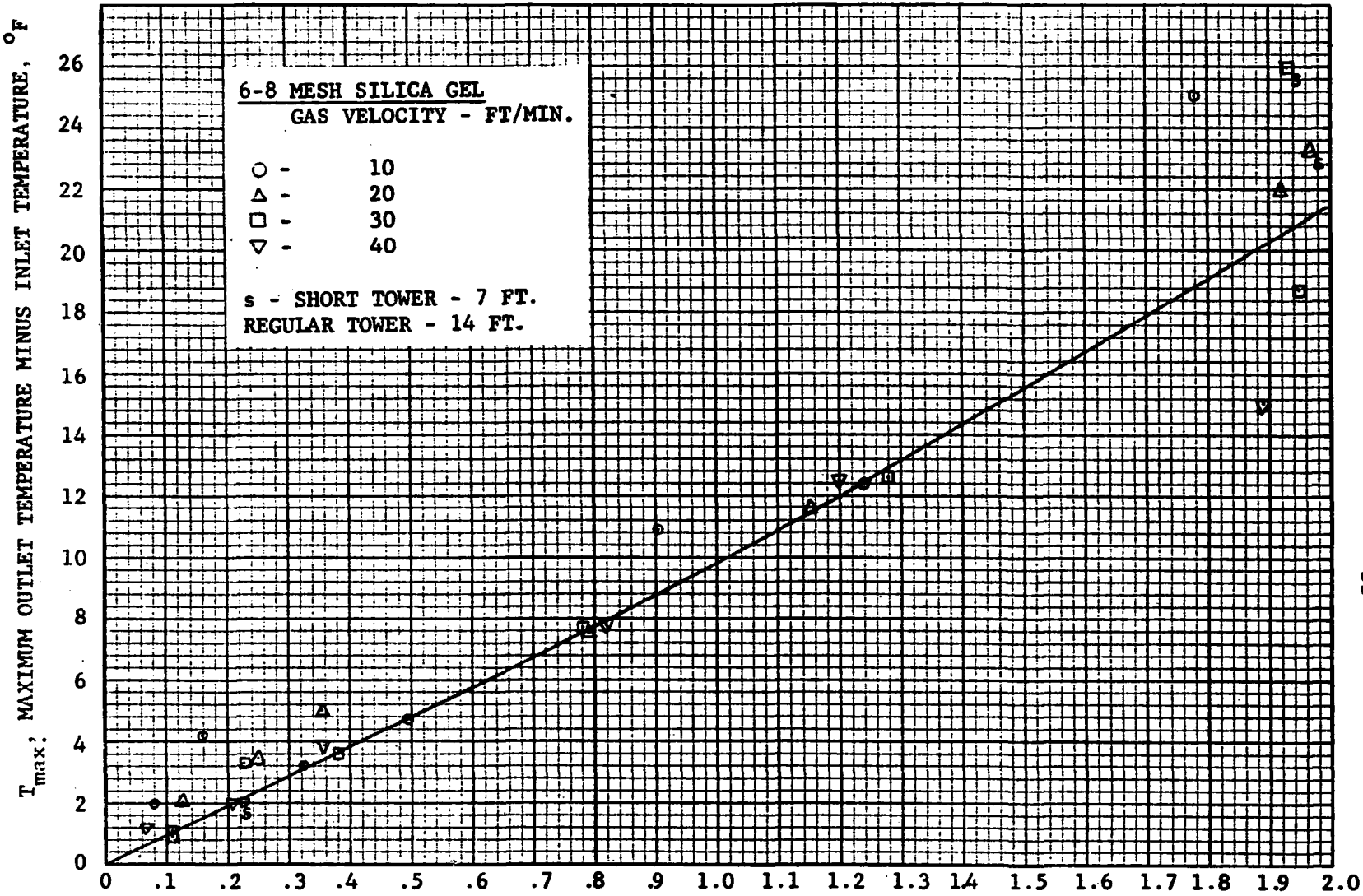

FIGURE 18.--MAXIMUM GAS TEMPERATURE INCREASE THROUGH TOWER

to decrease. This effect is a result of using the Klinkenberg (12,13) and Rosen (15) solutions to calculate the mass transfer constant. Both of these mathematical developments assume that the adsorption process is isothermal. Thus this decrease is erroneous and the mass transfer constants at high concentrations represented in Figures 16 and 17 are too low.

Utilizing the mass transfer constants obtained under isothermal conditions, the above effect was approximated. It was assumed that the first part of the breakout curve reflects the adsorption behavior at the maximum bed temperature attained and that the latter part of the curve represents the adsorption behavior at the temperature attained when adsorption is complete. This is roughly true since the breakout occurs when the outlet temperature reaches a maximum. Figure 19 was calculated for these conditions. Curve I represents the breakout for a temperature of 115°F; whereas, Curve II represents the breakout for 90°F in isothermal operations. In the case where the bed temperature starts at 90°F, increases to 115°F, and decreases again to 90°F, Curve III approximates the behavior by being fit to the $\frac{t_{.8} - t_{.2}}{Dz}$ obtained from Curves I and II. It is apparent that k = 0.941 at 115°F and k = 0.572 at 90°F for isothermal operations. However, if the temperature starts at 90°F, increases to 115°F, then decreases back to 90°F, a fit of the resulting curve yields k = 0.355. It is logical that the actual value of k in this non-isothermal case should be between 0.572 and 0.941. The case chosen for example was an extreme. For a temperature increase of 5°F the calculated k would be about 0.53 compared to 0.57 for 90°F. The data obtained below an adsorbate concentration of 0.6 mole per cent pentane had a maximum temperature variation less than 5°F.

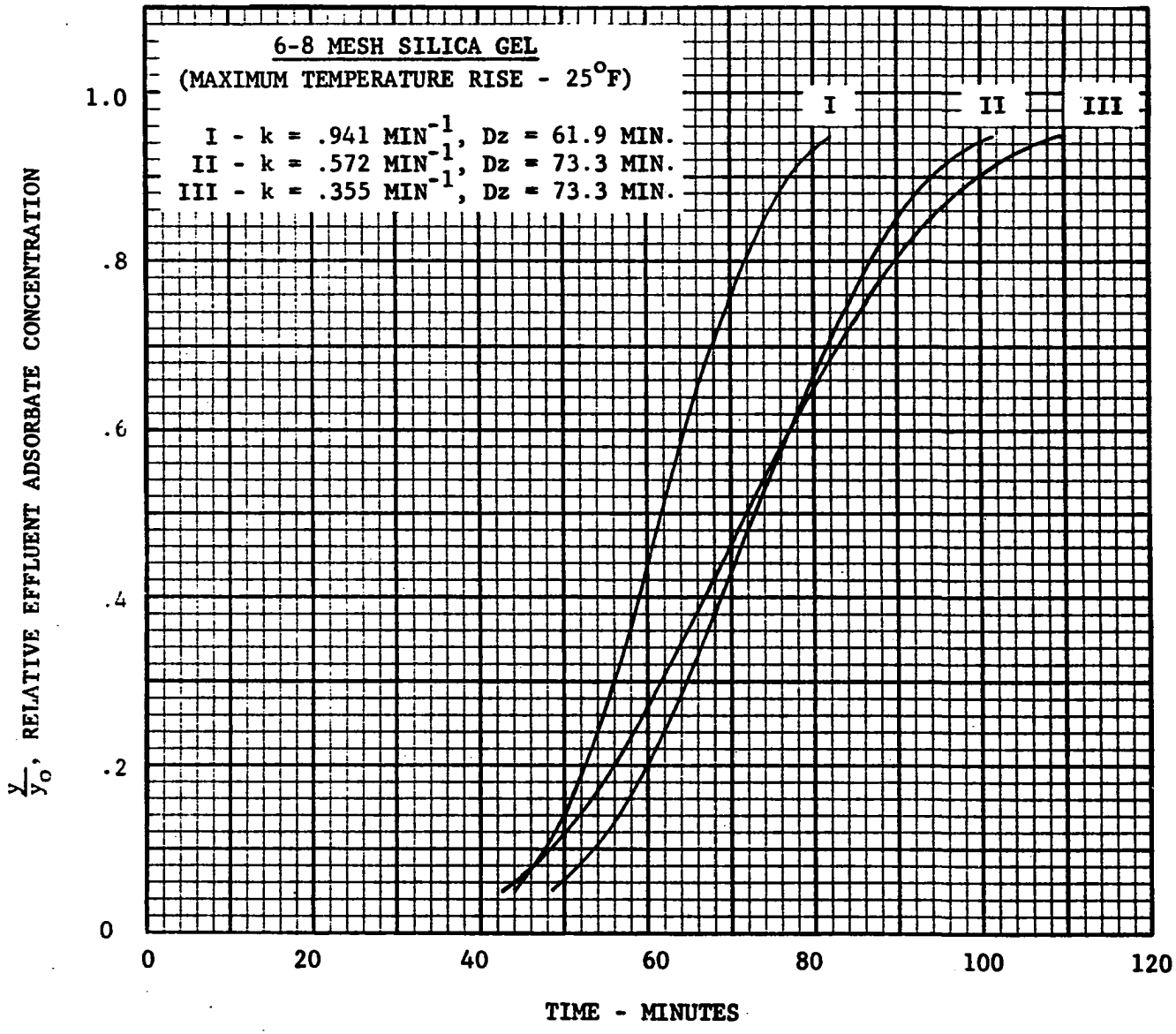

FIGURE 19.--REPRESENTATION OF THE SECOND TEMPERATURE EFFECT

The phenomenon presented above is partly counteracted by the favorable type of isotherm exhibited by pentane on silica gel. Since a favorable type of isotherm tends to sharpen the breakout curve, this result would act so as to decrease the second type of temperature effect. The counteracting of these two effects aids the application of the isothermal dynamic adsorption equations to non-isothermal conditions.

In order to more accurately describe the adsorption behavior at high adsorbate concentrations, both the adsorption and associated heat transfer would need to be considered in the utilized equations.

Dependence of Mass Transfer Constant on Adsorbate Concentration

As pointed out in the previous section, the mass transfer constant calculated by the Klinkenberg (12,13) solution at high adsorbate concentrations is lower than the true value of the mass transfer constant. Even so, there is a significant variation of the mass transfer constant with concentration. In all previous correlations the dependence upon concentration was through the gaseous diffusivity. At the concentrations currently utilized in pentane adsorption the gaseous diffusivity is essentially independent of concentration. Again it has been noted that the diffusion coefficient of normal butane through porous silica increases significantly with increasing surface coverage below an adsorbed monolayer. Figure 20 illustrates this change in the effective diffusion coefficient for butane on porous silica. This dependence of the mass transfer constant upon adsorbate concentration is another indication that the mass transfer is controlled by solid phase diffusion.

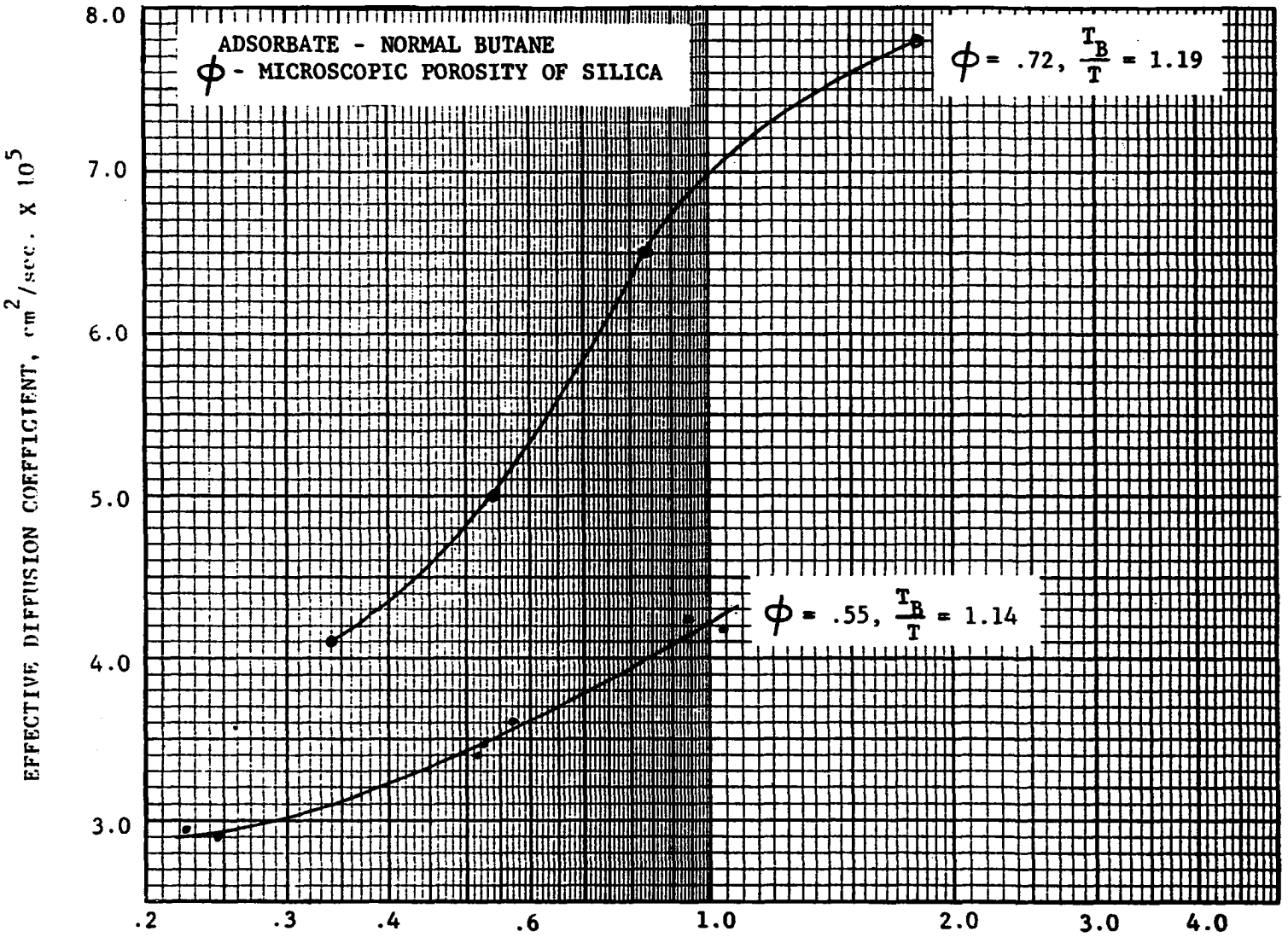

FIGURE 20.--EFFECTIVE DIFFUSION COEFFICIENT DEPENDENCE UPON ADSORBATE CONCENTRATION

Determination of a Diffusion Coefficient from the Mass Transfer Constant

When the mass transfer is controlled by the P mechanism and the film concept is valid, then the mass transfer constant is related to the solid diffusion coefficient by the following:(4)

$$k = k_p = \frac{10\ D_p\ a_v}{d_p}$$

where:

D_p = diffusion coefficient for the particle, $\frac{cm^2}{sec}$.

If the particle is assumed spherical, then:

$$a_v = \frac{6}{d_p}$$

and

$$k_p = \frac{60\ D_p}{d_p^2} \qquad \text{----------21)}$$

The value of the diffusion coefficient will be calculated in the range of a monolayer so that it can be compared to values reported in the literature. A monolayer forms for the silica gel used around an adsorbate concentration of 2 mole per cent pentane. In this region Figure 16 shows that $2.3\ min^{-1} < k < 3.0\ min^{-1}$ for the 6-8 mesh gel. Using the particle diameter of the 6-8 mesh gel as 0.2845 centimeters, the diffusion coefficient has the following value:

$$5.17 \times 10^{-5}\ \frac{cm^2}{sec} < D_p < 6.74 \times 10^{-5}\ \frac{cm^2}{sec} .$$

Carman (39) has shown that for a particular adsorbent, the diffusion coefficients of a wide range of materials correspond for a monolayer adsorbed, where the adsorbate is near its boiling point. In his work the

surface diffusion coefficient for butane on silica gel (microscopic porosity = 0.52) is given for a monolayer at $\frac{T_B}{T} = 1.04$ as $4.8 \times 10^{-5} \frac{cm^2}{sec}$. At 90°F the $\frac{T_B}{T}$ for pentane is 1.01. From this information it can be seen that the diffusion coefficient determined from the mass transfer constant agrees with the value expected from the surface diffusion of butane through silica gel. Again this indicates that the mass transfer is controlled by diffusion through the adsorbent particle.

The diffusion coefficient for the diffusion of hydrocarbons through silica consists of two types of transport operations. These two types of transport are Knudsen diffusion and activated surface diffusion. The individual contribution of each of these processes has been found to be important in the diffusion of butane through porous silica.(38) Figures 21 and 22 show some experimental results obtained by Haul.(38) The silica gel used in the dynamic adsorption study presented in Tables 2 and 3 had a porosity of 0.49. Comparing the diffusion of butane on porous silica to the diffusion of pentane through the 0.49 porosity silica gel, it would be consistent with Figure 21 to expect surface diffusion to contribute 70 per cent or more of the total transport.

The variation of the surface diffusion coefficient with temperature can be represented by the following equation:

$$D_s = D_{so} \, e^{-\frac{E_a}{RT}} \qquad (22)$$

where:

D_s = surface diffusion coefficient $\frac{cm^2}{sec}$.

D_{so} = surface diffusion coefficient for no hindrance.

T = absolute temperature.

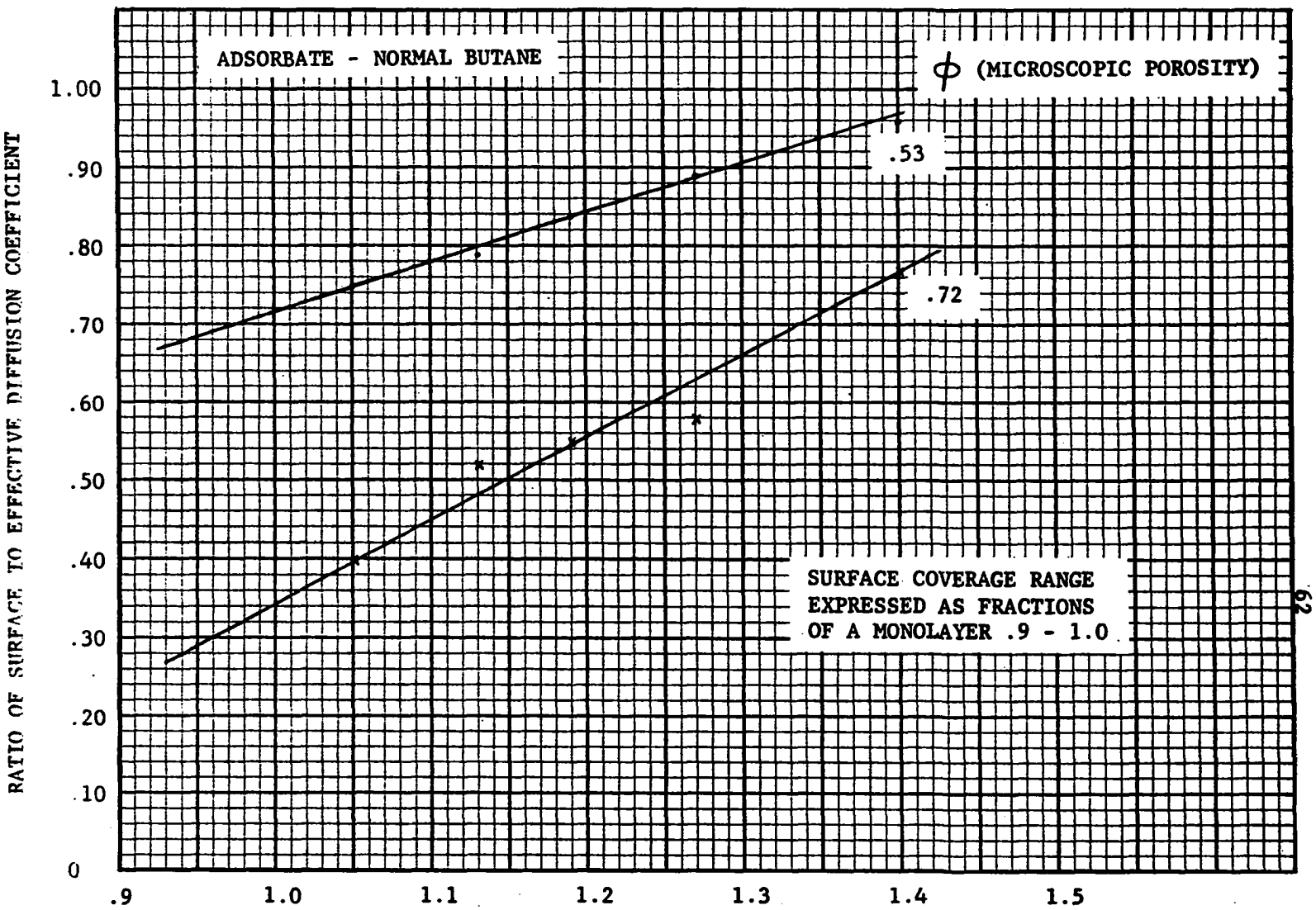

FIGURE 21.--CONTRIBUTION OF THE SURFACE DIFFUSION TO THE TOTAL SOLID DIFFUSION

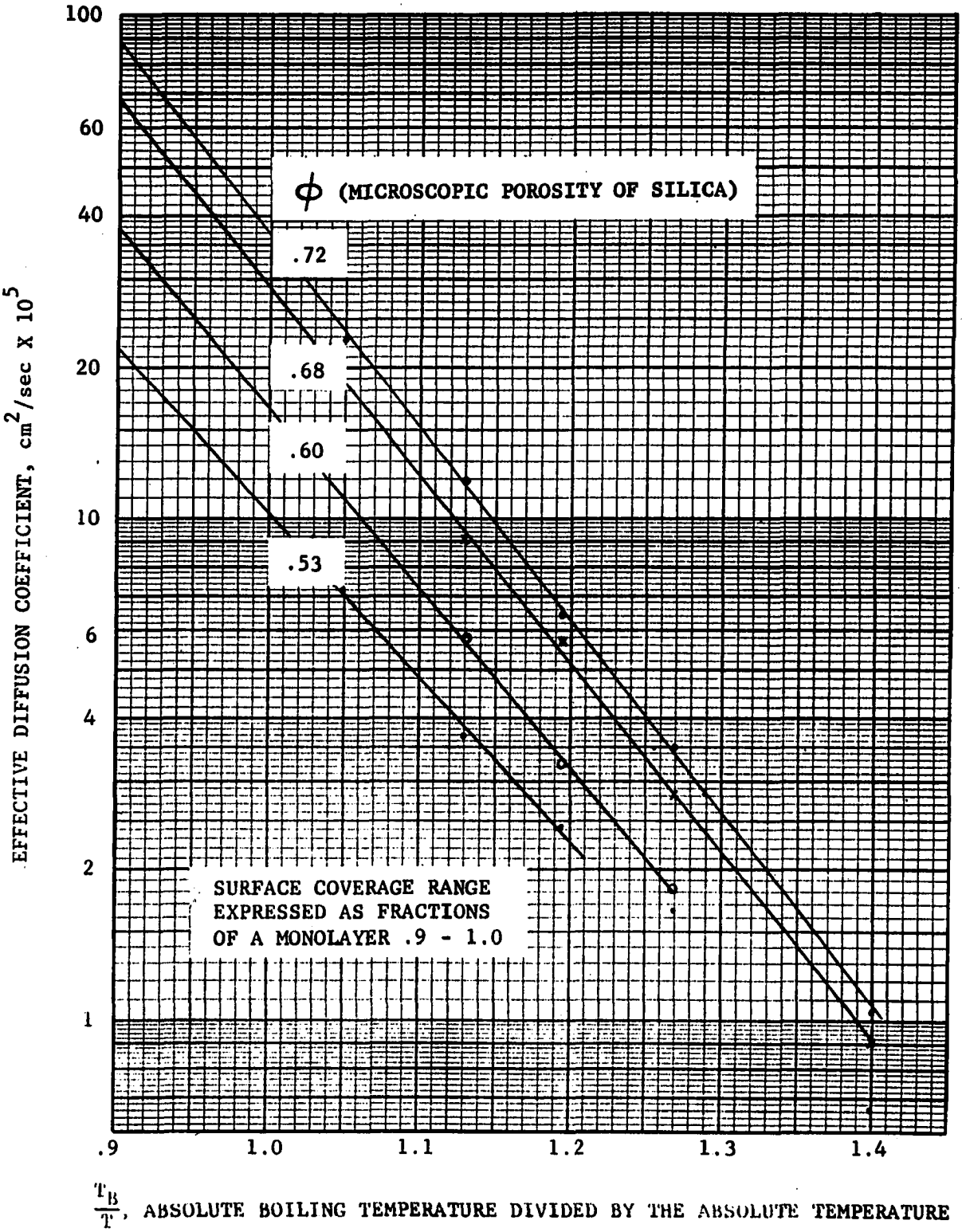

FIGURE 22.--THE EFFECTIVE DIFFUSION COEFFICIENT OF NORMAL BUTANE THROUGH POROUS SILICA

R = universal gas constant.

E_a = activation energy.

If it is assumed that the contribution of surface diffusion to the total transport is essentially constant for pentane between 90°F and 115°F, then the activation energy E_a can be calculated from the mass transfer constants. At a pentane concentration of 0.23 mole per cent, the mass transfer constant changes from 0.58 min^{-1} at 90°F to 0.94 min^{-1} at 115°F. Using this information, an activation energy of 6740 cal/mole was calculated with Equation 22. This is 87 per cent of the heat of adsorption as determined from the following equation used by Kiselev:(40)

$$Q_a = 1.5 + 1.23\ m$$

where:

Q_a = heat of adsorption on silica gel, cal/mole.

m = number of carbons in the adsorbing hydrocarbon.

The value of 6740 cal/mole is high for the activation energy, since the activation energy of butane is about 50 per cent of the adsorption energy and 80 per cent for heptane. Nevertheless, the deviation of the mass transfer constant is more representative of an activation energy than a change in gaseous diffusivity.

Comparison of Mass Transfer Correlations with Existing Correlations

The generalized mass transfer correlations of Gamson et al.(22) and Hougen and Marshall (10) have been previously presented. Since the Hougen and Marshall correlation is an application of the Gamson correlation to water adsorption, only a comparison with the Hougen and Marshall correlation is necessary. This correlation is primarily for the mass

transfer of water under conditions where the gas phase film diffusion is predominate; therefore, it is not surprising that it is not valid for hydrocarbon adsorption under the conditions studied.

The main features of the Hougen and Marshall correlation are:

1. The velocity dependence of the mass transfer constant is $G^{.49}$.

2. The adsorbent particle dependence of the mass transfer constant is $\frac{1}{d_p^{1.51}}$.

3. The temperature and adsorbate concentration dependence of the mass transfer constant is accounted for by the slope of the adsorption isotherm.

4. The mass transfer constant is independent of length.

The corresponding observations from this current investigation of dynamic pentane adsorption on silica gel are:

1. There is no velocity dependence on the mass transfer constant, with the possible exception of the low adsorbate concentration runs at a velocity of 10 feet per minute.

2. The adsorbent particle dependence of the mass transfer constant is $\frac{1}{d_p^{1.88}}$.

3. The temperature dependence of the mass transfer constant is of the order of magnitude of a solid surface diffusion activation energy.

4. The adsorbate concentration dependence of the mass transfer constant is approximately exponential. The exact variation is represented by Figure 16.

5. At low adsorbate concentrations there is no length dependence on the mass transfer constant. At high concentrations the effect

of length was remarkable and could not be account for by an $L^{1/2}$ term. However, a correction of this nature would be in the right direction.

A comparison of the features of the Hougen and Marshall correlation with those of this current investigation leads to the conclusion that the correlation for water adsorption is not applicable to pentane adsorption on silica gel for the conditions investigated.

A second correlation previously reviewed was that of Marks et al(3) This correlation was obtained for pentane adsorption on silica gel. The important features of this correlation are:

1. The velocity dependence of the mass transfer constant is $\frac{1}{G^{.245}}$.

2. The adsorbent particle dependence of the mass transfer constant is $\frac{1}{d_p^{2.745}}$.

3. The temperature and adsorbate concentration dependence of the mass transfer constant is accounted for by the term $K^{1/2}\left(\frac{D_v \rho}{\mu}\right)_g^{2/3}$.

4. The length dependence of the mass transfer constant is $L^{1/2}$.

This correlation was obtained for 33 runs where adsorbent particle size, adsorbate concentration, temperature, bed length, mixtures of other hydrocarbons, pressure and gas velocity were investigated.

The most significant differences between the Marks correlation and the results of this current study are features 1 and 2. The Marks correlation indicates a decrease of the mass transfer constant with an increase in velocity. This is inconsistent with any existing theory of mass transfer. However, since the exponent on the velocity is only 0.245, this result may be a consequence of a statistical type correlation and of

no theoretical significance. Feature 2 indicates a mass transfer constant dependence on adsorbent particle size of $\frac{1}{d_p^{2.745}}$. Whereas, theoretically the maximum value of the exponent is 2.0. The difference between the exponent of 2.745 and the value of 1.88 obtained in this study is significant; however, since the detailed data utilized in the Marks correlation are not available, no explanation is apparent.

The above correlation was used to calculate a mass transfer constant for a mass flux of 2990 lb/hr - ft^2, 6-8 mesh gel, 0.5 mole per cent pentane gas, 90°F adsorption temperature and 800 psia pressure. The value calculated was 1.25 min^{-1} which compares with a value of 0.90 min^{-1} measured in this study. Considering the reported 20 per cent variation in the Marks correlation, it can be seen that the values are in fair agreement.

The only other correlation which has been presented is that of Dale et al.(29) Part of the results of their work for the adsorption of isobutane and isopentane on 6-8 mesh silica gel are represented in a correlation for the adsorption zone length. For isopentane the following correlation was obtained:

$$h_z = \lambda_1 G^{.49}$$

where:

λ_1 is a function dependent upon adsorbent, adsorbate, temperature, desiccant bed length and other adsorption conditions.

Since their experiments were for large values of dimensionless length, the following equation is a direct result of the application of the Klinkenberg equation:

$$h_z = 4.65\left(\frac{L\ B\ G}{k\ \rho_B}\right)^{1/2}$$

This equation shows that if the mass transfer constant is independent of velocity then:

$$h_z = \lambda_o G^{1/2}$$

This result would agree well with the above empirical result of Dale. In the correlation of Dale, the B/k would change less than 5 per cent for the concentrations used for isopentane. The available correlations for hydrocarbon adsorption have been obtained utilizing a small amount of data with little or no consideration of the mass transfer mechanism. This current investigation not only includes more data than all previous investigations, but also places primary emphasis upon the determination of the mass transfer mechanism. Utilizing the determined mass transfer mechanism, the corresponding mathematical developments, and good engineering judgment, the results of this investigation can be extended beyond the range of the experimental data. Whereas, due to the purely empirical nature of previous correlations, they are applicable only within the range of their experimental data.

Discussion of the Mass Transfer Mechanism

There are many indications that the mass transfer mechanism is solid phase diffusion (mechanism P). This solid phase diffusion probably consists of both activated surface diffusion and Knudsen diffusion. The exact contribution of each diffusion process is unknown. However, from the butane data in Figure 21 it would be logical to assume that activated surface diffusion contributes at least 70 per cent of the total mass transport.

Although the evidence of mechanism P has been pointed out in the above sections, it should prove beneficial to list them together. Following is a list of the more important evidence:

1. Except for the low concentration, 6-8 mesh runs where the gas velocity is 10 feet per minute, there is no significant variation of the mass transfer constant with velocity.

2. The mass transfer constant dependence upon adsorbent particle size is $\frac{1}{d_p^{1.88}}$. The exponent of 1.88 indicates a particle diffusion mechanism (for spherical particles the exponent should be 2.0).

3. The order of magnitude of the diffusion coefficient calculated from the mass transfer constant agrees well with the value given by Carman (39) for activated surface diffusion. The agreement is excellent if it is considered that the diffusion coefficient given by Carman is only about 70 per cent of the effective diffusion coefficient.

4. The activation energy calculated from the deviation of the mass transfer constant with temperature is of the same order of magnitude as the surface diffusion activation energy.

5. The mass transfer constant varies significantly with adsorbate concentration.

6. If it is assumed that the mass transfer constant does not vary with the gas velocity, the correlation of Dale et al.(29) can be explained by the Klinkenberg equation for large dimensionless lengths. The data obtained in this current investigation is also predictable by the Klinkenberg equation.

7. The dynamic equilibrium capacity of silica gel varies with adsorbent particle size, tower length, and superficial gas velocity. The velocity effect is noticeable only for the high velocities and short tower runs. This phenomenon is further discussed in a subsequent section.

From the above evidence it is concluded that the dominating mass transfer mechanism is solid phase diffusion.

The Dynamic Equilibrium Capacity of Silica Gel

The dynamic equilibrium capacity was determined from the following equation:

$$Q_T = Q_s + q\ Dz \quad \text{----------23)}$$

where:

Q_T = total amount of adsorbate adsorbed at bed saturation.

Q_S = the amount of adsorbate adsorbed during the cooling of the bed.

q = injection rate of the adsorbate into the carrier gas.

Dz = previously defined.

Q_s is the only term which has not previously been determined. Since Q_s is a very small quantity compared to Q_T, it was approximated by plotting Q_T versus y_o for the runs where Q_s was zero. Then, since the bed was cooled by cycling gas long enough for the bed to be saturated with the lean gas, the equilibrium gas analysis was known. Thus the value of Q_s could be obtained utilizing the equilibrium gas analysis and the approximate isotherm.

The Dynamic Adsorption Isotherm

Figures 23 and 24 show the dynamic equilibrium capacity of the 6-8 mesh and 3-4 mesh silica gel respectively. It can be seen from these

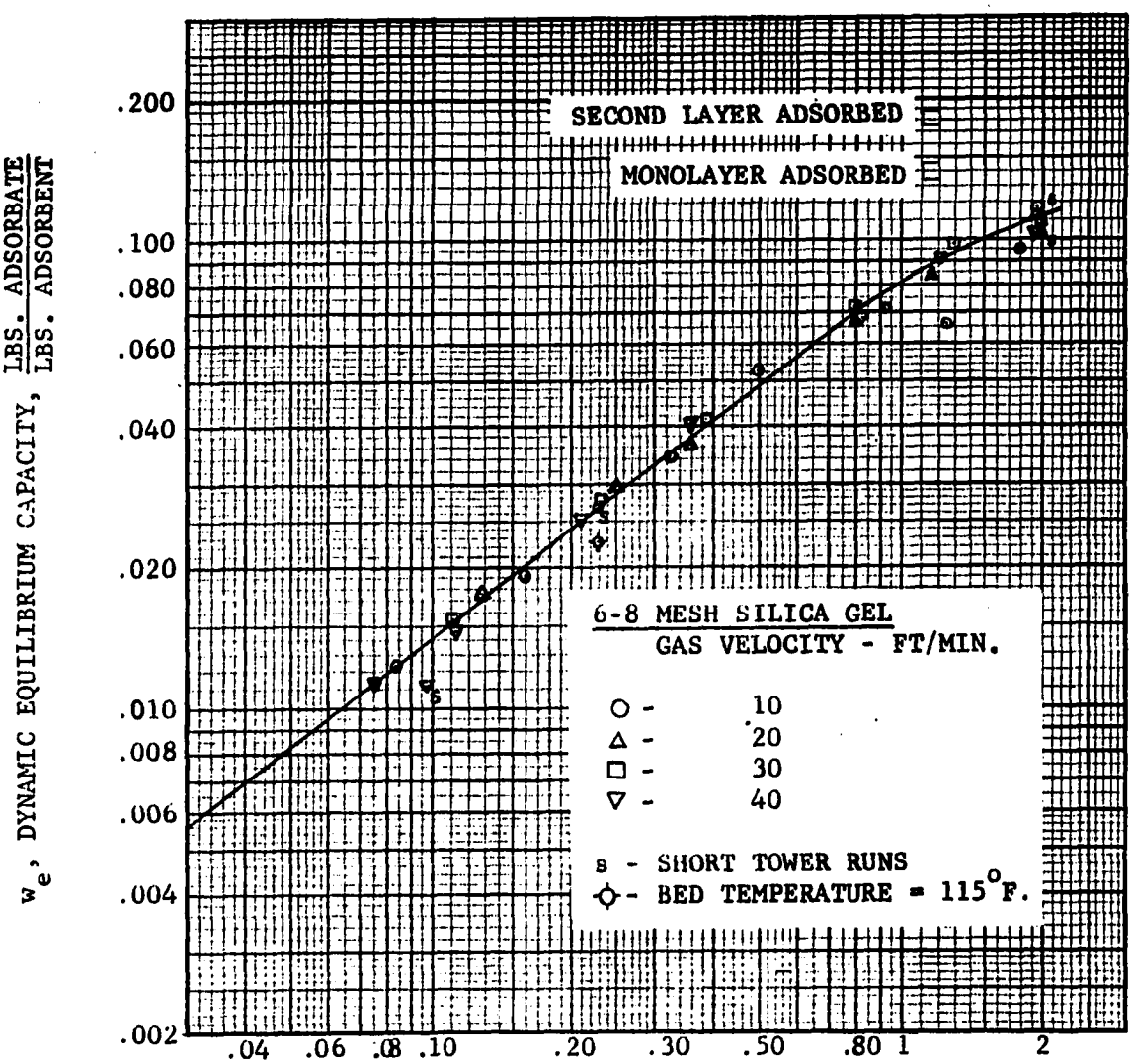

FIGURE 23.--DYNAMIC EQUILIBRIUM CAPACITY

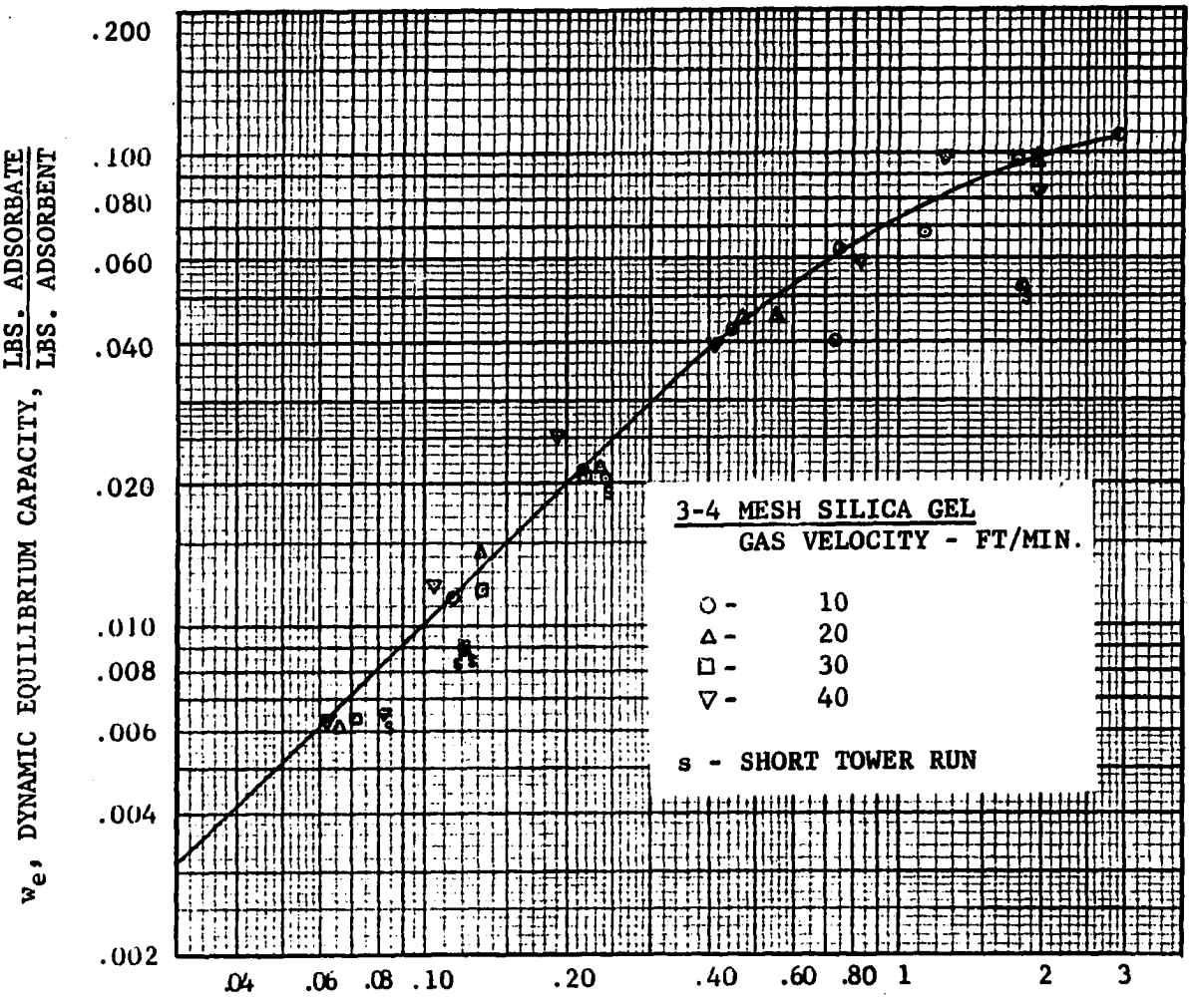

FIGURE 24.--DYNAMIC EQUILIBRIUM CAPACITY

figures that the data is independent of the gas velocity for the 14 foot tower length runs and can be represented by a Freundlich type of isotherm at low adsorbate concentrations. The resulting equations are:

For 6-8 mesh gel below 1.0 mole per cent pentane

$$w_e = 0.0842\ y_e^{.772} \qquad (24)$$

For 3-4 mesh gel below 0.5 mole per cent pentane

$$w_e = 0.0912\ y_e^{.966} \qquad (25)$$

where:

w_e is the dynamic equilibrium capacity of the adsorbent, $\frac{\text{lbs.adsorbate}}{\text{lbs. adsorbent}}$.

y_e is the adsorbate concentration, $\frac{\text{moles adsorbate}}{\text{mole gas}}$.

The short runs were excluded from the determination of these equations.

Variation of the Dynamic Equilibrium Capacity with Particle Size

The dynamic equilibrium capacity of silica gel decreases with an increase in adsorbent particle size. This is evident from a comparison of Figures 23 and 24. This result is consistent with a particle diffusional type of mechanism. This would seem to indicate that the dynamic capacity would also vary with column length and gas velocity. Figures 23 and 24 indicate that there is a definite effect of the gas velocity when the desiccant bed is decreased in length. That is, although there is no velocity effect for the long towers, the short tower lengths have a pronounced effect of velocity.

The observation of the change of the dynamic equilibrium capacity of silica gel with particle size has also been reported by Dale et al.(29)

They found that the capacity of 60-100 mesh gel was 50 per cent greater and that of 20-60 mesh gel was 20 per cent greater than the corresponding capacities of 6-8 mesh gel. The hydrocarbons used in their experiments were isobutane and isopentane.

The Role of Adsorbent Pore and Molecule Sizes in the Analysis of the Isotherm Behavior

An insite into the physical meaning of the shape of the dynamic adsorption isotherm can be obtained by some calculations based upon the following simplification:

1. All of the internal surface area and volume of the adsorbent particle can be represented by one long circular capillary whose diameter is equal to the pore diameter of largest frequency.
2. The pentane molecule can be represented by a circular cylinder with diameter 4.9 angstrom and length 10.0 angstrom. These values are the collision dimensions obtained from data on hydrocarbons from Hirschfelder et al.(41)
3. The pentane molecules are perfectly oriented in the pore.

The pore diameter of the silica gel used is approximately 21 angstrom. From the above data it was determined that the monolayer would accommodate 10 rows of pentane molecules and the second layer would hold 3 rows. A cross sectional view of this simplified capillary with the pentane molecules is presented in Figure 25. Since it was known that the surface area of the adsorbent was 750 to 800 square meters per gram, the monolayer was filled between 0.136 and 0.145 grams of pentane per gram of gel. The second layer was filled between 0.177 and 0.189 grams of pentane per gram of gel. These regions have been noted on the 6-8

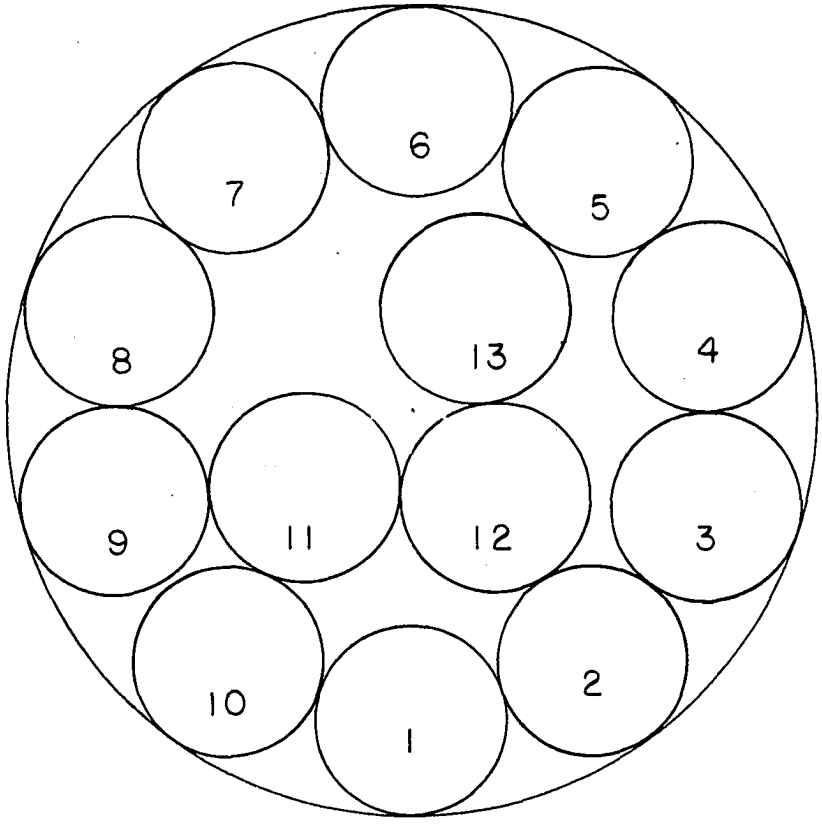

PORE DIAMETER 21 ANGSTROMS
PENTANE MOLECULE DIAMETER 4.9 ANGSTROMS
PENTANE MOLECULE LENGTH 10.0 ANGSTROMS

FIGURE 25.--SECTIONAL VIEW OF HYPOTHETICAL PORE-PENTANE SYSTEM

mesh isotherm in Figure 23. It can be seen that the deviation from the Freundlich isotherm is probably due to the filling up of the monolayer.

Since the above method of calculation is somewhat over simplified, it was decided to test this calculation procedure on some published static equilibrium data. Kiselev (40) shows that for pentane adsorption on a 25 angstrom silica gel the ultimate capacity is 3.6 micro-moles per square meter of adsorbent surface. Following the same procedure as outlined above, Figure 26 was constructed. This yields a value for the ultimate capacity of 4.0 micro-moles per square meter. Thus the calculated value is about 10 per cent larger than the value measured by Kiselev.(40) This deviation could easily be accounted for by the non-cylindrical shape of the pores or by a slight increase in the diameter and length of the pentane molecule adsorbed in the second layer.

Since the measured and calculated ultimate capacities agree, it can be hypothesized that:

1. The ultimate dynamic adsorption capacity of pentane on silica is determined solely by the available microscopic pore volume of the gel.
2. The pentane molecule exhibits a high degree of orientation when adsorbed upon silica gel.
3. A single circular cylinder is a simple representation of the pore network which is sufficient for practical considerations of the ultimate dynamic adsorption capacity of silica gel.

The above calculation procedure should be useful for the determination of ultimate adsorption capacities of hydrocarbon mixtures.

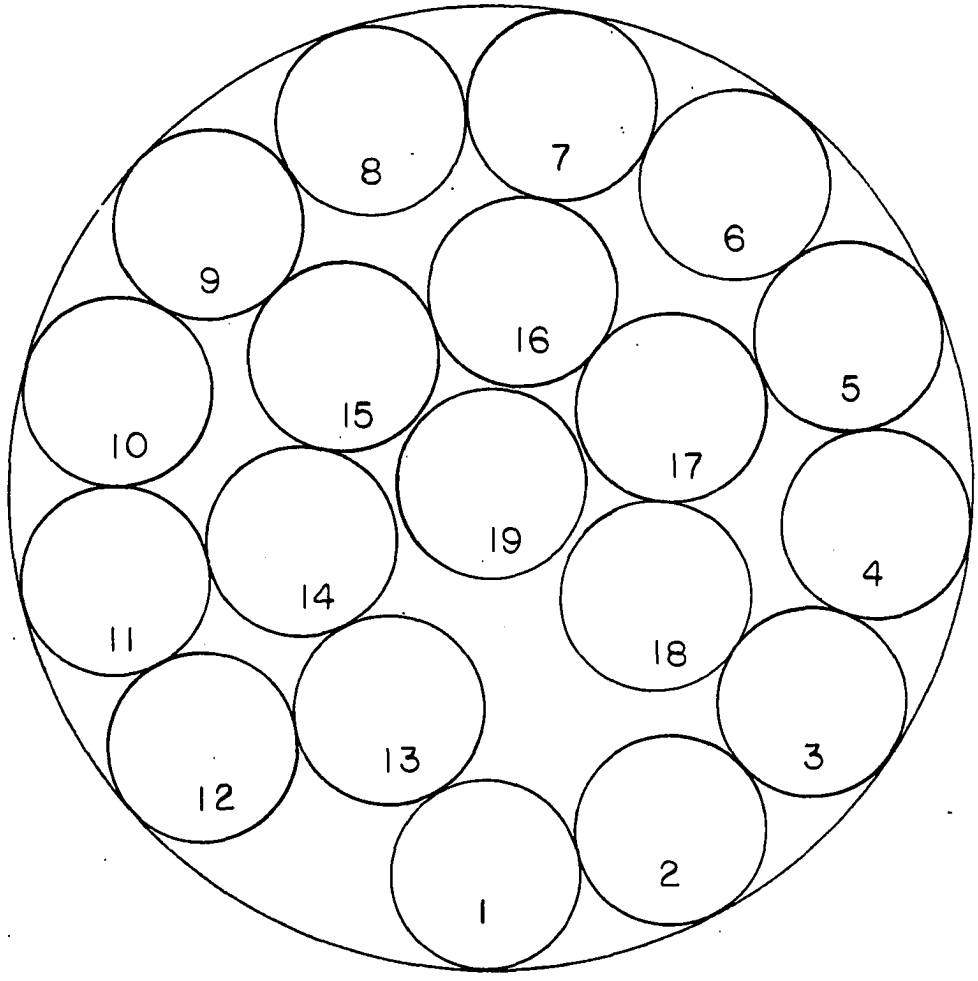

PORE DIAMETER 25 ANGSTROMS
PENTANE MOLECULE DIAMETER 4.9 ANGSTROMS
PENTANE MOLECULE LENGTH 10.0 ANGSTROMS

FIGURE 26.--SECTIONAL VIEW OF HYPOTHETICAL PORE-PENTANE SYSTEM

Presentation of Adsorption Zone Length Correlation

Once the mass transfer constant and the dynamic equilibrium capacity are known for the adsorption conditions, then the complete breakout performance of pentane can be predicted using either the Klinkenberg equation or the Rosen numerical solutions. Besides the breakout curve it is also of interest to know the adsorption zone length and the breakthrough capacity of the bed.

Figures 27, 28, 29, and 30 have been developed which yield these values directly without determination of the breakout curve. Figure 27 is a correlation of the dimensionless zone length with the dimensionless bed length. This correlation shows considerable scatter which is a result of a slight additional dependence upon concentration not accounted for by the mass transfer constant. The concentration dependence is evident from a comparison of Figures 27, and 28, since the latter figure excludes concentrations greater than 0.6 mole per cent pentane. Most field applications of adsorption are for gas compositions less than this value.

The adsorption zone is related to the breakthrough capacity by the following equation, obtainable from a mass balance around the adsorbent bed:

$$\frac{Q_B}{Q_T} = 1 - F \frac{h_z}{h_T}$$

where:

Q_B is the quantity of pentane adsorbed at breakthrough.

Q_T is the dynamic equilibrium capacity of the gel.

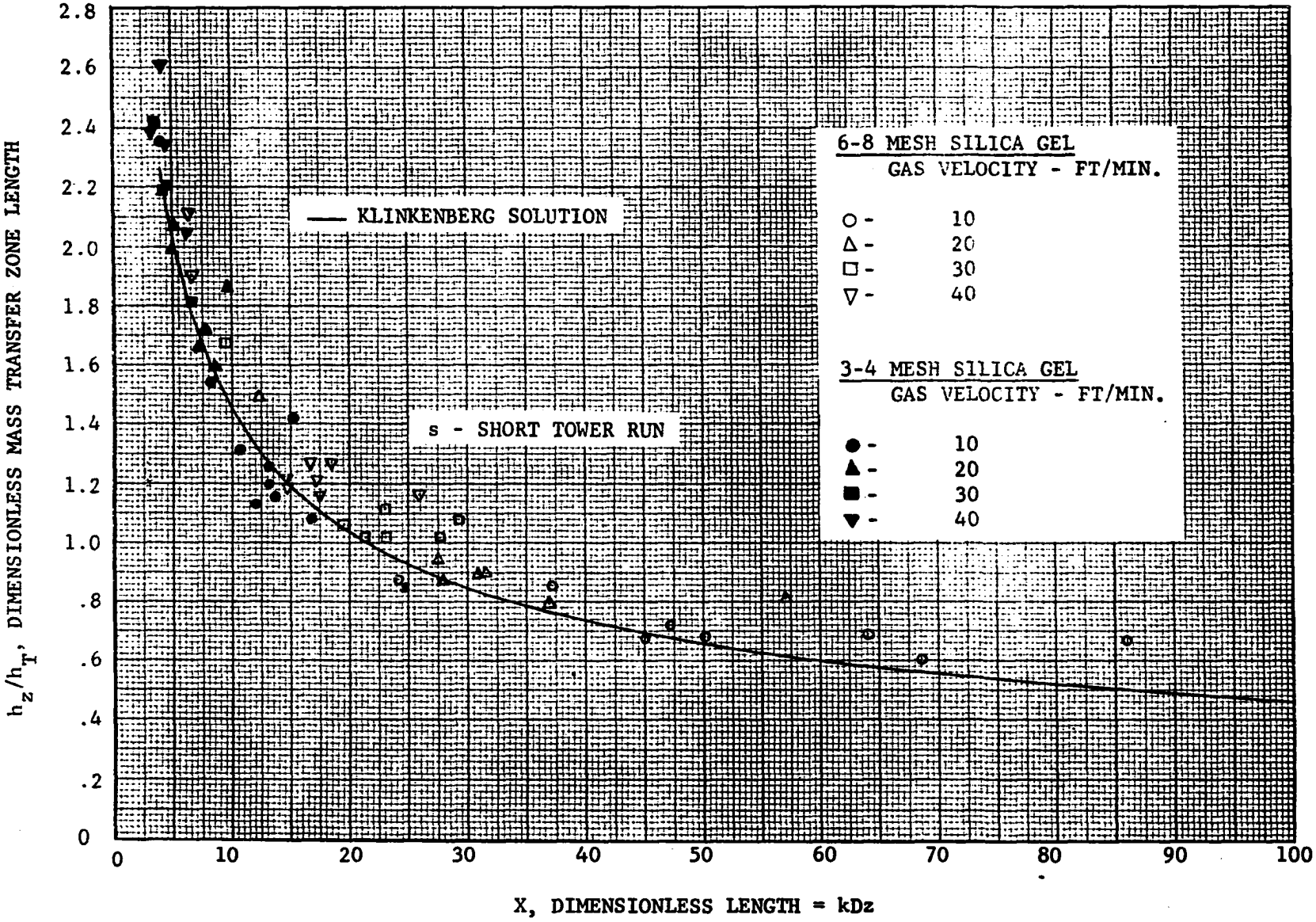

FIGURE 27.--ZONE LENGTH vs. DIMENSIONLESS LENGTH

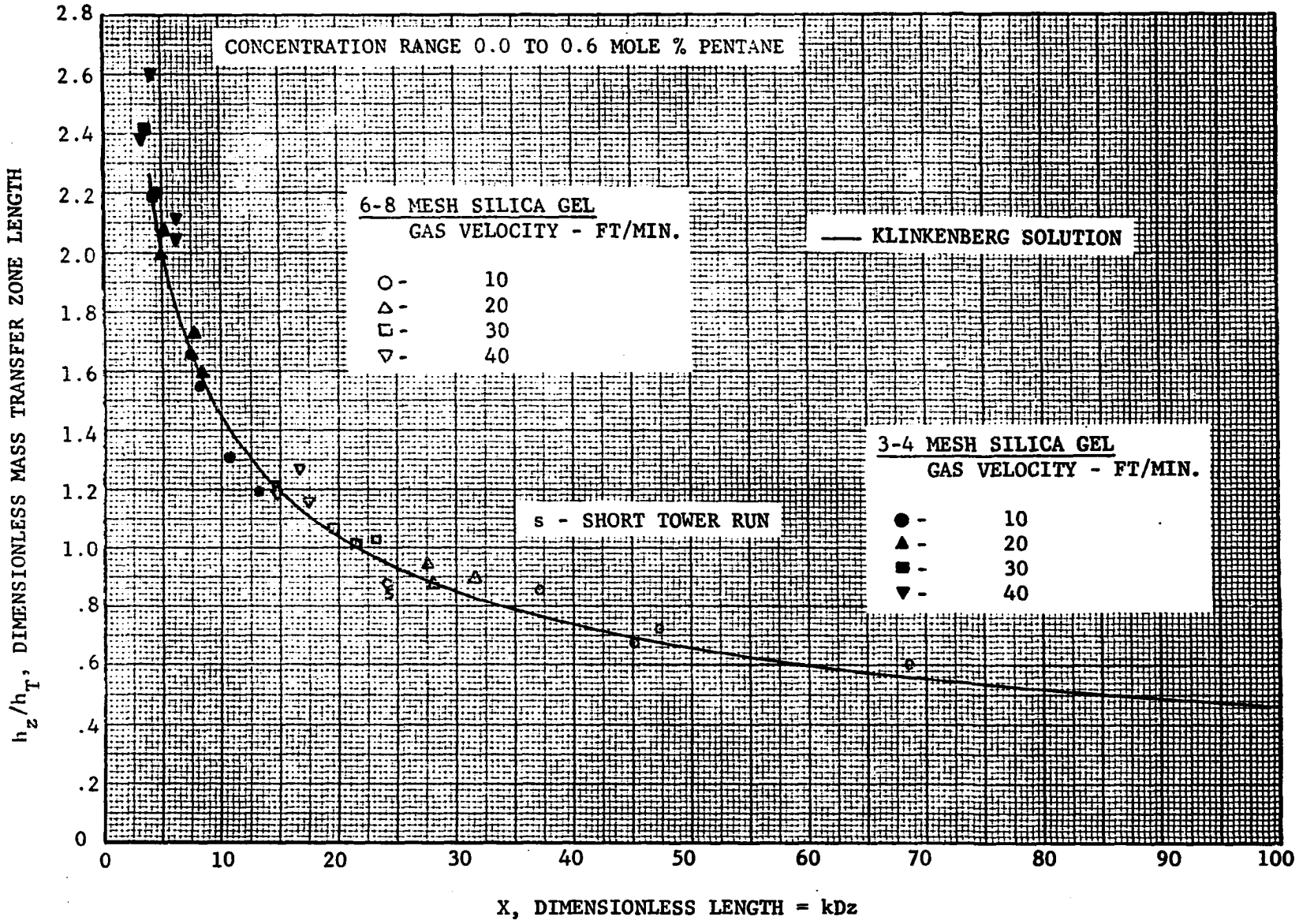

FIGURE 28.--ZONE LENGTH vs. DIMENSIONLESS LENGTH

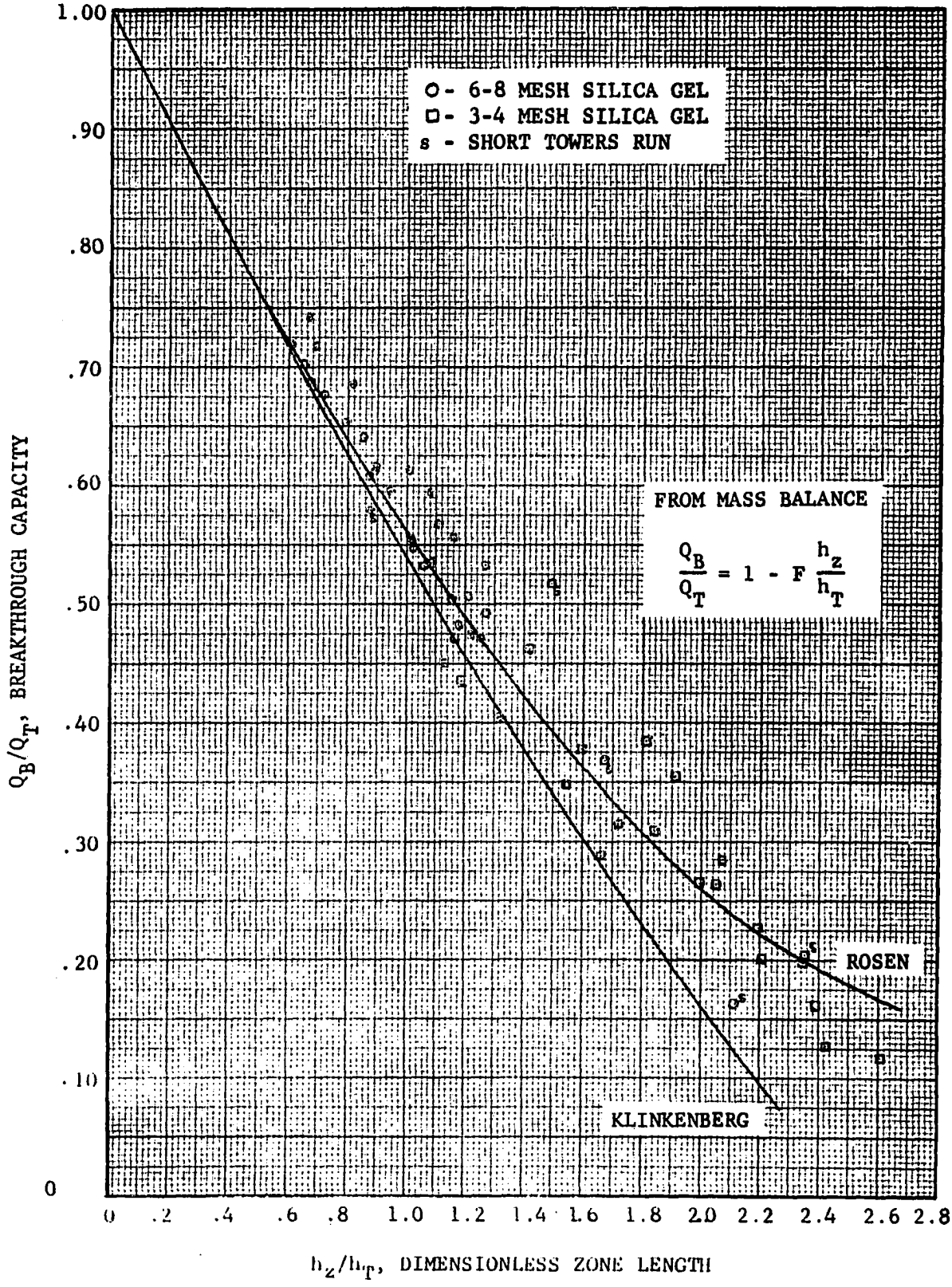

FIGURE 29.--BREAKTHROUGH CAPACITY vs. DIMENSIONLESS ZONE LENGTH

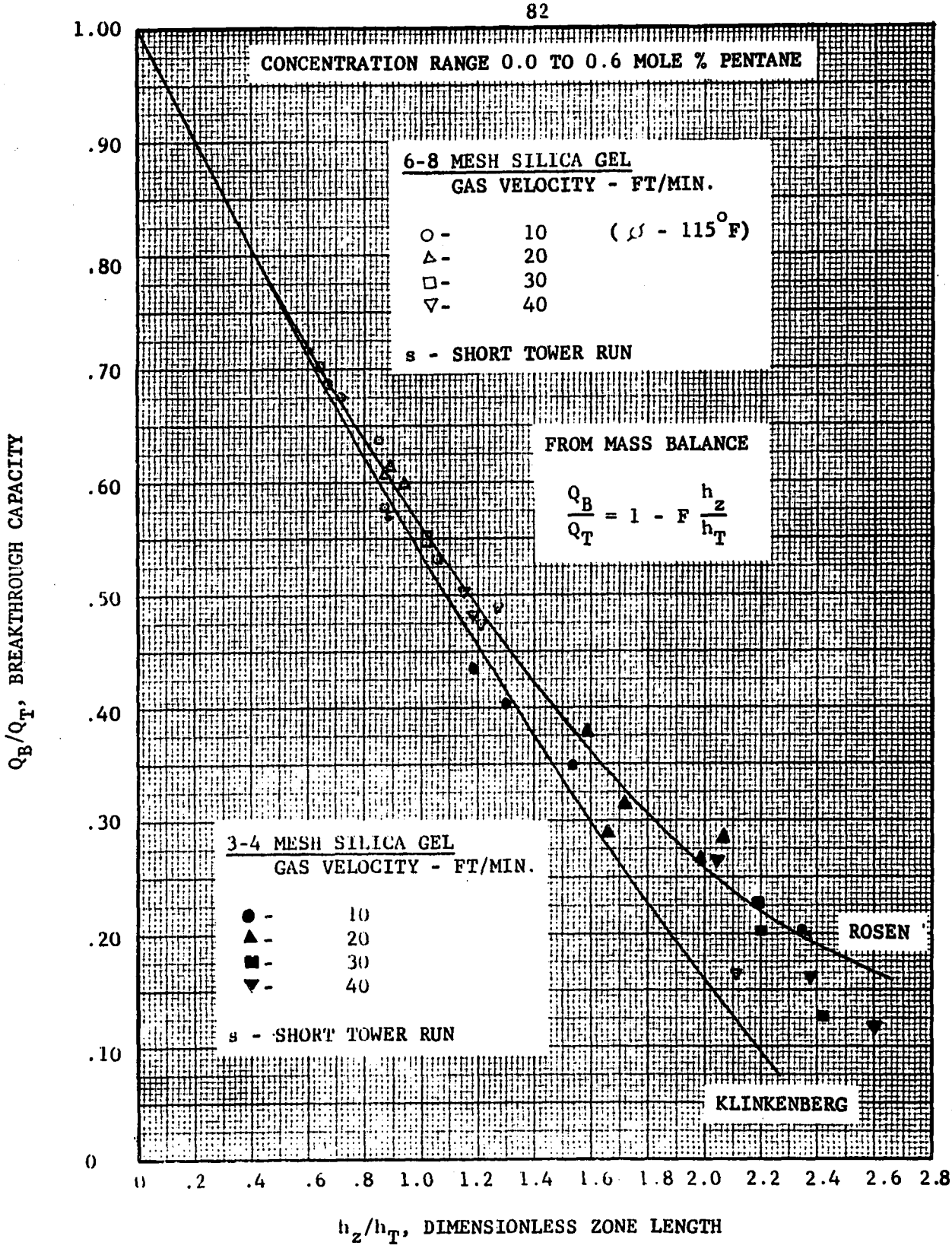

FIGURE 30.--BREAKTHROUGH CAPACITY vs. DIMENSIONLESS ZONE LENGTH

F is a dimensionless parameter defined as

$$\frac{\int_{t_{.05}}^{t_{.95}} \left(1 - \frac{y}{y_o}\right) dt}{t_{.95} - t_{.05}}$$

h_T is the total length of the adsorbent bed.

No acceptable method has been developed to correlate F;(27, 28, 42) therefore, it was decided to determine the breakthrough capacity by correlating it with dimensionless length through the intermediate correlation of adsorption zone length. Again the dependence of concentration produced scatter in the correlation for the breakthrough capacity. This is apparent from Figure 29. Figure 30 was then drawn to provide a better correlation for the concentrations below 0.6 mole per cent pentane.

Since it has been established that $\frac{h_z}{h_T}$ is a direct reflection of the breakthrough capacity, it is of interest to return to Figure 28. This figure shows that as the dimensionless length decreases, $\frac{h_z}{h_T}$ increases and thus the breakthrough capacity decreases. A guide which has been used in design is that the tower length should be at least as long as the adsorption zone length. Figure 28 shows this to be an excellent guide since the breakthrough capacity starts decreasing at a faster rate with each shortening of the dimensionless length when $\frac{h_z}{h_T} > 1.0$. These correlations should prove useful in preliminary design calculations.

In order to use these correlations, the dimensionless length must be determined from the mass transfer constant correlation and the dynamic equilibrium adsorption isotherm. This determination is presented in the following section.

Prediction of the Pentane Breakthrough Curve

In order to calculate the pentane breakthrough curve, a value for the dimensionless length (X) must be obtained. Once this value has been obtained the breakout curve can be calculated from the Klinkenberg equation or obtained from Figure 31 which is a graphical representation of this equation.

Determination of Dimensionless Length

The dimensionless length is defined as follows:

$$X = k\ D\ z$$

where:

k = the mass transfer constant in Figure 16, hr^{-1}, note that the units used on k in Figure 16 are min^{-1}.

z = the total tower length, feet.

$$D = \frac{\rho_B}{G\ B}$$

G = mass gas velocity, $\frac{lb.gas}{hr - ft^2}$.

ρ_B = bulk density of bed (47 $lb./ft^3$ for 6-8 mesh gel, 45 $lb./ft^3$ for 3-4 mesh gel)

$$B = \frac{y_e}{w_e}, \quad \frac{lb.gel}{lb.gas}$$

The value of k is determined from Figure 16 and the value of w_e is determined from Figure 23.

Example Calculation of Breakout Curve Showing the Influence of k and w_e

In order to show the influence of k and w_e, a breakout curve was calculated for the following conditions:

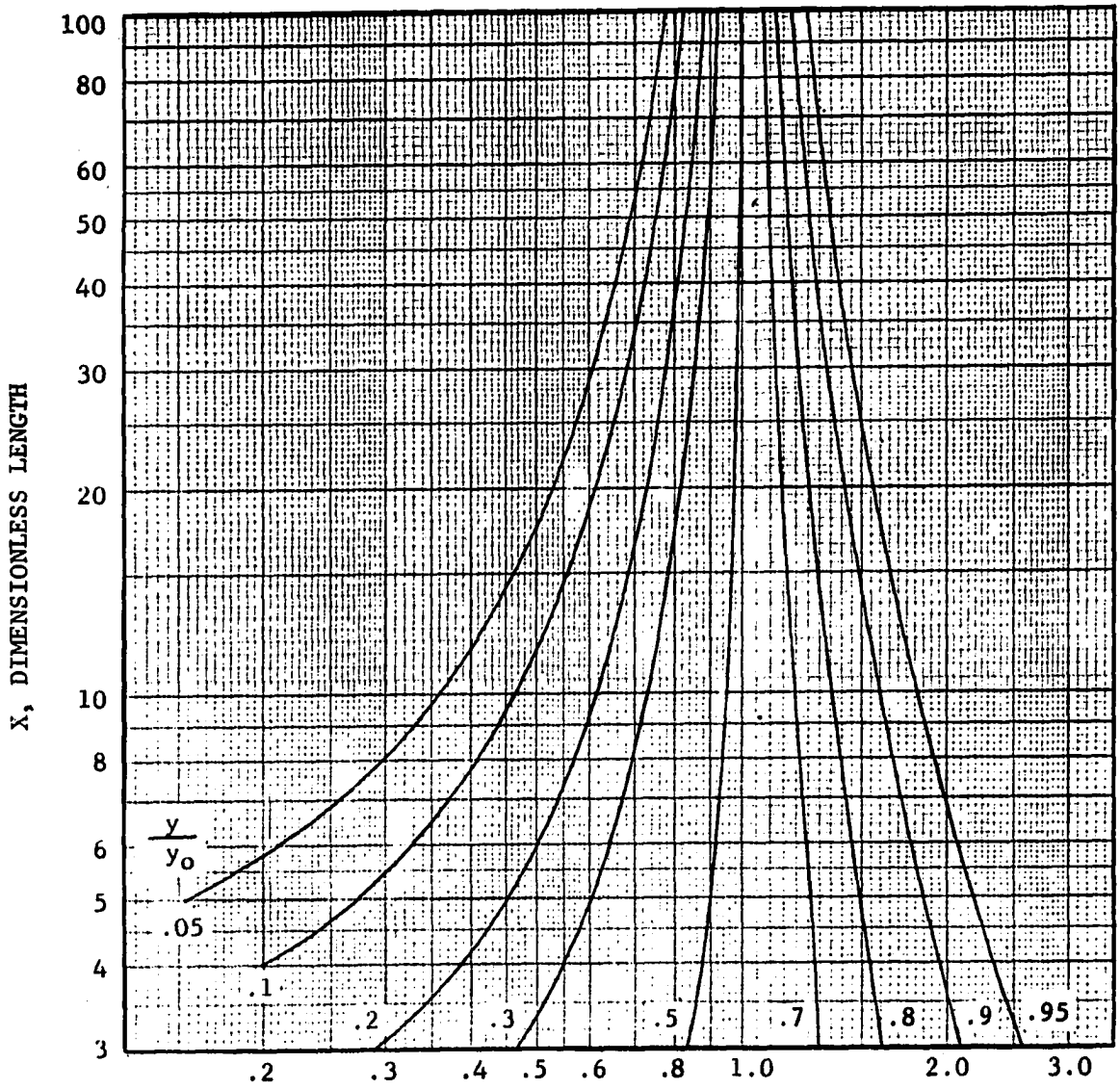

FIGURE 31.--GRAPHICAL SOLUTION OF THE KLINKENBERG EQUATION

$G = 2990$ lb./hr-ft^2 (about 20 ft./min.at 90°F and 800 psia).

$y_o = 0.36$ mole per cent pentane.

6-8 mesh gel.

$z = 14$ feet.

$\rho_B = 47$ lb./ft^3.

From Figures 16 and 23, $k = 0.80$ min^{-1} and $w_e = 0.038$ lb. pentane per lb. gel. Thus Dz is 36.5 min. Utilizing $k = 0.80$ min^{-1}, Dz = 36.5 min, and Figure 31, Curve II of Figure 32 was constructed. Then Curves I and III were calculated for a 20 per cent decrease in k and a 10 per cent decrease in Dz respectively.

A comparison of Curves I, II and III shows that a small deviation in Dz causes a large change in the breakout curve; whereas, a relatively large change in k is less significant.

Results of Particle Temperature Measurements

During the adsorption of hydrocarbons upon silica gel, the heat of adsorption results in a rise of the carrier gas temperature. Measurements of gas temperatures have shown temperature increases as large as 20°F for the adsorption of 2 mole per cent pentane on silica gel.(9) Therefore, it was decided to measure the temperature of the adsorbent particles as well as the adjacent gas temperature. The detailed construction of this special desiccant tower was reviewed in Chapter III. The results of measurements obtained for the particle and adjacent gas temperatures are shown in Figure 33. This figure shows the maximum deviation between the particle and the adjacent gas stream to be less than 0.5°F. From these results it can be concluded that for practical purposes the particle and gas temperatures can be considered as equal. The

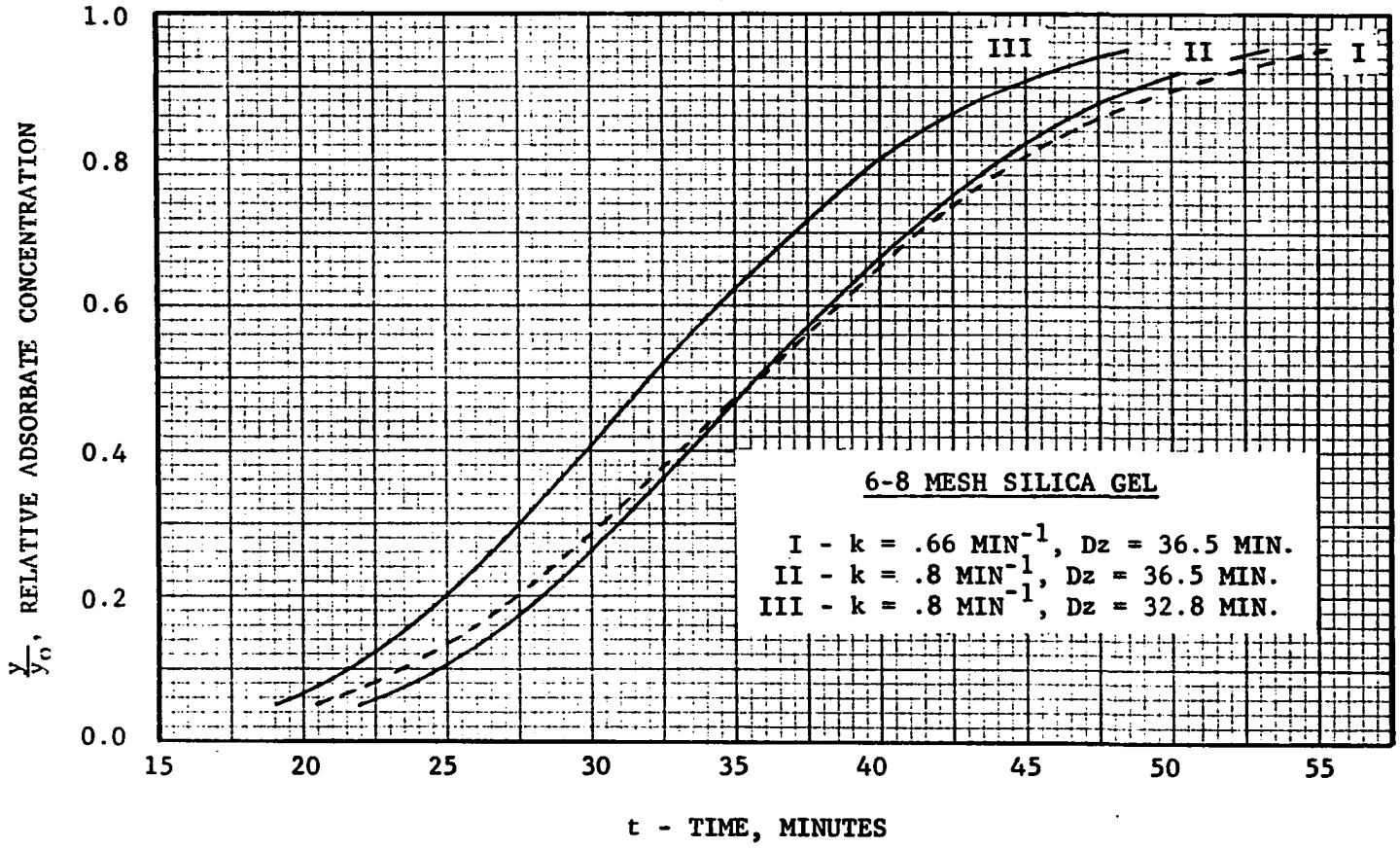

FIGURE 32.--THE EFFECT OF CHANGES IN k AND w_e ON THE BREAKOUT CURVE

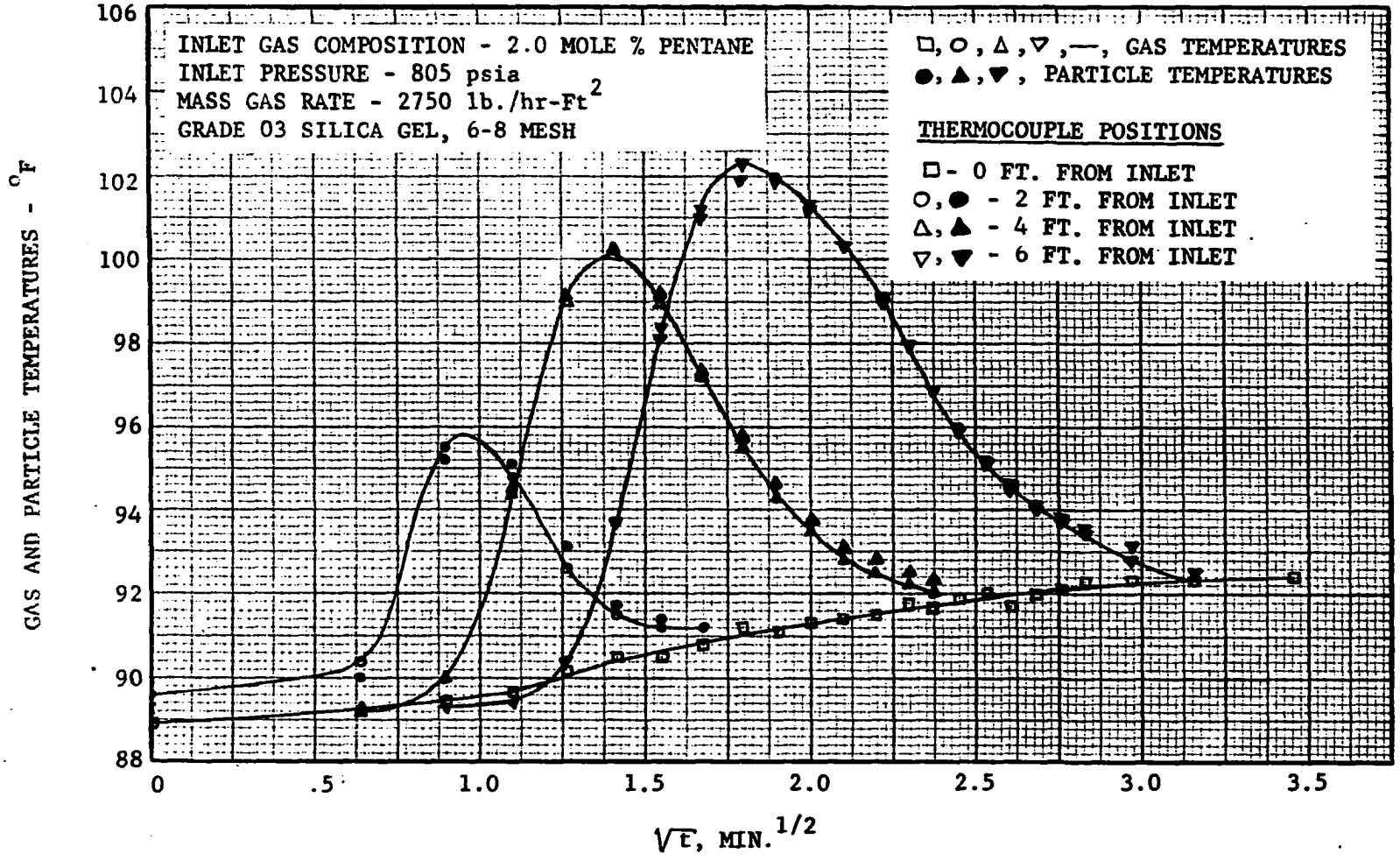

FIGURE 33.--GAS AND PARTICLE TEMPERATURES AT VARIOUS POSITION IN TOWER vs. TIME

above result can be verified by estimating the overall heat transfer coefficient U.

The maximum rate of heat generation is given by the following equation:

$$Q = h_a\left(\frac{\partial w}{\partial t}\right)_{max} = h_a\ k\ w^*$$

where:

Q = rate of heat generation, $\frac{BTU}{min}$.

h_a = heat of adsorption, $\frac{BTU}{lb.adsorbate}$.

The other terms are as previously defined.

For 6-8 mesh silica gel under the conditions of the above experiment, an overall heat transfer coefficient (U) of 11 BTU/hr-ft^2 ^oF would maintain the particle-gas temperature difference less than 0.5^oF. For 3-4 mesh silica gel under the same conditions, a U of 14 would produce the same result. Rough, conservative estimates of the overall U in the above cases were 30 and 19 BTU/hr-ft^2 ^oF respectively. Thus the particle and gas temperatures are logically very nearly equal.

Implications of this Research

The results and conclusions obtained from this research are in themselves important; also of significance are several resulting implications.

Mass Transfer Mechanism

It has been demonstrated that the mass transfer is controlled by solid phase diffusion. Once this has been established an immediate question arises. Can the properties of the gel be altered in such a fashion so as to increase the mass transfer rate? The reduction of the

particle size, which is an obvious solution, eventually results in undesirable increases in the pressure drop across the desiccant bed. Therefore, it would be most desirable to maintain the particle size and alter the internal desiccant structure to obtain the same result.

As shown by Figure 21 the effective rate of solid phase diffusion depends both upon Knudsen and activated surface diffusion. Both of these diffusion processes depend upon the average pore diameter or microscopic porosity. Figure 22 shows that the effective diffusion coefficient increases by a factor of 3.5 when the porosity of the gel is increased from 0.53 to 0.72. Although the data of Figure 22 are for the butane-silica system, the pentane-silica system will behave similarly. Thus it can be concluded that the effective diffusion coefficient of the pentane-silica system can be increased by increasing the average pore size. In turn the mass transfer constant will increase until the gas film diffusion controls the process. This effect is qualitatively represented in Figure 34 for a given set of adsorption conditions.

Although the increase in pore size increases the mass transfer constant, Kiselev (40) has shown that the static equilibrium capacity of pentane on silica gel is sharply reduced by an increase in pore size when the average pore diameter is less than 40 angstroms. If the dynamic capacity of the silica gel is controlled by diffusion as seems to be indicated by both the data in this current investigation and that of Dale et al.(29) then this reduction in static equilibrium capacity may not be reflected in the dynamic capacity. Indeed the dynamic capacity may even be increased as a result of an increased mass transfer constant.

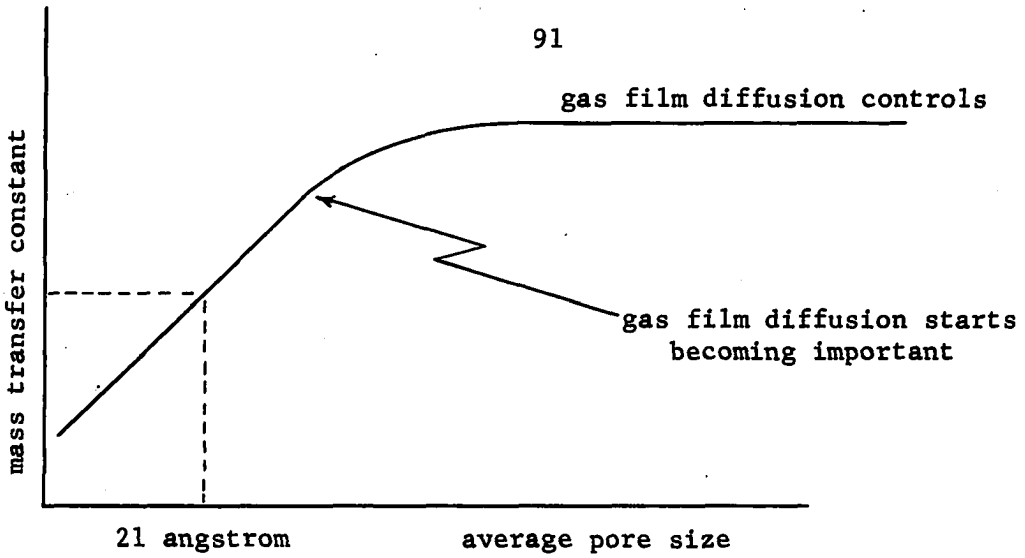

FIGURE 34.--QUALITATIVE REPRESENTATION OF THE MASS TRANSFER CHANGE WITH PORE SIZE

The implication here is that it is possible that a gel may be tailored to a particular range of gas concentrations. At very low concentrations, only a portion of the now available surface area may be sufficient. Thus the pore size could be increased, which necessarily decreases the surface area, to sharpen the breakout curve without decreasing the breakthrough capacity.

Breakout Curve Prediction at High Adsorbate Concentrations

Both the Rosen and Klinkenberg (for $X > 5$) solutions adequately predict for practical applications the behavior of pentane adsorption up to a concentration of about 0.6 mole per cent pentane. Above this value the solutions become increasingly empirical. An extention of the present mathematical developments will be necessary before the breakout curve for high concentrations can be predicted. The general problem of simultaneous adsorption and heat transfer has been studied by others.(43, 44) They have concluded that no general solution will be available in the foreseeable future. Thus it is appropriate to attempt the develop-

ment of a solution applicable to the special case of the hydrocarbon-silica gel system. From this research such a solution could justifiably incorporate the following assumptions:

1. The mass transfer rate can be represented by a film type diffusional mechanism. This is valid since in current practical hydrocarbon separations the dimensionless length would be greater than 5.
2. The mass transfer constant would need to be treated as a function of temperature.
3. The actual dynamic equilibrium capacity would need to be utilized in the rate equation.
4. This capacity should be treated as a function of temperature.
5. The gas and particle temperatures are identical.

It is believed that the use of these five statements would lead to a solution capable of describing hydrocarbon adsorption on silica gel even at relatively high concentrations. The effect of concentration upon the mass transfer constant was neglected since the temperature and the non-linear isotherm effects are probably more important. The results of such a solution would only be applicable for a single adsorbing component and much would remain to be done before multi-component behavior could be predicted.

CHAPTER V

CONCLUSIONS

This investigation of the characterization of dynamic pentane adsorption on silica gel has led to several important conclusions which are valid for the prevailing experimental conditions. The more important of these are:

1. The mass transfer for the pentane-silica gel system is controlled by solid phase diffusion below a concentration of 0.6 mole per cent pentane.
2. This diffusion is a combination of activated surface diffusion and Knudsen diffusion.
3. In dynamic adsorption of pentane on silica gel the gas and particle temperatures are identical.
4. The dynamic equilibrium capacity of silica gel varies with adsorbent particle size, desiccant bed length, and superficial gas velocity. For a seven foot bed length the effect of gas velocity is considerable; whereas, for a fourteen foot bed length the effect is negligible.
5. The generalized water adsorption mass transfer correlation is not applicable for the prediction of pentane adsorption on silica gel.

6. The Klinkenberg and Rosen solutions yield essentially identical results for practical values of dimensionless length (dimensionless length $\geqslant 10$). Therefore, since the Rosen solution must be obtained numerically, it is recommended that the Klinkenberg solution be utilized for the prediction of pentane adsorption for practical purposes.

7. The Klinkenberg and Rosen solutions are particularly applicable for low adsorbate concentrations.

8. The Klinkenberg and Rosen solutions become empirical at high adsorbate concentrations as a result of the non-linear adsorption isotherm and the heat generated by adsorption.

9. Accurate information on the dynamic equilibrium capacity is essential for a precise prediction of the breakout curve.

10. For commercial tower lengths, large errors in the mass transfer constant are not directly reflected in the determination of the breakout time.

These results lead to a better understanding of dynamic adsorption in general and in particular of the dynamic adsorption of pentane on silica gel. More importantly, they provide a firm basis for an improved method of designing processes utilizing silica gel.

BIBLIOGRAPHY

1) Halff, Howard. "Field Operation of Dry Bed Adsorption Units." Proceedings of Thirty-ninth Annual Convention, Natural Gasoline Association of America, (1960), pp. 97-100.

2) Lewis, W. K., Gilliland, E. R., Chertow, B., Cadogan, W. P. "Adsorption Equilibria: Pure Gas Isotherms." Joint Symposium on Adsorption sponsored by American Chemical Society, (Sept. 18-23, 1949), pp. 43-54.

3) Marks, D. E., Robinson, R. J., Arnold, C. W., Hoffmann, A. E. "Dynamic Behavior of Fixed-Bed Adsorbers." Journal of Petroleum Technology, Vol. 15, No. 4, (April, 1963), pp. 443-449.

4) Vermeulen, Theodore. Advances in Chemical Engineering. Edited by T. B. Drew and J. W. Hoopes, Jr. Vol. II, New York: Academic Press, Inc., 1958. pp. 147-208.

5) Carter, J. W. "Part I: Adsorption Drying of Gases." British Chemical Engineering, (July, 1960), p. 472.

6) Carter, J. W. "Part II: Adsorption Drying of Gases." British Chemical Engineering, (August, 1960), p. 552.

7) Carter, J. W. "Part III: Adsorption Drying of Gases." British Chemical Engineering, (Sept., 1960), p. 625.

8) Carter, J. W. "Adsorption Processes." British Chemical Engineering, (May, 1961), p. 308.

9) Needham, R. B., Campbell, J. M., McLeod, H. O. "A Critical Evaluation of the Mathematical Models Used for Dynamic Adsorption of Hydrocarbons." Unpublished. Presented at the February, 1964 meeting of AICHE at Memphis, Tennessee.

10) Hougen, O. A., Marshall, Jr., W. R. "Adsorption from a Fluid Stream Flowing Through a Stationary Granular Bed." Chemical Engineering Progress, Vol. 43, No. 4, (April, 1947), p. 197.

11) Jury, S. H., Licht, Jr., W. "Drying of Gases." Chemical Engineering Progress, Vol. 48, No. 2, (Feb., 1952), p. 102.

12) Klinkenberg, A. "Heat Transfer in Cross-Flow Heat Exchangers and Packed Beds." Industrial and Engineering Chemistry, Vol.46, No. 11, (Nov., 1954), p. 2285.

13) Klinkenberg, A. "Numerical Evaluation of Equations Describing Transient Heat and Mass Transfer in Packed Solids." Industrial and Engineering Chemistry, Vol. 40, No. 10 (Oct., 1948), p. 1992.

14) Rosen, J. B. "Kinetics of a Fixed Bed System for Solid Diffusion into Spherical Particles." Journal of Chemical Physics, Vol. 20 (1952), p. 387.

15) Rosen, J. B. "General Numerical Solution for Solid Diffusion in Fixed Beds." Industrial and Engineering Chemistry, Vol. 46, No. 8, (1954), p. 1590.

16) Michaels, A. S. "Simplified Method of Interpreting Kinetic Data in Fixed-bed Ion Exchange." Industrial and Engineering Chemistry, Vol. 44, No. 8, (1952), p. 1922.

17) Glueckauf, E., Coates, J. I. "Theory of Chromatography. Part IV. The Influence of Incomplete Equilibrium on the Front Boundary of Chromatograms and on the Effectiveness of Separation." Journal of Chemical Society, (1947), p. 1315.

18) Thomas, H. C. "Heterogeneous Ion Exchange in a Flowing System." Journal American Chemical Society, Vol. 66, (Oct., 1944), p. 1664.

19) Hiester, N. K., Vermeulen, Theodore. "Saturation Performance of Ion-exchange and Adsorption Columns." Chemical Engineering Progress, Vol. 48, No. 10, (1952), p. 505.

20) Hiester, N. K., Radding, S. B., Nelson, Jr., R. L., Vermeulen, T. "Interpretation and Correlation of Ion Exchange Column Performance under Nonlinear Equilibria." American Inst. Chemical Engineers Journal, Vol. 2, No. 3, (Sept. 1956), p. 404.

21) Tien, Chi, Thodos, George. "Ion Exchange Kinetics for Systems of Nonlinear Equilibrium Relationships." American Institute of Chemical Engineers Journal, Vol. 5, No. 3, (Sept., 1959), p. 373.

22) Gamson, B. W., Thodos, G., Hougen, O. A. "Heat, Mass and Momentum Transfer in the Flow of Gases Through Granular Solids." Transactions of American Institute of Chemical Engineers, Vol. 39, (1943), p. 1.

23) Leland, Jr., T. W., Holmes, R. E. "The Design of Hydrocarbon Recovery Units Using Solid Adsorbents." Journal of Petroleum Technology, (Feb., 1962), p. 179.

24) Wilke, C. R., Hougen, O. A. "Mass Transfer in the Flow of Gases through Granular Solids Extended to Low Modified Reynolds Numbers." Transactions of American Institute of Chemical Engineers, Vol. 41, (1945), p. 445.

25) Eagleton, L. C., Bliss, H. "Drying of Air in Fixed Beds." Chemical Engineering Progress, Vol. 49, No. 10, (1953), p. 543.

26) Sieg, K. G. "An Investigation of the Predictive Nature of the Differential Model of Adsorption." Unpublished Master's Thesis in Petroleum Engineering, University of Oklahoma, (1964).

27) Ashford, F. E. "Dynamic Adsorption of n-pentane and n-hexane on Silica Gel." Unpublished Master's Thesis in Petroleum Engineering, University of Oklahoma, (1962).

28) Campbell, J. M., Ashford, F. E., Needham, R. B., Reid, L. S. "More Insight into Adsorption Design." Hydrocarbon Processing and Petroleum Refiner, Vol. 42, No. 12, (1963), p. 89.

29) Dale, G. H., Haskell, D. M., Keeling, H. E., Warzel, L. A. "Dynamic Adsorption of Isobutane and Isopentane on Silica Gel." Chemical Engineering Progress Symposium Series, Vol. 57, No. 34, p. 42.

30) Wicke, E. "Empirische und theoretische Untersuchungen der Sorptionsgeschwindigkeit von Gasen an porosen Stoffen I." Kolloid-Zeitschrift, Band 86, Heft 2, (1939), p. 167.

31) Wicke, E. "Empirische und theoretische Untersuchungen der Sorptionsgeschwindigkeit von Gasen an porosen Stoffen II." Kolloid-Zeitschrift, Band 86, Heft 3, (1939), p. 295.

32) Wicke, E. "Untersuchungen uber ad-und Desorptionsvorgange in kornigen, durchstromten Adsorberschichten." Kolloid-Zeitschrift, Band 93, Heft 2, (1940), p. 9.

33) Sanlaville, J. "Etude de 1' adsorption de la vapeur d' eau par 1' alumine actvee, et du sechage dynamique des gaz." Genie Chimique, Vol. 78, No. 4 (Octobre, 1957), p. 102.

34) Getty, R. J., Armstrong, W. P. "Drying Air with Activated Alumina under Adiabatic Conditions." I & EC Process Design and Development, Vol. 3, No. 1, (1964), p. 60.

35) Leavitt, F. W. "Non-isothermal Adsorption in Large Fixed Beds." Chemical Engineering Progress, Vol. 58, No. 8, (1962), p. 54.

36) Bergeson, J. R. "Development of a Facility for Studying Adsorption Phenomena." Unpublished Master's Thesis in Petroleum Engineering, University of Oklahoma, (1961).

37) Bird, R. B., Stewart, W. E., Lightfoot, E. N. Transport Phenomena. New York: John Wiley and Sons, Inc., (1960), p. 504.

38) Haul, R. A. W. "Aktivierte Diffusion in Porosen Adsorbentien." Zeitschrift Phys. Chem. N.S.I., (1954), p. 153.

39) Carman, P. C. Flow of Gases Through Porous Media. London: Butterworths Scientific Publications, (1956), p. 118.

40) Kiselev, A. V. Proceedings of the Second International Congress of Surface Activity, Volume II (Solid/Gas Interface). New York: Academic Press, Inc.; London: Butterworths Scientific Publications, (1957), pp. 179-198 and p. 229.

41) Hirschfelder, J. O., Curtiss, C. F., Bird, R. B. Molecular Theory of Gases and Liquids, New York: John Wiley and Sons, Inc., (1954), p. 195.

42) Campbell, J. M., Ashford, F. E., Needham, R. B., Reid, L. S. "Design of Dynamic Hydrocarbon Adsorption Processes Employing Silica Gel." Proceedings Gas Conditioning Conference, University of Oklahoma, (April 2-3, 1963).

43) Deans, H. A., and Lapidus, L. "Derivation of Model for Non-reactive Systems," American Institute of Chemical Engineers Journal, (Dec., 1960), p. 656.

44) Lapidus, L. Society of Petroleum Engineers Paper no. 129, Presented at SPE-AICHE Symposium, Dallas, Texas, (October 8-11, 1961).

APPENDIX A

EXAMPLE CALCULATIONS

EXAMPLE CALCULATIONS

For the example calculation of breakout curve, mass transfer zone length, and breakthrough capacity, the following conditions were assumed:

$G = 2990$ lb./hr.-ft^2 (about 20 ft/min. at 90°F and 800 psia).

$y_o = 0.36$ mole per cent pentane.

6-8 mesh silica gel

Bed temperature = 90°F.

Bed pressure = 800 psia

$z = 14$ feet.

$\rho_B = 47$ lb./ft.^{3}

Gas specific gravity = .65

a) Determination of breakout curve --

From Figure 16, $k = 0.80$ min^{-1} and from Figure 23, $w_e = 0.038$ lb. pentane per lb. gel.

Assuming no pentane adsorbed during the cooling cycle ($Q_s = 0$)

$$Az\,\rho_B w_e = qDz + Q_s$$

and $Q_s = 0$

A = internal diameter of tower

$q = IA$

I = pentane feed Flux, $\frac{\text{lbs. pentane}}{\text{hr - ft}^2}$

Therefore: $Dz = \frac{w_e \rho_B z}{I}$

and

$$I = \frac{Gy_o MW_a}{29\ SG.}$$

MW_a = molecular weight of adsorbate (pentane = 72).

SG. = gas specific gravity.

$$I = \frac{(2990)\ (0.0036)\ (72)}{29\ (.65)} = 41.2\ \frac{\text{lbs. pentane}}{\text{hr. - ft}^2}$$

$$Dz = \frac{w_e\ \rho_B z}{I} = \frac{(0.038)\ (47)\ (14)}{41.2} = .608 \text{ hrs.} = 36.5 \text{ min.}$$

Thus

X (dimensionless length) = kDz = .80 (36.5) = 29.2

From Figure 31 (Graphical solution of the Klinkenberg equation):

and T = kt

$\frac{y}{y_o}$	$\frac{T}{X}$	T	t (minutes)
0.05	0.600	17.5	21.9
0.10	0.678	19.8	24.7
0.20	0.775	22.6	28.3
0.30	0.850	24.8	31.0
0.50	0.980	28.6	35.7
0.70	1.120	32.7	40.9
0.80	1.210	35.3	44.2
0.90	1.34	39.1	48.9
0.95	1.46	42.6	53.3

This calculated breakout curve is Curve II of Figure 32.

b) Determination of the pentane mass transfer zone length --

X = 29.2 as determined in a).

From Figure 28, $h_z/h_T = 0.85$

Thus for a bed length of 14 feet, $h_z = 11.9$ feet.

c) Determination of breakthrough capacity --

X = 29.2 as determined in a). From Figure 28, $h_z/h_T = .85$ and from Figure 30, $Q_B/Q_T = .61$. $w_e = 0.038$ lbs. pentane/lbs. gel. Therefore:

Breakthrough capacity = $\frac{Q_B\ w_e}{Q_T} = 0.0232$ lbs.pentane/lb.gel.

APPENDIX B

EXPERIMENTAL DATA

TABLE 4

EXPERIMENTAL AND CALCULATIONAL RESULTS FOR RUNS NO. 1 - 61 -- PART I

Run[b] No.	Tyler Mesh Size	Superficial Gas Velocity Ft/Min.	Gas Flow Rate SCF/hr.	Bed Length Ft.	y_o Mole %	[a] y_s Mole %	Bed Temp. ^oF	Bed Press. psia
1	3-4	19.8	4870	13.96	0.24	0.011	90	800
2	3-4	19.5	4800	13.96	0.46	0.021	91	800
3	3-4	9.5	2350	13.96	0.75	0.0	90	800
4	3-4	19.4	4770	13.96	0.13	0.013	90	800
5	3-4	29.8	7390	13.96	1.76	0.0	89	805
6	3-4	9.4	2340	13.96	1.95	0.0	90	805
7	3-4	9.6	2380	13.96	1.13	0.0	90	805
8	3-4	37.3	9230	13.96	0.19	0.009	88	800
9	3-4	9.7	2400	7.00	1.81	0.040	89	800
10	3-4	29.0	7150	7.00	0.12	0.021	90	800
11	3-4	19.5	4800	7.00	0.12	0.015	90	800
12	3-4	38.2	9400	7.00	0.083	0.016	90	800
13	3-4	36.8	9100	13.96	1.26	0.0	91	805
14	3-4	37.2	9250	13.96	0.82	0.0	89	805
15	3-4	38.6	9520	13.96	0.063	0.011	90	800
16	3-4	9.6	2390	13.96	2.89	0.0	89	805
17	3-4	29.2	7190	13.96	0.13	0.014	90	800
18	3-4	38.3	9440	13.96	0.11	0.010	90	800
19	3-4	38.5	9590	13.96	1.97	0.0	88	805
20	3-4	29.2	7190	13.96	0.071	0.014	90	800
21	3-4	19.5	4770	13.96	0.066	0.016	91	800
22	3-4	29.2	7230	13.96	0.22	0.010	89	800

[a] y_s is the equilibrium adsorbate concentration in the cooling gas.

[b] The adsorbent bed diameter for runs 1 - 61 was 3.826 inches and the adsorbate was pentane.

TABLE 4--Continued

Run No.	Tyler Mesh Size	Superficial Gas Velocity Ft/Min.	Gas Flow Rate SCF/hr.	Bed Length Ft.	y_o Mole %	y_s Mole %	Bed Temp. ^oF	Bed Press. psia
23	3-4	9.8	2430	13.96	0.22	0.011	90	805
24	3-4	19.7	4870	13.96	1.96	0.0	89	800
25	3-4	9.7	2380	13.96	0.12	0.018	90	800
26	3-4	9.8	2430	13.96	0.73	0.015	89	800
27	3-4	19.6	4870	13.96	0.55	0.0	89	805
28	3-4	37.4	9180	13.96	0.41	0.0	92	800
29	3-4	9.7	2410	13.96	0.45	0.015	89	805
30	3-4	9.6	2360	7.00	0.24	0.015	90	800
31	6-8	10.6	2510	13.82	0.23	0.003	115	800
32	6-8	9.7	2400	13.82	1.24	0.0	90	805
33	6-8	31.0	7840	6.83	1.93	0.0	87	815
34	6-8	20.3	5240	6.83	1.97	0.0	87	820
35	6-8	36.8	9060	13.82	1.89	0.0	91	800
36	6-8	9.8	2420	13.82	1.78	0.0	89	800
37	6-8	29.1	7170	13.82	1.95	0.0	90	800
38	6-8	37.0	9130	6.90	0.10	0.0	90	800
39	6-8	37.2	9180	13.82	0.82	0.0	90	800
40	6-8	19.6	4850	13.82	1.92	0.0	89	800
41	6-8	29.0	7150	13.82	1.28	0.0	91	800
42	6-8	28.8	7140	13.82	0.38	0.003	90	805
43	6-8	19.4	4800	13.82	1.15	0.0	91	805
44	6-8	36.9	9120	13.82	1.20	0.0	91	805
45	6-8	28.9	7140	13.82	0.78	0.0	92	805
46	6-8	36.4	8980	13.82	0.11	0.003	90	800
47	6-8	19.2	4740	13.82	0.36	0.006	91	800
48	6-8	36.4	8940	13.82	0.36	0.0	92	800
49	6-8	36.0	8870	13.82	0.21	0.004	90	800
50	6-8	30.4	7490	13.82	0.23	0.006	91	800

TABLE 4--Continued

Run No.	Tyler Mesh Size	Superficial Gas Velocity Ft/Min.	Gas Flow Rate SCF/hr.	Bed Length Ft.	y_o Mole %	y_s Mole %	Bed Temp. ^oF	Bed Press. psia
51	6-8	36.8	9080	13.82	0.075	0.003	90	800
52	6-8	19.3	4740	13.82	0.79	0.016	91	800
53	6-8	19.3	4760	13.82	0.25	0.005	89	800
54	6-8	9.1	2270	13.82	0.33	0.093	89	805
55	6-8	19.4	4770	13.82	0.13	0.002	91	800
56	6-8	29.7	7310	13.82	0.11	0.002	91	800
57	6-8	9.5	2339	6.90	0.23	0.002	88	800
58	6-8	9.2	2295	13.82	0.083	0.007	89	805
59	6-8	9.4	2315	13.82	0.16	0.011	88	800
60	6-8	9.1	2250	13.82	0.90	0.011	90	800
61	6-8	9.5	2370	13.82	0.49	0.0	88	805

TABLE 5

EXPERIMENTAL AND CALCULATIONAL RESULTS FOR RUNS NO. 1 - 61 -- PART II

Run No.	Dz Min.	$t_{.8}$ Min.	$t_{.2}$ Min.	$t_{.05}$ Min.	$\frac{t_{.8} - t_{.2}}{Dz}$	k Klinkenberg	k Rosen
1	30.242	47.0	16.2	8.9	1.02	0.17	0.16
2	32.900	45.3	18.7	12.7	0.81	0.26	0.24
3	58.244	77.1	40.0	28.0	0.64	0.24	0.23
4	37.085	53.1	20.8	11.0	0.87	0.20	0.18
5	11.970	16.5	6.4	4.8	0.84	0.64	0.60
6	34.770	44.6	24.4	19.2	0.58	0.48	0.46
7	40.830	53.4	26.9	19.8	0.65	0.32	0.31
8	23.498	38.1	6.4	-	1.35	-	0.06
9	8.996	12.7	5.0	-	0.86	0.83	0.78
10	7.757	9.1	-	-	-	-	-
11	11.631	19.8	3.5	-	1.40	-	-
12	6.291	8.2	-	-	-	-	-
13	13.980	19.8	7.1	5.1	0.91	0.47	0.44
14	12.790	19.4	5.3	2.7	1.10	0.34	0.22
15	17.413	26.1	6.6	2.2	1.12	0.25	0.22
16	25.710	32.8	17.2	12.5	0.61	0.59	0.56
17	19.977	30.6	8.8	4.25	1.09	0.23	0.20
18	20.177	33.7	7.8	3.4	1.28	0.16	0.11
19	7.054	9.7	3.3	-	0.91	0.94	0.87
20	19.801	31.6	7.6	2.70	1.21	0.18	0.15
21	30.944	47.4	15.1	8.5	1.04	0.16	0.15
22	20.756	32.7	8.6	4.9	1.16	0.19	0.16
23	65.396	89.0	41.9	27.0	0.72	0.16	0.15
24	16.170	21.7	9.4	6.1	0.76	0.60	0.56
25	64.301	90.9	38.2	23.0	0.82	0.13	0.12
26	36.056	48.5	23.9	16.8	0.68	0.33	0.32
27	27.390	39.9	14.7	8.9	0.92	0.24	0.22

TABLE 5--Continued

Run No.	Dz Min.	$t_{.8}$ Min.	$t_{.2}$ Min.	$t_{.05}$ Min.	$\frac{t_{.8} - t_{.2}}{Dz}$	k Klinkenberg	k Rosen
28	17.170	24.7	8.2	4.7	0.96	0.37	0.34
29	62.999	83.0	42.0	28.0	0.65	0.21	0.20
30	27.869	43.4	11.3	6.0	1.15	0.15	0.13
31	61.942	71.6	52.3	44.0	0.31	0.94	0.87
32	36.728	42.9	30.6	25.6	0.33	1.36	1.27
33	6.266	8.2	3.4	2.4	0.77	1.52	1.42
34	7.916	11.5	6.2	5.0	0.67	1.55	1.48
35	9.812	11.8	7.2	5.6	0.47	2.63	2.55
36	36.854	40.9	31.4	27.9	0.26	2.33	2.14
37	12.666	15.2	9.6	7.7	0.44	2.31	2.21
38	10.448	15.0	5.3	1.8	0.93	0.60	0.56
39	14.922	19.0	10.5	7.7	0.57	1.15	1.11
40	19.444	21.9	15.8	13.6	0.31	2.93	2.73
41	17.844	21.6	13.5	11.1	0.45	1.55	1.49
42	24.596	31.1	18.4	13.8	0.52	0.87	0.83
43	24.670	29.4	19.7	16.4	0.39	1.49	1.41
44	13.802	17.3	9.7	7.5	0.55	1.34	1.28
45	21.174	25.9	15.4	12.2	0.50	1.09	1.05
46	23.330	30.3	16.0	11.2	0.61	0.63	0.61
47	34.722	42.5	26.8	21.4	0.45	0.80	0.77
48	20.908	26.5	14.4	10.4	0.58	0.80	0.77
49	22.072	28.8	15.2	10.8	0.62	0.67	0.64
50	26.396	33.3	19.1	14.2	0.54	0.74	0.71
51	26.858	34.0	18.8	13.7	0.57	0.65	0.63
52	28.746	34.7	22.3	17.9	0.43	1.07	1.02
53	40.280	49.3	31.0	24.3	0.45	0.68	0.66
54	67.780	79.6	55.7	47.2	0.35	0.66	0.63
55	47.008	56.7	36.7	29.2	0.42	0.67	0.65
56	31.120	38.3	22.9	17.2	0.50	0.74	0.72

TABLE 5--Continued

Run No.	Dz Min.	$t_{.8}$ Min.	$t_{.2}$ Min.	$t_{.05}$ Min.	$\frac{t_{.8} - t_{.2}}{Dz}$	k Klinkenberg	k Rosen
57	40.924	50.7	30.9	24.0	0.48	0.59	0.57
58	93.743	109.4	76.9	64.0	0.35	0.50	0.48
59	82.148	97.9	65.7	53.1	0.39	0.45	0.43
60	56.482	64.3	47.4	41.1	0.30	1.13	1.06
61	74.382	85.0	63.5	53.9	0.29	0.92	0.85

TABLE 6

EXPERIMENTAL AND CALCULATIONAL RESULTS FOR RUNS NO. 1 - 61 -- PART III

Run No.	$\phi_{mac.}$	w_e lbs. adsorbate / lbs. adsorbent	Bed wt. Lbs.	F	h_z/h_T	Q_B/Q_T
1	0.348	0.0215	51.26	0.345	2.07	0.285
2	0.348	0.0452	51.26	0.390	1.60	0.378
3	0.348	0.0631	51.26	0.458	1.16	0.471
4	0.348	0.0142	51.26	0.428	1.66	0.289
5	0.348	0.0963	51.26	0.339	1.81	0.385
6	0.348	0.0981	51.26	0.429	1.08	0.535
7	0.348	0.0678	51.26	0.422	1.25	0.471
8	0.348	0.0252	51.26	-	-	-
9	0.364	0.0521	25.10	-	-	-
10	0.364	0.0090	25.10	-	-	-
11	0.364	0.0089	25.10	-	-	-
12	0.364	0.0065	25.10	-	-	-
13	0.348	0.0989	51.26	0.339	1.90	0.354
14	0.348	0.0599	51.26	0.341	2.35	0.199
15	0.348	0.0063	51.26	0.339	2.60	0.118
16	0.348	0.1097	51.26	0.378	1.42	0.463
17	0.348	0.0118	51.26	0.362	2.20	0.203
18	0.348	0.0122	51.26	0.352	2.38	0.162
19	0.348	0.0822	51.26	-	-	-
20	0.348	0.0064	51.26	0.361	2.42	0.127
21	0.348	0.0061	51.26	0.369	1.99	0.266
22	0.348	0.0204	51.26	0.353	2.19	0.227
23	0.348	0.0212	51.26	0.456	1.31	0.404
24	0.348	0.0953	51.26	0.344	1.86	0.360
25	0.348	0.0115	51.26	0.422	1.54	0.349
26	0.348	0.0401	51.26	0.487	1.13	0.450
27	0.348	0.0452	51.26	0.398	1.72	0.315

TABLE 6--Continued

Run No.	$\phi_{mac.}$	w_e lbs. adsorbate / lbs. adsorbent	Bed wt. Lbs.	F	h_z/h_T	Q_B/Q_T
28	0.348	0.0397	51.26	0.359	2.05	0.265
29	0.348	0.0421	51.26	0.473	1.19	0.435
30	0.364	0.0204	25.10	0.338	2.35	0.205
31	0.333	0.0227	51.94	0.460	0.65	0.702
32	0.333	0.0664	51.94	0.466	0.68	0.682
33	0.340	0.1180	25.41	0.376	1.68	0.370
34	0.340	0.1017	25.41	0.323	1.49	0.518
35	0.333	0.1025	51.94	0.382	1.16	0.557
36	0.333	0.0968	51.94	0.385	0.67	0.743
37	0.333	0.1081	51.94	0.376	1.08	0.594
38	0.333	0.0113	25.96	0.395	2.12	0.166
39	0.333	0.0682	51.94	0.407	1.21	0.507
40	0.333	0.1105	51.94	0.384	0.82	0.686
41	0.333	0.0992	51.94	0.383	1.01	0.612
42	0.333	0.0415	51.94	0.438	1.02	0.554
43	0.333	0.0834	51.94	0.436	0.80	0.654
44	0.333	0.0920	51.94	0.368	1.27	0.533
45	0.333	0.0720	51.94	0.388	1.12	0.568
46	0.333	0.0147	51.94	0.432	1.22	0.474
47	0.333	0.0363	51.94	0.446	0.88	0.609
48	0.333	0.0408	51.94	0.399	1.28	0.491
49	0.333	0.0253	51.94	0.436	1.19	0.483
50	0.333	0.0279	51.94	0.442	1.06	0.532
51	0.333	0.0114	51.94	0.428	1.16	0.505
52	0.333	0.0674	51.94	0.433	0.89	0.613
53	0.333	0.0299	51.94	0.428	0.94	0.597
54	0.333	0.0345	51.94	0.463	0.67	0.688
55	0.333	0.0177	51.94	0.430	0.89	0.615

TABLE 6--Continued

Run No.	$\phi_{mac.}$	$\frac{w_e}{\text{lbs. adsorbate}}{\text{lbs. adsorbent}}$	Bed wt. Lbs.	F	h_z/h_T	Q_B/Q_T
56	0.333	0.0155	51.94	0.443	1.02	0.547
57	0.333	0.0270	25.96	0.478	0.88	0.580
58	0.333	0.0124	51.94	0.450	0.72	0.676
59	0.333	0.0193	51.94	0.420	0.86	0.640
60	0.333	0.0713	51.94	0.411	0.69	0.718
61	0.333	0.0531	51.94	0.469	0.60	0.717

TABLE 7

PENTANE CONCENTRATION RATIO EXIT THE DYNAMIC ADSORPTION TOWER

Run No. 1		Run No. 2		Run No. 3		Run No. 4	
Time Min.	$\frac{y}{y_o}$	Time Min.	$\frac{y}{y_o}$	Time Min.	$\frac{y}{y_o}$	Time Min.	$\frac{y}{y_o}$
2	0.016	5	0.0	23	0.0	5	0.0
5	0.020	8	0.011	26	0.043	8	0.022
8	0.038	11	0.016	29	0.075	11	0.044
11	0.079	14	0.078	32	--	14	0.080
14	0.156	17	0.141	35	0.121	17	0.124
17	0.224	20	0.291	38	0.167	20	0.177
20	0.312	23	0.340	41	0.216	23	0.249
23	0.396	26	0.412	44	0.285	26	0.323
26	0.470	29	0.470	47	0.339	29	0.392
29	0.547	32	0.582	50	0.374	32	0.459
32	0.606	35	0.615	53	0.461	35	0.536
35	0.651	38	0.720	56	0.522	38	0.586
38	0.697	41	0.718	59	0.531	41	0.644
41	0.728	44	0.781	62	0.599	44	0.685
44	0.774	47	0.814	65	0.656	47	0.721
47	0.794	50	0.899	68	0.704	50	0.760
50	0.832	53	0.886	71	0.711	53	0.801
53	0.841	56	0.895	74	0.785	56	0.829
56	0.873	59	0.935	77	0.794	59	0.859
59	0.896	62	0.933	80	0.855	62	0.887
62	0.921	65	--	83	0.850	65	0.898
65	0.927	68	0.922	86	0.864	68	0.909
68	0.934	71	0.924	89	0.889	71	0.914
71	0.950	74	0.953	92	0.915	74	0.964
74	0.957	77	0.964	95	0.963	77	0.967
77	0.984	80	0.971	98	0.980	80	0.981
80	0.968	83	1.002	101	0.958	83	0.992
83	1.011	86	1.020	104	0.986	86	0.994
86	0.986	89	1.007	107	0.989	89	1.003
89	1.007	92	0.998	110	0.997	92	1.006
92	1.002	95	0.982	113	1.032	95	1.008
95	0.991	98	0.984	116	0.994	98	0.994
98	0.998	101	1.013	119	0.997	101	0.997
						104	1.000

TABLE 7--Continued

Run No. 5		Run No. 6		Run No. 7		Run No. 8	
Time Min.	$\frac{y}{y_o}$	Time Min.	$\frac{y}{y_o}$	Time Min.	$\frac{y}{y_o}$	Time Min.	$\frac{y}{y_o}$
3	0.0	14	0.0	17	0.0	2	0.006
5	0.068	17	0.038	20	0.093	5	0.051
7	0.257	20	0.065	23	0.106	8	0.234
9	0.421	23	0.152	26	0.122	11	0.348
11	0.564	26	0.253	29	0.260	14	0.426
13	0.675	29	0.352	32	0.332	17	0.465
15	0.743	32	0.459	35	0.401	20	0.505
17	0.814	35	0.533	38	0.541	23	0.553
19	0.856	38	0.653	41	0.554	26	0.604
21	0.884	41	0.745	44	0.665	29	0.655
23	0.894	44	0.760	47	0.676	32	0.703
25	0.930	47	0.840	50	0.762	35	0.751
27	0.960	50	0.926	53	0.782	38	0.787
29	0.975	53	0.931	56	0.762	41	0.823
31	0.982	56	--	59	0.887	44	0.862
33	0.980	59	0.937	62	0.908	47	0.877
35	1.008	62	0.964	65	0.908	50	0.910
37	0.995	65	1.052	68	0.931	53	0.937
39	1.005	68	0.989	71	0.951	56	0.940
41	1.010	71	1.000	74	0.973	59	0.958
43	1.013	74	1.031	77	0.965	62	0.970
45	1.005	77	1.008	80	0.975	65	0.985
47	1.003	80	0.981	83	1.001	68	0.985
49	0.995	83	0.969	86	1.031	71	0.997
51	0.985	86	0.998	89	0.973	74	0.988
53	0.987	89	1.015	92	0.996	77	1.012
						80	1.003

TABLE 7--Continued

Run No. 9		Run No. 10		Run No. 11		Run No. 12	
Time Min.	$\frac{y}{y_o}$	Time Min.	$\frac{y}{y_o}$	Time Min.	$\frac{y}{y_o}$	Time Min.	$\frac{y}{y_o}$
2	0.0	2	0.303	2	0.071	2	0.419
5	0.201	5	0.639	5	0.307	5	0.687
8	0.530	8	0.772	8	0.482	8	0.845
11	0.731	11	0.833	11	0.599	11	0.850
14	0.845	14	0.864	14	0.686	14	0.884
17	0.919	17	0.878	17	0.754	17	0.902
20	0.964	20	0.878	20	0.806	20	0.922
23	0.987	23	0.898	23	0.848	23	--
26	0.992	26	0.901	26	0.900	26	0.946
29	0.997	29	0.918	29	0.948	29	0.966
32	1.015	32	0.946	32	0.968	32	0.990
35	1.000	35	0.946	35	0.984	35	0.977
38	1.000	38	1.007	38	0.990	38	0.995
41	0.992	41	1.003	41	0.987	41	1.003
44	0.990	44	1.000	44	0.994	44	1.000
		47	0.993	47	1.006	47	1.021
				50	1.013	50	1.016

TABLE 7--Continued

Run No. 13		Run No. 14		Run No. 15		Run No. 16	
Time Min.	$\frac{y}{y_o}$	Time Min.	$\frac{y}{y_o}$	Time Min.	$\frac{y}{y_o}$	Time Min.	$\frac{y}{y_o}$
2	0.014	2	0.014	2	0.046	8	0.0
5	0.045	5	0.181	5	0.135	11	0.017
8	0.269	8	0.397	8	0.261	14	0.085
11	0.452	11	0.531	11	0.384	17	0.181
14	0.601	14	0.666	14	0.507	20	0.341
17	0.724	17	0.756	17	0.610	23	0.483
20	0.800	20	0.805	20	0.691	26	0.615
23	0.872	23	0.865	23	0.736	29	0.724
26	0.902	26	0.900	26	0.822	32	0.785
29	0.897	29	0.922	29	0.842	35	0.836
32	0.948	32	0.959	32	0.857	38	0.870
35	0.970	35	0.952	35	0.871	41	0.906
38	0.980	38	0.972	38	0.885	44	0.934
41	1.031	41	0.999	41	0.923	47	0.936
44	1.005	44	0.980	44	0.940	50	0.963
47	0.995	47	0.989	47	0.940	53	0.968
50	1.005	50	1.000	50	0.954	56	0.984
		53	1.032	53	1.034	59	0.992
				56	0.980	62	0.995
				59	0.991	65	0.981
				62	0.971	68	1.000
				65	1.026	71	1.001
						74	1.000

TABLE 7--Continued

Run No. 17		Run No. 18		Run No. 19		Run No. 20	
Time Min.	$\frac{y}{y_o}$	Time Min.	$\frac{y}{y_o}$	Time Min.	$\frac{y}{y_o}$	Time Min.	$\frac{y}{y_o}$
2	0.017	2	0.018	1	0.0	2	0.031
5	0.063	5	0.097	3	0.147	5	0.111
8	0.171	8	0.210	5	0.452	8	0.185
11	0.298	11	0.319	7	0.640	11	0.342
14	0.419	14	0.420	9	0.817	14	0.419
17	0.515	17	0.509	11	0.828	17	0.524
20	0.598	20	0.593	13	0.894	20	0.585
23	0.675	23	0.655	15	0.919	23	0.656
26	0.727	26	0.695	17	0.934	26	0.705
29	0.777	29	0.746	19	0.959	29	0.767
32	0.824	32	0.779	21	0.973	32	0.832
35	0.848	35	0.812	23	0.986	35	0.844
38	0.934	38	0.936	25	0.977	38	0.865
41	0.906	41	0.894	27	0.957	41	0.890
44	0.920	44	0.916	29	0.986	44	0.905
47	0.942	47	0.920	31	1.029	47	0.945
50	0.953	50	0.940	33	0.995	50	1.044
53	0.961	53	0.936	35	1.007	53	0.961
56	0.986	56	1.035	37	1.005	56	0.976
59	0.989	59	0.973	39	0.995	59	1.000
62	0.989	62	1.049	41	0.989	62	0.992
65	0.989	65	1.035	43	0.984	65	0.989
68	1.000	68	0.993	45	0.986	68	0.989
71	1.011	71	0.982	47	1.014	71	1.038
74	1.014	74	0.982	49	1.000	74	0.992
						77	1.000

TABLE 7--Continued

Run No. 21		Run No. 22		Run No. 23		Run No. 23-Cont.	
Time Min.	$\frac{y}{y_o}$	Time Min.	$\frac{y}{y_o}$	Time Min.	$\frac{y}{y_o}$	Time Min.	$\frac{y}{y_o}$
2	0.0	3	0.0	14	0.0	122	0.981
5	0.056	5	0.053	17	0.005	125	0.962
8	--	7	0.133	20	0.014	128	1.005
11	0.101	9	0.220	23	0.025	131	0.973
14	0.174	11	0.300	26	0.046	134	1.000
17	0.258	13	0.394	29	0.060	137	1.008
20	0.334	15	0.452	32	0.074	140	1.000
23	0.404	17	0.514	35	0.117	143	1.005
26	0.474	19	0.569	38	0.145		
29	0.540	21	0.608	41	0.197		
32	0.582	23	0.651	44	0.235	Run No. 24	
35	0.659	25	0.697	47	0.270		
38	0.697	27	0.725	50	0.301		
41	0.780	29	0.755	53	0.358	2	0.0
44	0.756	31	0.771	56	0.382	5	0.013
47	0.808	33	0.814	59	0.445	8	0.111
50	0.829	35	0.837	62	0.503	11	0.317
53	0.857	37	0.849	65	0.530	14	0.511
56	0.868	39	0.869	68	0.598	17	0.647
59	0.892	41	0.886	71	0.623	20	0.756
62	0.916	43	0.901	74	0.675	23	0.831
65	0.934	45	0.915	77	0.678	26	0.856
68	0.934	47	0.933	80	0.762	29	0.902
71	0.955	49	0.936	83	0.770	32	0.924
74	0.965	51	0.959	86	0.765	35	0.952
77	--	53	0.961	89	0.790	38	0.952
80	1.003	55	0.963	92	0.817	41	1.005
83	1.021	57	0.975	95	0.861	44	1.025
86	0.990	59	0.963	98	0.863	47	0.970
89	0.986	61	0.984	101	0.893	50	0.982
92	0.997	63	1.007	104	0.880	53	1.025
95	1.017	65	1.041	107	0.926	56	1.005
98	1.031	67	0.984	110	0.943	59	0.985
101	0.990	69	0.993	113	0.953		
104	0.986	71	0.991	116	0.970		
107	0.990	73	1.002	119	0.962		

TABLE 7--Continued

Run No. 25		Run No. 25-Cont.		Run. No. 27		Run No. 27-Cont.	
Time Min.	$\frac{y}{y_o}$	Time Min.	$\frac{y}{y_o}$	Time Min.	$\frac{y}{y_o}$	Time Min.	$\frac{y}{y_o}$
8	0.0	128	0.965	3	0.0	83	1.006
11	0.003	131	0.962	5	0.013	85	1.006
14	0.006	134	0.987	7	0.024	87	0.998
17	0.006	137	0.997	9	--	89	0.982
20	0.025	140	0.994	11	0.090	91	1.017
23	0.044	143	1.035	13	0.148	93	1.026
26	0.076	146	0.990	15	0.203		
29	0.092			17	0.275		
32	0.124			19	0.336	Run No. 28	
35	0.165	Run No. 26		21	0.382		
38	0.200			23	0.458		
41	0.229			25	0.502	2	0.0
44	0.270	11	0.0	27	0.587	5	0.060
47	0.327	14	0.018	29	0.600	8	0.196
50	0.378	17	0.052	31	0.659	11	0.352
53	0.406	20	0.109	33	0.699	14	0.495
56	0.454	23	0.177	35	0.696	17	0.590
59	0.495	26	0.250	37	0.753	20	0.654
62	0.530	29	0.336	39	0.803	23	0.778
65	0.571	32	0.419	41	0.862	26	0.813
68	0.613	35	0.495	43	0.832	29	0.854
71	0.644	38	0.565	45	0.862	32	0.884
74	0.670	41	0.633	47	0.886	35	0.918
77	0.698	44	0.701	49	0.906	38	0.926
80	0.733	47	0.771	51	0.893	41	0.967
83	0.822	50	0.836	53	0.904	44	0.971
86	0.775	53	0.891	55	0.947	47	0.985
89	0.781	56	0.917	57	0.952	50	1.010
92	--	59	0.969	59	0.993	53	1.004
95	0.829	62	0.992	61	0.971	56	0.992
98	0.851	65	1.013	63	0.971	59	1.009
101	0.857	68	1.013	65	0.985	62	0.990
104	0.863	71	0.995	67	0.982	65	0.986
107	0.870	74	0.992	69	0.982	68	1.004
110	0.895			71	1.015	71	1.010
113	0.914			73	0.989		
116	0.927			75	1.037		
119	0.933			77	1.048		
122	0.949			79	0.989		
125	0.968			81	0.991		

TABLE 7--Continued

Run No. 29		Run No. 30		Run No. 31		Run No. 31-Cont.	
Time Min.	$\frac{y}{y_o}$	Time Min.	$\frac{y}{y_o}$	Time Min.	$\frac{y}{y_o}$	Time Min.	$\frac{y}{y_o}$
23	0.0	2	0.0	29	0.0	101	0.981
26	0.039	5	0.024	31	0.004	103	0.973
29	0.055	8	0.099	33	0.004	105	1.038
32	0.073	11	0.193	35	0.006	107	0.998
35	0.110	14	0.285	37	0.008	109	0.987
38	0.139	17	0.377	39	0.010	111	0.979
41	0.202	20	0.457	41	0.023		
44	0.215	23	0.519	43	0.036		
47	0.277	26	0.580	45	0.061	Run No. 32	
50	0.334	29	0.633	47	0.092		
53	0.393	32	0.669	49	0.128		
56	0.420	35	0.715	51	0.174	20	0.0
59	0.461	38	0.754	53	0.234	23	0.019
62	0.505	41	0.780	55	0.295	26	0.054
65	0.578	44	0.804	57	0.358	29	0.126
68	0.622	47	0.829	59	0.427	32	0.276
71	0.679	50	0.850	61	0.496	35	0.441
74	0.721	53	0.908	63	0.569	38	0.617
77	0.730	56	0.889	65	0.626	41	0.737
80	0.732	59	0.981	67	0.684	44	0.833
83	0.793	62	0.918	69	0.736	47	0.910
86	0.826	65	0.930	71	0.793	50	0.942
89	0.835	68	0.949	73	0.833	53	0.964
92	0.899	71	0.949	75	0.862	56	1.051
95	0.905	74	0.954	77	0.893	59	0.981
98	0.923	77	0.954	79	0.912	62	0.983
101	0.927	80	0.952	81	0.925	65	0.991
104	0.956	83	0.957	83	0.944	68	0.987
107	0.960	86	0.973	85	0.954	71	0.996
110	0.980	89	0.983	87	0.971	74	0.998
113	0.984	92	1.027	89	0.969	77	0.987
116	0.996	95	0.986	91	1.033	80	0.996
119	0.973	98	0.998	93	0.983	83	0.994
122	1.020	101	0.998	95	0.975	86	1.024
125	1.009	104	1.000	97	1.054	89	1.006
		107	1.005	99	0.990	92	1.004
						95	1.013

TABLE 7--Continued

Run No. 33		Run No. 34		Run No. 35		Run No. 36	
Time Min.	$\frac{y}{y_o}$	Time Min.	$\frac{y}{y_o}$	Time Min.	$\frac{y}{y_o}$	Time Min.	$\frac{y}{y_o}$
2	0.0	2	0.0	3	0.0	23	0.0
5	0.443	5	0.042	5	0.010	25	0.013
8	0.784	8	0.403	7	0.178	27	0.031
11	0.918	11	0.749	9	0.497	29	0.079
14	0.964	14	0.907	11	0.713	31	0.177
17	0.979	17	0.955	13	0.881	33	0.328
20	0.989	20	0.979	15	0.943	35	0.478
23	1.000	23	1.000	17	0.950	37	0.666
26	1.001	26	1.008	19	0.958	39	0.727
		29	1.004	21	0.974	41	0.803
		32	1.001	23	0.990	43	0.856
		35	0.995	25	1.004	45	0.880
		38	0.993	27	1.000	47	0.900
		41	0.992	29	0.996	49	0.889
				31	1.000	51	0.930

TABLE 7--Continued

Run No. 37		Run No. 38		Run No. 39		Run No. 40	
Time Min.	$\frac{y}{y_o}$	Time Min.	$\frac{y}{y_o}$	Time Min.	$\frac{y}{y_o}$	Time Min.	$\frac{y}{y_o}$
5	0.0	1	0.038	3	0.0	11	0.0
7	0.010	3	0.071	5	0.006	13	0.021
9	0.145	5	0.179	7	0.029	15	0.132
11	0.405	7	0.340	9	0.108	17	0.329
13	0.638	9	0.481	11	0.248	19	0.531
15	0.790	11	0.607	13	0.417	21	0.748
17	0.866	13	0.731	15	0.579	23	0.824
19	0.955	15	0.840	17	0.706	25	0.897
21	0.945	17	0.855	19	0.802	27	0.915
23	0.969	19	0.876	21	0.869	29	0.950
25	0.980	21	0.919	23	0.921	31	0.963
27	0.972	23	0.947	25	0.938	33	0.971
29	0.988	25	0.964	27	0.958	35	1.019
31	0.988	27	0.964	29	0.983	37	0.990
33	0.986	29	0.977	31	0.990	39	1.062
35	1.020	31	0.998	33	0.985	41	0.981
37	0.998	33	0.966	35	1.010	43	0.981
39	1.006	35	0.981	37	1.000	45	0.988
41	1.012	37	0.998	39	1.000	47	0.994
		39	1.011	41	1.000	49	0.990
		41	1.021	43	0.990	51	0.996
		43	1.024	45	1.000	53	0.992

TABLE 7--Continued

Run No. 41		Run No. 42		Run No. 43		Run No. 44	
Time Min.	$\frac{y}{y_o}$	Time Min.	$\frac{y}{y_o}$	Time Min.	$\frac{y}{y_o}$	Time Min.	$\frac{y}{y_o}$
7	0.0	9	0.0	13	0.0	5	0.0
9	0.008	11	0.007	15	0.022	7	0.029
11	0.047	13	0.033	17	0.067	9	0.146
13	0.163	15	0.075	19	0.157	11	0.342
15	0.341	17	0.141	21	0.294	13	0.536
17	0.527	19	0.227	23	0.451	15	0.685
19	0.667	21	0.340	25	0.586	17	0.792
21	0.792	23	0.472	27	0.708	19	0.860
23	0.833	25	0.570	29	0.782	21	0.963
25	0.908	27	0.653	31	0.857	23	0.936
27	0.920	29	0.742	33	0.898	25	0.951
29	0.949	31	0.852	35	0.939	27	0.963
31	0.965	33	0.850	37	0.959	29	0.977
33	0.975	35	0.894	39	0.976	31	0.979
35	0.976	37	0.934	41	0.982	33	0.984
37	1.035	39	0.958	43	0.990	35	0.986
39	0.982	41	0.958	45	0.996	37	0.984
41	0.990	43	1.011	47	0.998	39	0.990
43	1.008	45	1.004	49	1.004	41	0.990
45	0.982	47	0.987	51	1.000	43	0.998
47	1.012	49	0.989	53	1.000	45	1.006
49	1.002	51	1.018	55	1.000	47	1.006
51	0.992	53	1.000	57	1.000	49	1.000
		55	0.989	59	0.998	51	1.002
		57	0.996	61	1.002	53	0.996
						55	1.002
						57	0.992

TABLE 7--Continued

Run No. 45		Run No. 46		Run No. 47		Run No. 48	
Time Min.	$\frac{y}{y_o}$	Time Min.	$\frac{y}{y_o}$	Time Min.	$\frac{y}{y_o}$	Time Min.	$\frac{y}{y_o}$
9	0.0	5	0.0	15	0.0	5	0.0
11	0.020	7	0.008	17	0.008	7	0.005
13	0.077	9	0.016	19	0.019	9	0.023
15	0.174	11	0.045	21	0.043	11	0.062
17	0.310	13	0.091	23	0.082	13	0.135
19	0.452	15	0.159	25	0.133	15	0.233
21	0.590	17	0.243	27	0.207	17	0.342
23	0.696	19	0.342	29	0.298	19	0.459
25	0.773	21	0.443	31	0.399	21	0.573
27	0.830	23	0.542	33	0.476	23	0.671
29	0.879	25	0.627	35	0.574	25	0.753
31	0.907	27	0.707	37	0.644	27	0.817
33	0.927	29	0.769	39	0.699	29	0.852
35	0.951	31	0.819	41	0.766	31	0.890
37	0.952	33	0.862	43	0.793	33	0.906
39	0.956	35	0.891	45	0.854	35	0.986
41	0.973	37	0.924	47	0.891	37	0.934
43	0.974	39	0.946	49	0.918	39	0.979
45	0.985	41	0.961	51	0.941	41	0.966
47	0.995	43	0.969	53	1.016	43	0.975
49	0.989	45	0.981	55	0.944	45	0.989
51	0.991	47	0.990	57	0.963	47	1.009
53	0.996	49	1.002	59	0.965	49	0.993
55	1.007	51	1.000	61	0.979	51	0.986
57	1.005	53	1.004	63	1.048	53	0.995
59	0.996	55	1.002	65	0.995	55	1.000
61	1.015	57	0.996	67	0.997	57	1.007
		59	1.000	69	0.997	59	0.998
		61	0.992	71	1.003	61	0.998
				73	0.995	63	0.995
				75	0.997	65	1.005
				77	0.989	67	1.002
						69	1.016

TABLE 7--Continued

Run No. 49		Run No. 50		Run No. 51		Run No. 52	
Time Min.	$\frac{y}{y_o}$	Time Min.	$\frac{y}{y_o}$	Time Min.	$\frac{y}{y_o}$	Time Min.	$\frac{y}{y_o}$
5	0.0	5	0.0	7	0.0	11	0.0
7	0.004	7	0.006	9	0.004	13	0.002
9	0.018	9	0.004	11	0.010	15	0.012
11	0.055	11	0.009	13	0.037	17	0.031
13	0.115	13	0.028	15	0.078	19	0.073
15	0.185	15	0.064	17	0.134	21	0.147
17	0.286	17	0.118	19	0.210	23	0.235
19	0.392	19	0.210	21	0.290	25	0.347
21	0.497	21	0.284	23	0.379	27	0.459
23	0.626	23	0.381	25	0.475	29	0.571
25	0.677	25	0.475	27	0.566	31	0.671
27	0.755	27	0.565	29	0.654	33	0.749
29	0.806	29	0.656	31	0.720	35	0.808
31	0.845	31	0.727	33	0.774	37	0.855
33	--	33	0.792	35	0.823	39	0.896
35	--	35	0.836	37	0.868	41	0.924
37	--	37	0.880	39	0.893	43	0.945
39	0.974	39	0.921	41	0.912	45	0.957
41	0.986	41	0.943	43	0.938	47	0.967
43	0.986	43	0.958	45	0.951	49	0.984
45	0.998	45	0.972	47	0.963	51	1.000
47	1.004	47	0.983	49	0.971	53	0.996
49	1.000	49	0.989	51	0.977	55	0.988
51	1.000	51	0.996	53	0.975	57	0.988
53	1.014	53	0.998	55	0.986	59	0.992
55	0.995	55	1.002	57	0.990	61	1.014
57	0.991	57	1.004	59	0.994	63	1.002
59	0.991	59	1.002	61	0.998	65	1.010
61	0.996	61	0.996	63	0.996	67	1.002
63	1.004	63	1.006	65	1.010	69	1.004

TABLE 7--Continued

Run No. 53		Run No. 54		Run No. 55		Run No. 56	
Time Min.	$\frac{y}{y_o}$	Time Min.	$\frac{y}{y_o}$	Time Min.	$\frac{y}{y_o}$	Time Min.	$\frac{y}{y_o}$
15	0.0	43	0.0	17	0.0	7	0.0
17	0.005	45	0.023	19	0.002	9	0.002
19	0.008	47	0.043	21	0.002	11	0.004
21	0.018	49	0.068	23	0.004	13	0.008
23	0.035	51	0.106	25	0.017	15	0.021
25	0.074	53	0.151	27	0.024	17	0.043
27	0.097	55	0.184	29	0.048	19	0.083
29	0.148	57	0.232	31	0.076	21	0.145
31	0.200	59	0.282	33	0.110	23	0.201
33	0.267	61	0.340	35	0.158	25	0.280
35	0.349	63	0.390	37	0.204	27	0.381
37	0.421	65	0.453	39	0.265	29	0.455
39	0.498	67	0.514	41	0.333	31	0.540
41	0.570	69	0.554	43	0.400	33	0.623
43	0.639	71	0.610	45	0.481	35	0.702
45	0.700	73	0.665	47	0.536	37	0.762
47	0.748	75	0.710	49	0.604	39	0.812
49	0.790	77	0.753	51	0.665	41	0.857
51	0.832	79	0.791	53	0.718	43	0.878
53	0.909	81	0.824	55	0.770	45	0.913
55	0.888	83	0.917	57	0.808	47	0.938
57	0.904	85	0.899	59	0.858	49	0.950
59	0.921	87	0.904	61	0.869	51	0.952
61	0.951	89	0.922	63	0.891	53	0.969
63	0.965	91	0.932	65	0.908	55	0.973
65	0.963	93	0.950	67	0.923	57	0.977
67	0.973	95	0.962	69	0.937	59	0.983
69	0.987	97	0.965	71	0.943	61	0.986
71	0.993	99	0.972	73	0.976	63	0.994
73	0.995	101	0.992	75	0.967	65	0.992
75	1.003	103	0.990	77	0.983	67	0.996
77	1.003	105	1.005	79	0.983	69	0.996
79	1.007	107	1.010	81	0.998	71	1.012
81	1.002	109	0.992	83	0.994	73	1.008
83	1.000	111	1.005	85	0.996	75	1.004
85	0.993	113	1.000	87	1.009	77	1.000

TABLE 7 --Continued

Run No. 57		Run No. 58		Run No. 59		Run No. 60	
Time Min.	$\frac{y}{y_o}$	Time Min.	$\frac{y}{y_o}$	Time Min.	$\frac{y}{y_o}$	Time Min.	$\frac{y}{y_o}$
15	0.0	50	0.0	35	0.0	29	0.0
17	0.003	53	0.009	38	0.004	31	0.002
19	0.010	56	0.016	41	0.006	33	0.004
21	0.021	59	0.022	44	0.006	35	--
23	0.038	62	0.029	47	0.020	37	0.018
25	0.060	65	0.054	50	0.030	39	0.029
27	0.101	68	0.107	53	0.048	41	0.047
29	0.146	71	0.112	56	0.068	43	0.077
31	0.202	74	0.159	59	0.102	45	0.124
33	0.269	77	0.199	62	0.144	47	0.180
35	0.332	80	0.251	65	0.186	49	0.259
37	0.411	83	0.309	68	0.246	51	0.339
39	0.478	86	0.369	71	0.325	53	0.420
41	0.548	89	0.434	74	0.367	55	0.508
43	0.613	92	0.510	77	0.441	57	0.582
45	0.671	95	0.573	80	0.503	59	0.663
47	0.711	98	0.624	83	0.571	61	0.726
49	0.762	101	0.673	86	0.625	63	0.762
51	0.808	104	0.736	89	0.715	65	0.847
53	0.846	107	0.770	92	0.729	67	0.841
55	0.884	110	0.796	95	0.774	69	0.872
57	0.914	113	0.852	98	0.800	71	0.901
59	0.940	116	0.850	101	0.832	73	0.901
61	0.932	119	0.886	104	0.854	75	0.912
63	0.940	122	0.910	107	0.868	77	0.928
65	0.950	125	0.917	110	0.892	79	0.942
67	0.971	128	0.935	113	0.898	81	0.953
69	0.983	131	0.957	116	0.928	83	0.971
71	1.005	134	0.957	119	0.944	85	0.977
73	0.983	137	0.969	122	0.942	87	0.978
75	0.983	140	0.969	125	0.962	89	0.989
77	1.003	143	0.962	128	0.998	91	1.000
79	1.009	146	0.991	131	0.970	93	1.007
81	1.027	149	0.975	134	0.982	95	1.000
		152	1.051	137	0.992	97	1.009
		155	0.996	140	0.998	99	0.993
		158	1.000	143	0.998	101	0.996
		161	0.980	146	1.016	103	0.991
				149	1.000	105	1.000

TABLE 7--Continued

Run No. 61		Run No. 61 -Cont.	
Time Min.	$\frac{y}{y_o}$	Time Min.	$\frac{y}{y_o}$
45	0.0	115	0.996
47	0.014	117	0.996
49	0.019	119	0.994
51	0.029	121	1.002
53	0.041	123	1.004
55	0.052	125	0.998
57	0.081		
59	0.105		
61	0.143		
63	0.188		
65	0.236		
67	0.298		
69	0.357		
71	0.424		
73	0.496		
75	0.552		
77	0.620		
79	0.674		
81	0.721		
83	0.764		
85	0.800		
87	0.831		
89	0.864		
91	0.886		
93	0.907		
95	0.926		
97	0.934		
99	0.952		
101	0.965		
103	0.973		
105	0.975		
107	0.988		
109	0.988		
111	0.990		
113	1.025		

TABLE 8

RESULTS OF GAS AND PARTICLE TEMPERATURE MEASUREMENTS FOR RUN NO. 62

Adsorbent: 6-8 mesh silica gel
Adsorbate: 2.0 mole % pentane
Bed Pressure: 805 psia

Superficial gas velocity: 17.6 ft/min.
Bed length: 5.83 feet
Bed diameter: 2 inches

Time Min.	T_1	T_2	T_3	T_4	T_5	T_6	T_7	T_8	T_9	T_{10}	T_{11}
0.0	89.6	89.6	89.4	89.4	89.2	89.2	89.4	89.4	89.5	89.6	88.9
0.4	90.4	90.0	89.6	89.4	89.2	89.2	89.4	89.4	89.2	89.4	89.2
0.8	95.5	95.2	93.5	92.6	90.0	90.0	89.6	89.4	89.3	89.2	89.4
1.2	94.8	95.1	98.0	97.4	94.4	94.5	90.5	90.5	89.4	89.4	89.7
1.6	92.6	93.1	98.0	98.0	99.0	99.1	94.3	94.4	90.4	90.4	90.2
2.0	91.5	91.7	95.7	96.0	100.1	100.2	99.1	99.0	93.7	93.7	90.5
2.4	91.2	91.4	93.9	94.2	99.0	99.1	101.3	101.2	98.3	98.0	90.5
2.8	91.2	91.2	92.6	92.8	97.2	97.3	101.5	101.5	101.2	101.0	90.8
3.2	91.2	91.3	92.1	92.3	95.5	95.7	100.4	100.3	102.3	102.0	91.2
3.6	91.5	91.5	92.0	92.0	94.3	94.6	99.2	99.2	102.0	101.9	91.1
4.0	91.6	91.6	91.7	91.9	93.5	93.7	97.8	97.7	101.3	101.2	91.3
4.4	91.7	91.7	91.7	91.7	92.8	93.1	96.6	96.6	100.3	100.3	91.4
4.8	91.8	91.8	91.8	91.8	92.5	92.8	95.5	95.5	99.1	99.0	91.5
5.2	92.0	92.0	92.0	92.0	92.2	92.5	94.6	94.8	98.0	98.0	91.8
5.6	92.0	92.0	92.0	92.0	92.0	92.3	94.0	94.0	96.9	96.9	91.7
6.0	92.2	92.1	92.0	92.0	92.0	92.2	93.4	93.6	95.9	96.0	91.9
6.4	92.3	92.3	92.3	92.3	92.1	92.3	93.2	93.2	95.1	95.2	92.0
6.8	92.5	92.4	92.3	92.3	92.1	92.3	92.8	93.1	94.5	94.6	91.7
7.2	92.5	92.5	92.4	92.4	92.3	92.4	92.7	92.8	94.0	94.1	92.0
7.6	92.5	92.5	92.5	92.5	92.3	92.4	92.7	92.8	93.7	93.8	92.1
8.0	92.5	92.5	92.5	92.5	92.4	92.5	92.7	92.7	93.4	93.5	92.3
8.8	92.5	92.5	92.5	92.5	92.4	92.4	92.5	92.5	92.8	93.1	92.3

TABLE 8--Continued

Time Min.	T_1	T_2	T_3	T_4	T_5	T_6	T_7	T_8	T_9	T_{10}	T_{11}
10.0	92.6	92.5	92.5	92.4	92.1	92.3	92.3	92.3	92.3	92.5	92.3
12.0	92.6	92.6	92.6	92.6	92.5	92.5	92.5	92.5	92.4	92.4	92.4

Note:

Thermocouple Location

T_1 - Gas temperature 2 feet from inlet
T_2 - Particle temperature 2 feet from inlet
T_3 - Gas temperature 3 feet from inlet
T_4 - Particle temperature 3 feet from inlet
T_5 - Gas temperature 4 feet from inlet
T_6 - Particle temperature 4 feet from inlet
T_7 - Gas temperature 5 feet from inlet
T_8 - Particle temperature 5 feet from inlet
T_9 - Gas temperature 6 feet from inlet
T_{10} - Particle temperature 6 feet from inlet
T_{11} - Gas temperature 0 feet from inlet

TABLE 9

RESULTS OF TEMPERATURE MEASUREMENTS FOR RUNS 31 - 61

Run No.	$\triangle T_{10}$	$\triangle T_5$
31	-	3.0
32	12.4	10.5
35	15.0	15.5
36	25.0	20.3
37	18.7	18.0
38	0.0	0.0
39	7.8	7.7
40	21.9	20.4
41	12.6	12.3
42	3.6	4.0
43	11.6	9.9
44	12.5	13.7
45	7.7	7.5
46	1.1	2.1
47	5.0	4.4
48	3.9	4.6
49	2.0	2.5
50	3.3	3.7
51	1.2	1.7
52	7.5	6.9
53	3.5	3.9
54	3.2	4.1
55	2.1	2.2
56	0.9	1.8
57	-	0.6
58	2.0	2.9
59	4.2	4.9
60	10.9	8.6
61	4.7	4.6

Note:

$\triangle T_{10}$ is the maximum difference between the outlet gas temperature and the inlet gas temperature.

$\triangle T_5$ is the maximum difference between the gas temperature out the first half of the tower and the inlet gas temperature.